# Best
# Available
# Copy

L. J. P. Salo                        Services Branch                        15 Nov 71
Chief, Soils Div                                                            GEDDINGS/lmh/2571

1.  Attached is a Xerox copy of Change 3 to Appendix II of AR 70-31, **Standards for Technical Reporting (Incl 1)**.  Also inclosed are the pages from our complete List of Publications listing reports of your Division having restrictive statements (Incl 2).  Affected titles are indicated in red.

2.  Existing Statement 2, "This document is subject to special export controls and each transmittal to foreign governments or foreign nationals may be made only with prior approval of (controlling office)," on our reports must be changed to either Statement A or Statement B (see pages 4 and 5 of Incl 1) before the end of 1971.  Therefore, it is requested that you review the reports bearing Statement 2 and indicate by each title on the list the new statement to be imposed on document and return completed list to Publications as soon as possible.

3.  If Statement B is to be imposed on document, please give full statement (see page 5 of Incl 1) so that we can have new statement printed and placed on remaining copies of reports in Publications and those on file in our Research Center Library.  All recipients on primary distribution lists will have to be notified so that their copies can be marked accordingly.  This will be done by the Publications Distribution Unit after receipt of pertinent information from you.

4.  Any questions about this . . .          . . . . ac . . . . . . . . may . . . dressed to
Mrs. Laura Hardsee, Exte. . . .       . . . . .

2 Incl                                              EDL
as

## CONTRACT REPORTS (Continued)

| Number | Date | Title | Restrictions |
|--------|------|-------|--------------|
| | | **Soils Division, 1969** | |
| S-69-1 | May 1967 | The Use of Sodium Silicate and Sulphur as a Dust Palliative | Transmittal outside U. S. Govt agencies must be approved by AMC |
| S-69-2 | June 1968 | Study of Wave Propagation in Confined Soils | |
| S-69-3 | Apr 1969 | Effect of Degree of Saturation on Compressibility of Soils from the Defence Research Establishment, Suffield | |
| S-69-4 | Oct 1969 | Dutch Friction-Cone Penetrometer Exploration of Research Area at Field 5, Eglin AFB, Florida | |
| *S-69-5 | Apr 1969 | Cracking of Earth and Rockfill Dams; A Theoretical Investigation by Means of the Finite Element Method | |
| *S-69-6 | Sept 1969 | Finite Element Analyses of Port Allen and Old River Locks | |
| *S-69-7 | July 1969 | A Theoretical Study of Landing Mat Behavior | Subject to special export controls by AMC |
| *S-69-8 | Nov 1969 | Finite Element Analyses of Stresses and Movements in Embankments During Construction | |
| | | **Miscellaneous Subjects, 1969** | |
| O-69-1 | May 1969 | A Water Resources Ecology Capability for the Waterways Experiment Station and Corps of Engineers | |

---

\* Issued in 1970.

CONTRACT REPORT S-69-7

# A THEORETICAL STUDY OF LANDING MAT BEHAVIOR

by

M. E. Harr, J. C. Rosner

July 1969

ARMY MRC VICKSBURG MISS

# FOREWORD

The work reported herein was performed by the Purdue Research Foundation, Purdue University, Lafayette, Indiana, for the U. S. Army Engineer Waterways Experiment Station (WES) under Contract DACA 39-67-C-0044, during the period July 1967 to March 1969. The study was conducted as a part of the landing mat program under Research and Development Project No. 1T062103A046, "Trafficability and Mobility Research," Task 05, "Mobility Engineering Support," under the sponsorship of the Research and Development Directorate, U. S. Army Materiel Command (AMC). The principal investigators were Messrs. Milton E. Harr, Professor of Soil Mechanics, and John C. Rosner, Graduate Instructor.

WES Soils Division personnel directly concerned with monitoring this contract were Messrs. D. N. Brown, Chief, Design and Analysis Section, and D. W. White, Mat Section, under the general supervision of Mr. J. P. Sale, Chief, Soils Division. COL Levi A. Brown, CE, was Director of the WES and Mr. F. R. Brown was Technical Director during this study.

72093

# TABLE OF CONTENTS

# LIST OF TABLES

# LIST OF FIGURES

# LIST OF SYMBOLS

| | |
|---|---|
| A | Coefficient |
| $a_D$ | Shift factor |
| $c_j$ | Coefficients |
| $C(\sigma)$ | Stress dependent parameter |
| CA | Contact area |
| $CA_R$ | Relative contact area |
| CBR | California Bearing Ratio |
| $D_0$ | Elastic compliance |
| $D_1$ | Coefficient |
| $D(t)$ | Inelastic compliance |
| $D_u(t)$ | Total compliance |
| $D(\sigma)$ | Deviator stress |
| E | Young's modulus of mat or beam |
| $E_0$ | Young's modulus of subgrade |
| $EI_R$ | Relative rigidity |
| H | Thickness of subgrade layer |
| I | Moment of inertia of the mat or beam |
| k | Model characteristic |
| $k_{INT}$ | Model characteristic at zero coverages |
| $k_N$ | Model characteristic at N coverages |
| $(k_e)_{INT}$ | Model characteristic at the end joint at zero coverages |

| $(k_e)_N$ | Model characteristic at the end joint at $N$ coverages |
|---|---|
| $L$ | Elastic characteristic of the beam |
| $m$ | Slope of strain-time relationship |
| $N$ | Number of coverages |
| $p(x)$ | Loading function |
| $q(x)$ | Loading function |
| $r^2$ | Coefficient of governing differential equation |
| $s^4$ | Coefficient of governing differential equation |
| $T$ | Membrane tension |
| $t$ | Model characteristic |
| $t$ | Time |
| $t_1$ | Time duration of load |
| $TP_R$ | Relative tire pressure |
| $V$ | Deflection |
| $w$ | Deflection |
| $\dot{w}$ | Water content |
| $WL$ | Wheel load |
| $WL_R$ | Relative wheel load |
| $WS_R$ | Relative wheel spacing |
| $x$ | Coordinate |
| $y$ | Coordinate |
| $\gamma$ | Dimensionless parameter |
| $\gamma_d$ | Dry unit weight of subgrade |
| $\gamma_N$ | Value of dimensionless parameter at $N$ coverages |
| $\delta$ | Width of beam |

| | |
|---|---|
| $\Delta_f$ | Deflection at failure |
| $\Delta_r(t)$ | Residual deflection |
| $\Delta\varepsilon(t)$ | Time dependent strain |
| $\varepsilon(t)$ | Strain |
| $\varepsilon_0$ | Elastic strain |
| $\varepsilon_r(t)$ | Residual strain |
| $\eta$ | Dimensionless coordinate |
| $\mu_0$ | Poisson's ratio of the subgrade |
| $\pi_j$ | Dimensionless parameter |
| $\sigma$ | Normal stress |
| $\tau$ | Shear stress |
| $\psi$ | Displacement distribution function |
| $\nabla^2$ | Laplacian operator |

# ABSTRACT

Rosner, John Christopher. Ph.D., Purdue University, August 1969. Theoretical Study of Landing Mat Behavior. Major Professor: Dr. Milton E. Harr.

Mechanistic models are developed to help predict the behavior of landing mat systems. The first model, which is based upon elastic theory, is capable of duplicating the action of such systems under static loads. The associated assumptions are: 1) that an infinite beam is the structural equivalent of the mat; 2) that the subgrade is homogeneous; 3) that horizontal displacements within the subgrade are negligible; and 4) that the mat always remains in contact with the subgrade. The model parameters are established from simulations of full-scale experimental tests. These parameters are also correlated with prototype test variables.

Results from prototype tests indicate that the model parameter k, the subgrade modulus, decreases as trafficking of the section progresses. Contrary to common belief the model behavior is found to be extremely sensitive to the magnitude of the subgrade modulus. Results also indicate that the performance of dual-wheel prototype tests can be predicted with reasonable confidence by the procedure developed herein: use for the single-wheel tests appears to be somewhat limited.

An investigation of the effect of end joint connections indicates that some increase in service life can be attained by strengthening the standard end joint connectors.

A second mechanistic model is developed to simulate actual loading sequences and to provide a means of estimating the residual deformations of the mat surface. The applicability of this model is demonstrated for both single-wheel and dual-wheel tests. Complete evaluation of the potentialities of this model is not possible from the available data.

# INTRODUCTION

Present indications are that landing mats will be used extensively in the forward areas of any future air operations. This is particularly true in theaters of operations where time and the availability of native construction materials will not permit a more permanent type of installation. Since the efforts and cost required to produce and deliver landing mats to theaters of operations are so great, the efficient use of the mat is essential. Inefficient use of mats may prevent the timely accomplishment of assigned missions.

Existing criteria for designing runways to be surfaced with landing mats have developed, by and large, from full-scale experimental tests. Prototype tests were conducted by the Corps of Engineers [10, 12][1] on individual mat types under various conditions of load, number of coverages, wheel spacing, tire pressure, tire ply rating, base thickness, and California Bearing Ratio (CBR) of the subbase material. Most of these tests were conducted until failure occurred. Failure was judged on the basis of the roughness of the mat surface or excessive breakage in the mat. In regards to the roughness requirement, the test section was considered to have failed when permanent deviations of 3 inches or more occurred in a 10 foot length in any direction within the traffic lane. When breakage developed in 10 percent or more of the mat panels within the traffic lane, the test section was considered to have failed. In most tests both failure criteria were met simultaneously.

The results of each test when failure occurred were used in connection with established design curves developed originally for flexible pavements. Such design curves are given by Yoder [68] and the procedure for using the obtained data is given in Corps of Engineers publications [8, 10]. An effective thickness of flexible pavement was assigned to the mat using the design curves. The performance of a landing mat could then be estimated by interpolation and extrapolation.

---

[1] The numbers in brackets refer to references given in the List of References.

In tests where failure was not in evidence after a maximum established number of coverages, the effective thickness of the mat was determined using the same procedure given above. For these, the effective thickness assigned to the mat was less than optimal for the established failure criteria.

For each type of mat tested a set of design curves has been developed. In line with this procedure, each alteration in the structure or configuration of the individual mat elements has necessitated a new series of performance tests.

The objective of this study was to develop a reliable procedure or method for predicting the performance of landing mats. It was anticipated that the success of this study would serve to reduce greatly the need for costly performance testing and the procedure could be used for comparisons of the relative effectiveness of existing mat types. In addition, it was hoped that the study would provide a means whereby more efficient utilization of landing mats could be achieved.

For this study the results of the prototype tests as reported by the Corp of Engineers [10, 12] were used.

# REVIEW OF LITERATURE

## Existing Theories of Surface Displacements

The benefits to be accrued from the use of selected surface materials as agents for the transmission of wheel loads to the existing sub-soils have long been realized. The behavior of these materials, be they concrete, asphaltic mixtures, chemically stabilized soils, or landing mats, has been of considerable interest to the engineer. Many theories for the analysis of such systems have been proposed; yet, no general theory exists today.

## Winkler Concept

One of the initial analyses of load transfer between surface materials and a subgrade was provided by Winkler [67]. In his work he assumed that the action of the subgrade was analogous to a dense fluid or a system of linear independent springs wherein the reactive pressures developed in the subgrade were proportional to the deflection of the surface. Winkler's hypothesis stated that

$$p = kw \qquad (1)$$

where      p is the pressure exerted by the subgrade
           k is a proportionality constant
           w is the deflection of the subgrade surface.

However he did not indicate what value or values should be associated with the proportionality constant, k.

In his analyses of railway ties and rails, Zimmermann [70] utilized the Winkler concept and concluded that the proportionality constant was dependent upon the type of subgrade. Experimental studies conducted by Foppl [19] indicated that the response of such systems could be approximated by using the Winkler hypothesis.

In a mathematical treatment of the subject, Hayashi [25] employed the Winkler hypothesis to analyse beams resting on soil. He presented the solution for the condition where shearing forces existed at the interface of the beam and the soil. The governing differential equation took the form

$$\frac{d^4 w}{dx^4} - \frac{A}{EI} \frac{d^2 w}{dx^2} + \frac{k}{EI} w = \frac{q(x)}{EI} \tag{2}$$

wherein    EI is the rigidity of the beam
           A is a constant
           q(x) is the loading function.

If interfacial shear can be neglected, the second term in Eqn. (2) may be omitted. From a later investigation which considered the presence of interfacial shear forces, Florin [18] concluded that these frictional forces had negligible influence on the distribution of the vertical pressure exerted by the soil.

In 1926, Westergaard [64] used the Winkler hypothesis to compute the stresses in concrete highway pavements. Later [65] he extended his analysis to airport pavements. In his initial study, he observed that an increase of the subgrade modulus from 50 lbs./cu. in. to 200 lbs./cu. in. produced only minor variations in pavement stresses. Therefore it was surmised that an approximate single value of the subgrade modulus, k, should be sufficient for determination of the stresses in pavements. It was also suggested that a standard procedure be developed whereby the value of k could be determined.

Prior use of the Winkler hypothesis assumed that the subgrade followed the structural member. This necessitated the development of normal tensile stresses at the interface of the load transfer mechanism and the subgrade. Murphy [39] investigated the stresses and deflections of plates whose edges were free of foundation support. In addition to observing that the size of the plate had a considerable effect upon the developed stresses, calculations indicated that an increase in the stiffness of the foundation reduced appreciably the stresses and deflections of the plate. In an analogous manner, Harr and Leonards [24], employing the Winkler hypothesis, demonstrated that appreciable stresses and deflections could be produced in concrete slabs when moisture and/or temperature gradients across the depth were present.

4

In 1946, Hetenyi [26] presented a collection of solutions for beams on Winkler foundations; finite as well as infinite length beams. To remove the discontinuity in the deflection pattern that occurs at the end of a finite length beam using the Winkler hypothesis, he suggested that the finite beam be placed over an infinite beam which in turn was embedded in the system of springs. Hetenyi did not give numerical values for the subgrade modulus, nor did he suggest what factors may influence this measure.

In a study conducted in 1955, Drapkin [16] obtained the solution for finite length beams utilizing the principle of superposition. He noted that contrary to prevailing practice increasing the length of a beam did not reduce substantially the maximum vertical foundation pressures.

In 1955, Terzaghi [62] presented a critical review of the history and development of existing theory based upon the subgrade modulus. He pointed out that the magnitude of the subgrade modulus was dependent upon the dimensions of the loaded area as well as the elastic properties of the soil. He also established a procedure whereby consistent values for the subgrade modulus could be obtained. Terzaghi noted that intelligent use of the Winkler hypothesis would produce reliable stresses and bending moments but the theory failed to provide reasonable estimates for settlements.

In 1962, Lenczer [36] experimentally investigated the effect of soil depth on the magnitude of the subgrade modulus. He observed that for shallow depths, less than 12 inches, the variation in the numerical values of k was appreciable. He, as did Terzaghi before him, found that the subgrade modulus was dependent upon the size of loaded area. In addition, he presented an empirical relationship wherein the subgrade modulus could be taken as a function of deposit depth.

Many other investigators [21, 29, 38, 51] have employed the Winkler hypothesis or minor variations thereof to the analysis of load transfer systems.

Elastic Solid Models

In the 1930's with the advance of soil mechanics, questions were directed concerning the validity of the Winkler hypothesis. In 1937, Biot [4] presented the means of com-

5

puting the contact pressures on the base of an infinite elastic beam resting on a semi-infinite elastic solid. This solution made it possible to determine an equivalent value for the subgrade modulus, k. Subsequent investigations led to the conclusion that the subgrade modulus was a complicated function dependent not only on the elastic modulus of the soil and the width of the beam but also upon the beam's flexural rigidity. Biot concluded that no unique value of the subgrade modulus could be assigned to a given subgrade.

In 1943, Burmister [ 6 ] obtained the solution for a two layered system acted upon by a uniform circular load. Each layer was assumed to be a homogeneous, isotropic, and linearly elastic solid. A perfectly rough interface condition was assumed to exist between layers with the lower layer providing continuous support to the upper layer. Lemcoe [ 35 ] confirmed the results given by Burmister and also investigated the condition of a frictionless interface. He reported that only a very slight change occurred in the vertical normal stresses as the interface condition changed from perfectly rough to perfectly smooth.

The semi-infinite elastic solid model and an elastic layer of finite thickness were employed by Pickett [ 43 ] in his investigation of the behavior of concrete pavements. Influence charts for deflections and moments at different points in the concrete slab were presented for both an elastic solid subgrade and a dense liquid subgrade. However, he gave no suggestions for associating the model parameters with given subgrade conditions. The solution for an elastic solid of finite depth was also presented by Sovinc 60 . As an aid to obtaining this solution he approximated the displacements within the solid by a double Fourier Series.

In 1961, Davis and Taylor [ 13 ] investigated the influince of horizontal loading on the surface displacements of an elastic layer. They concluded that care in selecting the values of the elastic constants was necessary for this type of loading because some portions of the soil mass experiences a stress reduction. In 1963, Lee [ 34 ] concluded that for horizontal surface loads the normal stress distribution along the contact surface of a flexible strip was essentially independent of the magnitude of the contact shearing stresses. Lee also expressed the belief that the assumption of a smooth contact surface leads to conservative estimates of the bending moment and shearing force induced in the strip. In an earlier study, Leonov [ 37 ] also found that horizontal forces have practically no influence on the distribution of the vertical reactive pressure.

6

In an attempt to simplify future computations, DeBeer [14] using an iterative procedure, obtained the contact pressure distribution beneath a beam. He suggested that a second or fourth order polynominal could be used to approximate the contact pressure distribution. Using this relationship he obtained reasonably correct deflections and bending moments. From the results of an experimental investigation DeBeer [15] concluded that the second degree parabolic distribution reflected the results of the tests regardless of the beam stiffness. Comparisons of the test results with computations based upon the Winkler hypothesis were also made. Barden [2] in his studies of finite beams employed DeBeer's approximation for the contact pressure and concluded that the results obtained were more valid than those obtained from the Winkler analysis.

Many procedures and techniques have been developed [57, 41, 23, 34, 48] to approximate the distribution of surface contact pressures. A method developed by Zhemochkin [69] assumed that the load transfer element was connected to the elastic solid by linkages (two-force members). By treating the forces in these linkages as unknowns and using the "method of virtual displacements", he was able to approximate the contact pressures transmitted by the elastic solid. A high degree of accuracy could be achieved by using many linkages in the system. This procedure gave results which agreed well with the more rigorous mathematical solution. Sinitsyn [59] extended the application of Zhemochkin's procedure and Barden [1] later presented another variation. In his discussion to Barden's paper, Chueng [7] indicated a further simplification and noted that this method had been used in Asiatic countries in design for many years.

A recent theory for analyzing structures on elastic foundations based upon a general variational method was developed by Vlasov and Leont'ev [63]. This theory is more complex than the Winkler theory yet simpler than the elastic half-space analysis. The form of the basic differential equation given to describe the state of strain in a loaded single-layer foundation had the same form as that obtained earlier by Filonenko-Borodich [17] and by Pasternak [42]. The method possesses great flexibility. By judicious selection of the coefficients in the differential equation, the equation for either the Winkler hypothesis or the elastic solid model may be obtained. In addition, boundary conditions are easily introduced and the developed procedure can be readily extended for complex three-dimensional considerations. This method forms the background of a large part of the analysis developed in this report.

7

# Viscoelastic Models

Recently attention has been directed toward application of viscoelastic theory to the response of soils subjected to static and dynamic loading. Many rheological models have been proposed for simulating the stress-strain-time behavior of soils and for modeling studies of creep phenomena and stress relaxation in soil.

Freudenthal and Lorsch [20] were among the first investigators who employed a linear viscoelastic analysis to infinite beams. In their study the soil support was replaced by a series of Kelvin, Maxwell, or Standard Linear Solid elements. For each of these elements the authors were able to develop relationships for the deflection of an infinite beam subjected to time invariant concentrated and uniform loads.

In a brief note in 1958, Reissner [52] presented the solution of a thin plate resting on a viscoelastic foundation which possessed shear interaction; a frictionless plate-foundation interface was assumed. Two years later, Pister and Williams [47] extended the work of Reissner to incorporate a rough interface condition. In addition, they presented response curves for the maximum deflection and moment for an applied step force. Later Pister [46] presented the solution for the axisymmetric bending of a viscoelastic plate of finite thickness supported by a viscoelastic foundation of infinite extent. He, as did Reissner, assumed a frictionless interface condition.

In his study of the creep behavior of snow foundations, Kerr [28] employed a linear viscoelastic media. The time invariant load was applied directly to the foundation rather than by a load transfer mechanism (such as a beam or a plate).

Hoskin and Lee [27] used linear viscoelastic models for their analysis of the stress and deformation characteristics of a subgrade, strengthened by a flexible surface plate and subjected to a suddenly applied uniformly distributed invariant load. They concluded that the Maxwell model gave unrealistic values for deflections, subgrade pressures, and plate bending moments for long time loading; however, the use of the Standard Linear Solid model was found to be satisfactory. They also noted that under certain circumstances (by use of transform theory the time dependence of the system could be removed) stress and deflection analyses of a system containing linear viscoelastic components could be treated as an

8

analogous elastic problem having the same geometric boundary conditions. This analogy is known as the "correspondence principle". They concluded that the response of a linear viscoelastic material to stress could be predicted by an elastic material wherein the elastic constants were replaced by time-dependent parameters.

Schapery [53, 54] reported that the solution of many non-linear viscoelastic problems may also be closely approximated by reducing them to an equivalent elastic condition wherein the parameters, which characterize the non-linear viscoelastic material, are taken as functions of time. The validity of this procedure (quasi-elastic method of analysis) was demonstrated by Schapery [53] for a viscoelastic cantilever beam subjected to a concentrated load at the free end. Schapery [54] also applied this procedure to the analysis of the creep of glass fiber reinforced resin under an uniaxial stress condition and demonstrated that the procedure could also predict the creep response of Polystyrene under a varying stress condition. Three different samples of Polystyrene were subjected to a triple-step stress application. Predictions of the magnitude of the strains were within 9% of those observed from experimental investigation over an elapsed time of 1512 hours.

Konder and Krizek [31] investigated the creep response of a commercially available cohesive soil, Jordan Buff, under uniaxial and constant compressive stress. They were able to predict creep response for this material which exhibited definite non-linear behavior with an expression of the form

$$\varepsilon = C(\sigma) + C_1 (\sigma)(\log t - C_2 \log^2 t) \tag{3}$$

where $C(\sigma)$, $C_1 (\sigma)$ are constants with respect to time but are stress dependent
$C_2$ is a constant
$t$ is the time variable.

Singh and Mitchell [58] studied the creep response of a number of soil types subjected to various test conditions. They developed an expression for the strain of the form

$$\varepsilon = C(\sigma) + C_1 e^{\alpha D(\sigma)}(t)^{1-m} \qquad (m \neq 1) \tag{4}$$

9

where      $C(\sigma)$ is a constant which is dependent on the strain at unit time

$C_1$ is a constant

$\alpha$ is a dashpot constant

$D(\sigma)$ is the deviator stress

M is the slope of logarithm of strain rate versus logarithm of time (straight line)

t is time.

They concluded that the expression was applicable irrespective of whether the soils were undisturbed or remolded, wet or dry, normally consolidated or over-consolidated, or tested in a drained or undrained condition. They stated that the developed creep function reflected the effect of soil composition, soil structure, stress history, stress intensity and the slope of the strain rate vs. time relationship on a log-log plot. They indicated that further research was being conducted to attest the validity of their creep function for repetitive load conditions.

In his analysis of viscoelastic layered pavement systems, Barksdale [3] was able to develop a creep compliance response for an asphalt mixture and one for a clay subgrade. Both relationships were developed for materials subjected to repetitive stationary step loadings.

The primary limitation of applying viscoelastic models to real soil behavior has been the difficulty in assigning representative numerical values to the parameters for even the simplest model.

## Prototype Tests on Landing Mats

Accelerated traffic tests simulating aircraft taxiing operations were conducted by the Corps of Engineers [10] on test sections constructed with a range of subgrade strengths that represented airstrips surfaced with landing mats. The purpose of these tests was to provide data on the service life of mat-surfaced airstrips under various conditions of wheel load, tire pressure, and subgrade strength. As noted previously, design curves were developed by modification of the conventional CBR (California Bearing Ratio) design curves for flexible pavements.

The traffic simulated the operations of military aircraft with both single- and dual-wheel assemblages. Single-wheel loads ranged from 10,000 to 50,000 lbs and tire pressures ranged from 40 to 300 psi. For dual-wheel assembly, loads of 50,000 lbs were used with a wheel spacing of 37.5 in. (center to center) and tire pressures ranged from 100 to 300 psi. These loading arrangements were applied by a load cart [10]. Each test section was approximately 26 ft. wide and 30 ft. long with the traffic applied over a width of 12 ft.

Two types of subgrades were used: (1) a fat clay (CH) with an average liquid limit of 60 and a plasticity index of 39 and (2) a lean clay (CL) with an average liquid limit of 36 and a plasticity index of 15. The strength of the subgrade was classified into three groups: (1) high strength with a CBR above 20, (2) medium strength with a CBR between 7 and 20, and (3) low strength with a CBR between 3 and 7.

The tests were made on standard M6, M8, and M9 landing mats. The M6 mat is a pierced steel plank with a moment of inertia per foot of width of 0.069 in.$^4$; the M8 mat is a heavy, deep-ribbed steel mat with a moment of inertia per foot of width of 0.269 in.$^4$ The M9 mat is a deep-ribbed aluminum mat with an average moment of inertia per foot of width of 0.618 in.$^4$ These mats, which are rectangular in shape, were placed on the subgrade in a masonry type arrangement and connected by integral locking lugs on the sides and hooked connectors on the ends.

The tests were continued until the test section failed or until 700 coverages had been completed by the load cart. Failure of the sections was judged on the basis of: (1) development of roughness of the mat surface to the point of endangering aircraft operations and (2) excessive mat breakage.

In 1967, the Corps of Engineers conducted an extensive study [12] to develop criteria for the efficient design of aircraft landing gear for aircraft required to operate from mat-surfaced airfields. Traffic tests were conducted with numerous combinations of wheel configurations, loads, and tire pressures. The wheel configurations varied from a single-wheel up to 12 wheels: the loading varied from 35,000 to 273,000 lbs and the tire pressures ranged from 50 to 250

psi. The two soils, which formed the subgrade, exhibited only minor differences in characteristics. One soil was a fat clay (CH) with a liquid limit of 58 and a plasticity index of 31 while the other soil was a fat clay (CH) with a liquid limit of 61 and a plasticity index of 37. The in-place, initial strength of these subgrades as indicated by CBR values ranged from 1.1 to 9.0.

These tests were made on the M8 mat (previously described) and the modified T11 mat which is a lightweight, extruded-aluminum panel with an abrasive surface [11]. The moment of inertia per foot of width of the T11 mat is 1.368 in.[4] The method of placement of the rectangular-shaped T11 mat was also of the masonry design. The behavioral characteristics and performance of the mat surfaces, whether loaded or unloaded, are well documented [12] for each test at various coverage levels. The single-wheel and dual-wheel data from this test series constitute the basis of the investigation reported herein.

## Application of Theories to Landing Mats

It is well recognized [9] that the action of landing mats in distributing wheel loads to the subgrade is complicated and that the exact mechanism through which distribution is accomplished has not been defined. The consensus of opinion is, however, that the mat distributes loads in a manner similar to that of a beam or flat plate. Consequently, most theoretical studies of landing mats have employed this type of analysis.

In 1951, Pickett [44] conducted a theoretical investigation of the behavior of landing mats. In this investigation, he considered the landing mat capable of: (1) tensile strength only, (2) flexural strength only, and (3) both flexural and tensile strength. Initially, the assumption was made that the composite mat and subgrade material could be represented by a model composed of a thin membrane of infinite extent supported on a liquid subgrade incapable of supporting shear stresses. Vertical loads were applied directly to the membrane. The governing differential equation for this model was

$$T \, \Delta^2 w - kw = -q \tag{5}$$

12

where $T$ is the membrane tension (assumed to be constant)
$\Delta^2$ is the Laplacian operator
w is the deflection of the surface
k is the density of the liquid
q is the intensity of pressure in the direction
of positive deflection.

In earlier studies, Schiel [56] and Filonenko-Borodich [17] arrived at this identical differential equation in their analyses of beams on elastic foundations. After obtaining the solution of Eqn. (5), Pickett developed an influence chart by which the deflection of the surface and the reactive pressure could be determined graphically for a uniform load of any configuration.

Next Pickett [44] assumed that the composite mat and subgrade material could be represented by a membrane supported on an elastic solid. For this model, influence charts were prepared for both deflection and reactive pressures for two finite thicknesses of the elastic solid in addition to the case of infinite thickness. As could be expected, the presence of the membrane reduced the magnitude of the deflection as compared to the simple elastic half-space model. A model composed of a thin plate type of membrane (wherein the membrane tension could vary with direction at a point and vary from point to point) and a subgrade, assumed to be a dense liquid with respect to vertical reactions but providing elastic resistance to horizontal displacements of the membrane, was investigated by the finite difference method. Mathematical difficulties prevented the completion of this solution.

In a later study, Pickett [45] extended his analytical work to include considerations of orthotropic mats on elastic subgrades. In these investigations, he considered the mat capable of only flexural resistance and assigned to the mat a wide range of combinations of transverse, longitudinal, and torsional stiffnesses. He concluded that a given amount of transverse flexural rigidity was several times as effective in reducing maximum deflection as an equal amount of torsional rigidity and that both of these rigidities were of less relative importance than the longitudinal rigidity. It was further noted for widely distributed loads that all mat rigidities were of less relative importance than the subgrade rigidity.

In all of Pickett's studies it was assumed that the mat and subgrade remained in contact at all points and that the shear developed at the interface could be neglected. In none of the studies did he actually utilize his models to predict the performance of landing mats.

In 1955, the Corps of Engineers [9] presented the results of full-scale landing mat tests and model tests which were compared with the analytical studies conducted by Pickett [44, 45]. It was concluded that the beneficial effects of the landing mat was dependent upon its longitudinal, transverse, and to a very minor extent its torsional rigidity. It was further noted that because of slack in the end joint connections and practical considerations in laying the mat little, if any, over-all membrane action was possible. The report concluded that landing mats act primarily "in flexure" and that additional stiffness at the end joints add considerably to the smoothness of the operating surface under traffic conditions, approximately doubling the service life of the mat.

# MODEL DEVELOPMENT AND SIMULATION

## Introduction

A mechanistic model was sought whose deflection behavior reflected the action of landing mats. Initial consideration was given to the selection of a representative load transfer element. In accordance with the findings of the Corps of Engineers [9], a membrane was eliminated as a possible element. Also as indicated in Photograph 5 of this report, (particularly for a group of M8 type mats) there is an apparent lack of resistance to lateral bending due to the presence of longitudinal joints. This would tend to exclude a thin plate from consideration. Thus for the sake of expediency, a beam was selected for the basic load transfer element.

The second consideration was the idealization of the soil media. The Winkler hypothesis, Eqn. (1), was not considered suitable due to its shortcomings as pointed out by Terzaghi [62] and its neglection of interfacial shear stresses. Initially, a viscoelastic model was not used because of its complexity and the anticipated difficulty of correlating the model parameters with the given soil properties. Since it was shown [12] that the "average deflection" increased with the number of coverages, a conventional elastic solid model was also not directly applicable. However, this behavioral characteristic could be accommodated by an elastic solid model wherein the model parameters are made coverage dependent. Such a quasi-elastic model for the soil media was employed initially in this study.

## Development of Mat-Soil Model

Since it was anticipated that the mat-soil model parameters would have to be established by analytical simulation of prototype test data, careful consideration was given to the method of analysis. The general variational method of

analysis, developed by Vlasov and Leont'ev [63] for elastic foundations, appeared to provide the desired degree of flexibility. A detailed presentation of this method for a single layer foundation is given in Appendix A.

The reaction of a beam of infinite length to loading was selected as the mechanistic equivalent to that of the mat under similar circumstances. This selection was predicated upon several prevailing conditions. First, actual field operations and test procedures employed by the Waterways Experiment Station [12] demonstrated that the mat elements extend laterally for an appreciable distance outside the normal traffic lane. The traffic lane widths for the single wheel tests ranged from 4.75 ft. to 12.00 ft. A minimum extension of 10.16 ft. beyond the traffic lane existed for all cases. Typically the width over which the wheel load was applied was only 14.7 inches. Secondly, the longitudinal joint used for the mats (necessitated by the construction procedure) provided virtually no moment transfer from one mat element to the next. However, as attested by Photograph 4 of reference 9, in the transverse direction an appreciable amount of moment transfer was afforded by the end joint connectors. Tests [9] on the M8 mat indicated that the longitudinal rigidity was approximately 150 times larger than the lateral rigidity.

The width of the infinite beam was taken as the length of a rectangle whose area was equivalent to the tire print area and whose width was equal to the maximum width of the tire print. In those cases where this equivalent beam width was greater than the width of the actual mat element the longitudinal joint was neglected. Initially, it was assumed that complete continuity existed at the end joints of the mat elements; that is, the end joint connections provided total shear and moment transfer between mat elements.

In addition to the above, the following assumptions were made:

1. The wheel loads can be represented by uniformly distributed loads.

2. The beam obeys Eulerian conditions regardless of the stress level.

3. The beam and the soil always remain in contact.

4. Horizontal displacements within the soil media are negligible.

16

Under these assumptions, the response of the mat-soil model is given by the differential equation (Eqn. (B5), Appendix B)

$$\frac{d^4 V(\eta)}{d\eta^4} - 2r^2 \frac{d^2 V(\eta)}{d\eta^2} + s^4 V(\eta) = \frac{p(x)L^4}{EI} \qquad (6)$$

where

$$r^2 = \frac{tL^2}{EI} = \frac{1-\mu_0}{2L} \int_0^H \psi_1^2 \, dy \qquad (7)$$

$$s^4 = \frac{kL^4}{EI} = 2L \int_0^H \psi_1'^2 \, dy \qquad (8)$$

and

$$L = \sqrt[3]{\frac{2EI(1-\mu_0^2)}{E_0 \, \delta}} \qquad (9)$$

At the present time there is no reliable information available as to the actual distribution of displacements with depth in a soil layer. This is particularly true for the selected soil model wherein horizontal displacements in the soil media are assumed to be of negligible magnitude. Information available for homogeneous deposits indicates that the distribution of displacements with depth is non-periodic and has a maximum at the surface. Tests conducted by the Corps of Engineers [9] on a rubber subgrade loaded both without a mat and through a steel mat indicate an asymptotic attenuating distribution of displacement with depth (see Plate 17 of reference 9). It appears reasonable to assume that with different mat rigidities the same general shape would be maintained but that the rate of attenuation would vary with depth. Functional representations of this type of distribution may take many forms. One form, suggested by Vlasov and Leont'ev [63], assumed a ratio of hyperbolic functions as

$$\psi_1(y) = \frac{\sinh \gamma \frac{H-y}{L}}{\sinh \gamma \frac{H}{L}} \qquad (10)$$

17

where     H is the thickness of the soil layer
          y is the distance from the subgrade surface
          $\gamma$ is the dimensionless parameter

With the distribution of displacements described by Eqn. (10) and after applying the assumption of negligible horizontal displacements, the stresses can be expressed as (from Eqns. (A16), Appendix A)

$$\sigma_y = \frac{E_o}{1-\mu_o^2} V_1(x) \frac{d\psi_1(y)}{dy} \tag{11a}$$

$$\tau_{xy} = \frac{E_o}{2(1+\mu_o)} V_1'(x)\psi_1(y) \tag{11b}$$

A typical distribution of the above stresses is given in Figure 1.

With the form of $\psi_1(y)$ taken as in Eqn. (10), any variation in the rate of attenuation of the displacement due to different mat rigidities can be incorporated by judicious selection of the parameter $\gamma$. As indicated in Figure 2, $\psi_1(y)$ does not produce a unique distribution until the dimensionless parameter $\gamma$ is established. Since the value of $\gamma$ could not be established from any previous studies, it was necessary to examine the "average deflection" patterns for the cases at hand with the hope that a simulation procedure could be developed which would yield reasonable measures of this parameter.

In addition to the parameter $\gamma$, some measure was required for the equivalent layer thickness, H. In most of the test sections, the natural soil was excavated to a depth of 6 ft. and the excavation was backfilled under controlled conditions to produce the required soil strengths. In some test sections, the subgrade was controlled only for a depth of two feet. An analytical study of the effect of layer thickness on the deflection pattern was made. For this investigation the layer thickness was varied in increments from 12 in. to an infinite depth. From the simulation of the "average deflection" patterns, results (to be discussed later, see Table 3) for the extreme conditions indicate that the layer thickness was immaterial. For simplicity, the soil media was assumed to be of infinite extent. Under this assumption, the model characteristics k and t in Eqns. (7) and (8), become

18
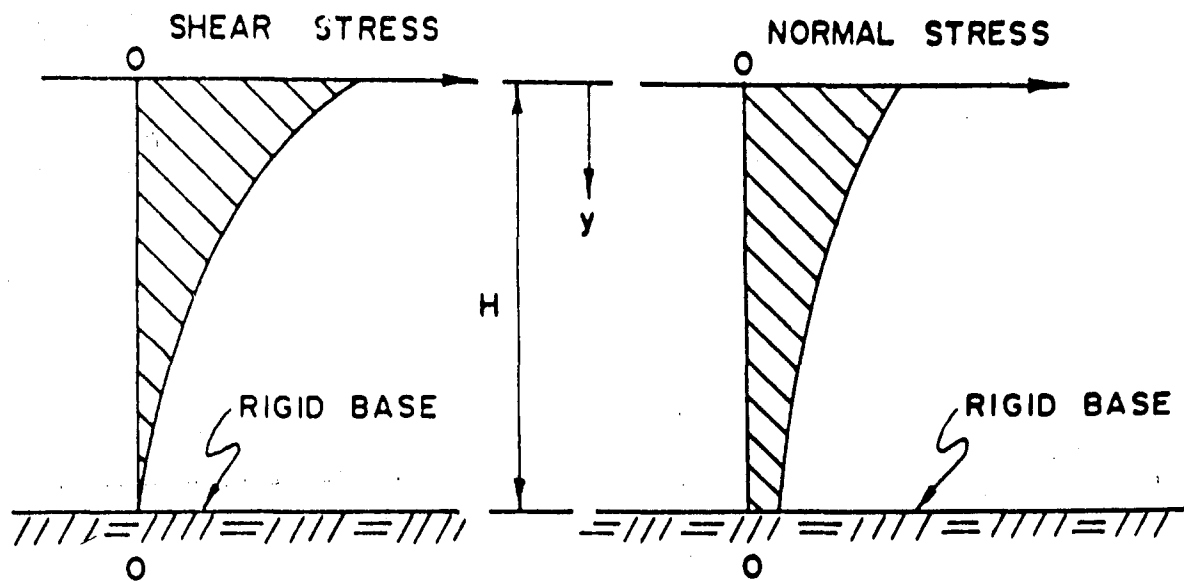
FIGURE I. DISTRIBUTION OF STRESSES
WITH DEPTH



$$\psi(y) = \frac{\sinh \dfrac{\gamma(H-y)}{L}}{\sinh \dfrac{\gamma H}{L}}$$
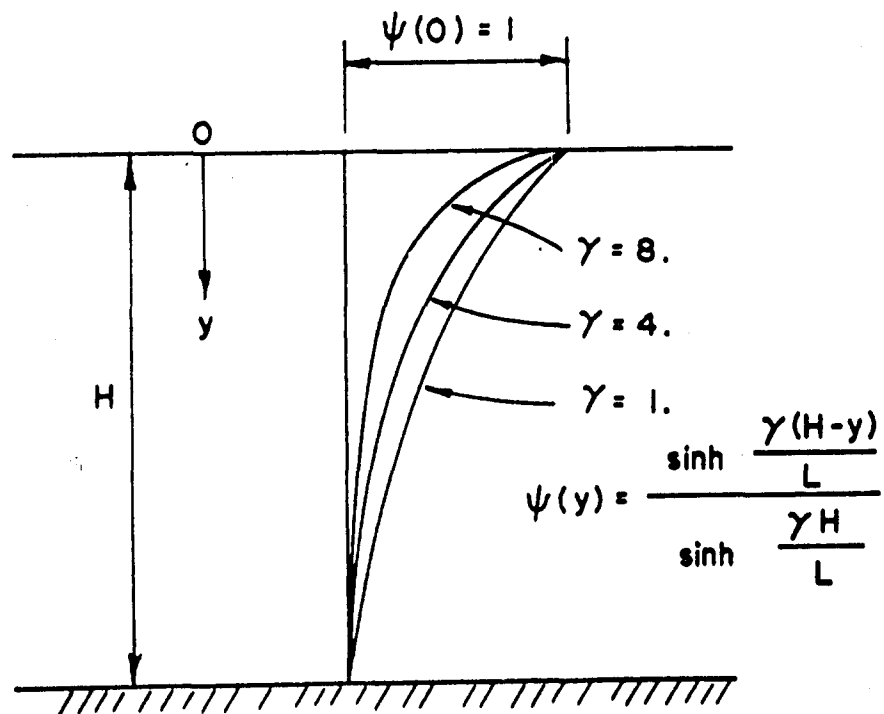
FIGURE 2. DISTRIBUTION OF DISPLACEMENT
WITH DEPTH

$$k = \frac{E_O \delta}{2(1-\mu_0^2)} \frac{\gamma}{L} \qquad (12a)$$

$$t = \frac{E_O \delta}{\epsilon(1+\mu_O)} \frac{L}{\gamma} \qquad (12b)$$

As can be noted from the above relations, the two model characteristics are functions of the unknown parameters $E_O$ (modulus of elasticity of the soil), $\mu_O$ (Poisson's ratio for the soil), and $\gamma$. Therefore to use the developed mat-soil model, the parameters $E_O$ and $\mu_O$ must be numerically identified in addition to the parameter $\gamma$. The identification of these parameters could be accomplished by simulating the "average deflection" patterns; however, to consider the effect of each parameter independently would necessitate extensive computer time.

Previous studies of beams on elastic foundations indicated that $\mu_O$ generally has a negligible effect on the resulting deflection pattern. To assess the validity of this assertion for the present problem, the deflections of two points in the mat, one directly under a wheel and one 36.75 in. from the centerline of the wheel, were determined for conditions identical to those of Section 13, Lane 2E, Item 2 for Poisson's ratios of 0.3 and 0.5. The resulting deflections are tabulated in Table 1. For this particular test, a Poisson's ratio of 0.4 appears adequate. Hence in this study, $\mu_O$ is assumed to be 0.4. This assumption is also in line with that made previously by Pickett[43, 44]. In any event, any appreciable error incurred by this assumption would be compensated for, in part, by the other parameters, $E_O$ and $\gamma$, obtained from the simulation procedure.

## Table 1

### Effect of Poisson's Ratio on Deflection

| | $\gamma$ | $E_o$ (psi) | Deflection at $\ell$ of Wheel (in.) | Deflection 36.75 in. from $\ell$ of Wheel (in.) |
|---|---|---|---|---|
| $\mu_o = 0.3$ | 3.00 | 250 | 1.098 | 0.099 |
| $\mu_o = 0.5$ | 3.00 | 250 | 0.900 | 0.054 |
| Actual (from "average deflection" pattern) | | | 1.0 | 0.0 |

## Parameter Identification Techniques

Several identification methods were applied to the deflection data obtained from the prototype tests to determine equivalent mat-soil model parameters. The first method, which has been used successfully by mechanical engineers for similar systems, utilizes a state variable filter. Unfortunately, for the present problem it proved to be totally unsatisfactory. The second approach, the so-called "steep descent" method, proved to be adequate for the identification of the model characteristic k, Eqn. (12a). A simplification was introduced to this method to reduce computer time. The "steep descent" method failed to provide a reliable measure of the parameter $\gamma$. Finally, success was registered in this regard by employing a trial and error procedure.

For each method and modification, input conditions were imposed upon the developed mat-soil model identical to those of the prototype tests. The criterion followed in the identification of the model parameters was to minimize the response differences in deflection of at least nine discrete points taken from the "average deflections" patterns. In cases where the curvature of the deflection pattern changed appreciably from point to point, more reference points were selected. In some cases as many as sixteen reference points were used.

## State Variable Filter

The initial procedure utilized a state variable filter in conjunction with a steep descent linear identifier as outlined by Kohr [30]. The procedure (see Appendix C) was programmed using the field data; however, unrealistic values for the parameters resulted. Additional modifications also proved unsuccessful and the method was eventually abandoned. Failure of this procedure to produce meaningful values was believed to be primarily due to the selection of a step function as the forcing function for the load. The lack of success for a step load had been noted previously in other cases by Kohr [30].


## Steep Descent Method

The second method employed to provide a measure of the parameters, $E_o$ and $\gamma$, was based upon the "steep descent" method [40, 68]. A brief explanation of the procedural aspects of this method is given in Appendix D.

This procedure was initially applied to data from the test designated as Section 1, Lane 2, Item 3, for zero coverages. The initial values assumed for $E_o$ and $\gamma$ were 100 psi. and 1.55, respectively. Using the steep descent procedure, a minimum of the error functional (defined in Appendix D) of 0.060 was obtained when $E_o$ = 750 psi. and $\gamma$ = 1.598; this is indicated as trial 1 in Figure 3. To determine whether the minimum obtained was global rather than local another trial was performed. Trial 2, Figure 3, which was initiated with $E_o$ = 200 psi. and $\gamma$ = 6.00, produced a minimum of 0.079 when $E_o$ = 280 psi. and $\gamma$ = 6.006. With these results it was apparent that the surface of the error functional was not bowl-like in form. Additional trials were made as indicated in Figure 3. As can be seen from Figure 3, the error functional possessed a curved valley of minimal values which for all practical purposes were identical. Unfortunately, the shape of the error functional proved not to be unique as shown for another test section in Figure 4.

It was apparent that unique values of $E_o$ and $\gamma$ could not be obtained with the selected form of the error functional. Fortunately, as can be seen in Table 2, the values of the parameter k varied only slightly along the valley of the error functional. Therefore, representative values of the characteristic k could be generated regardless of the value of $\gamma$.

22
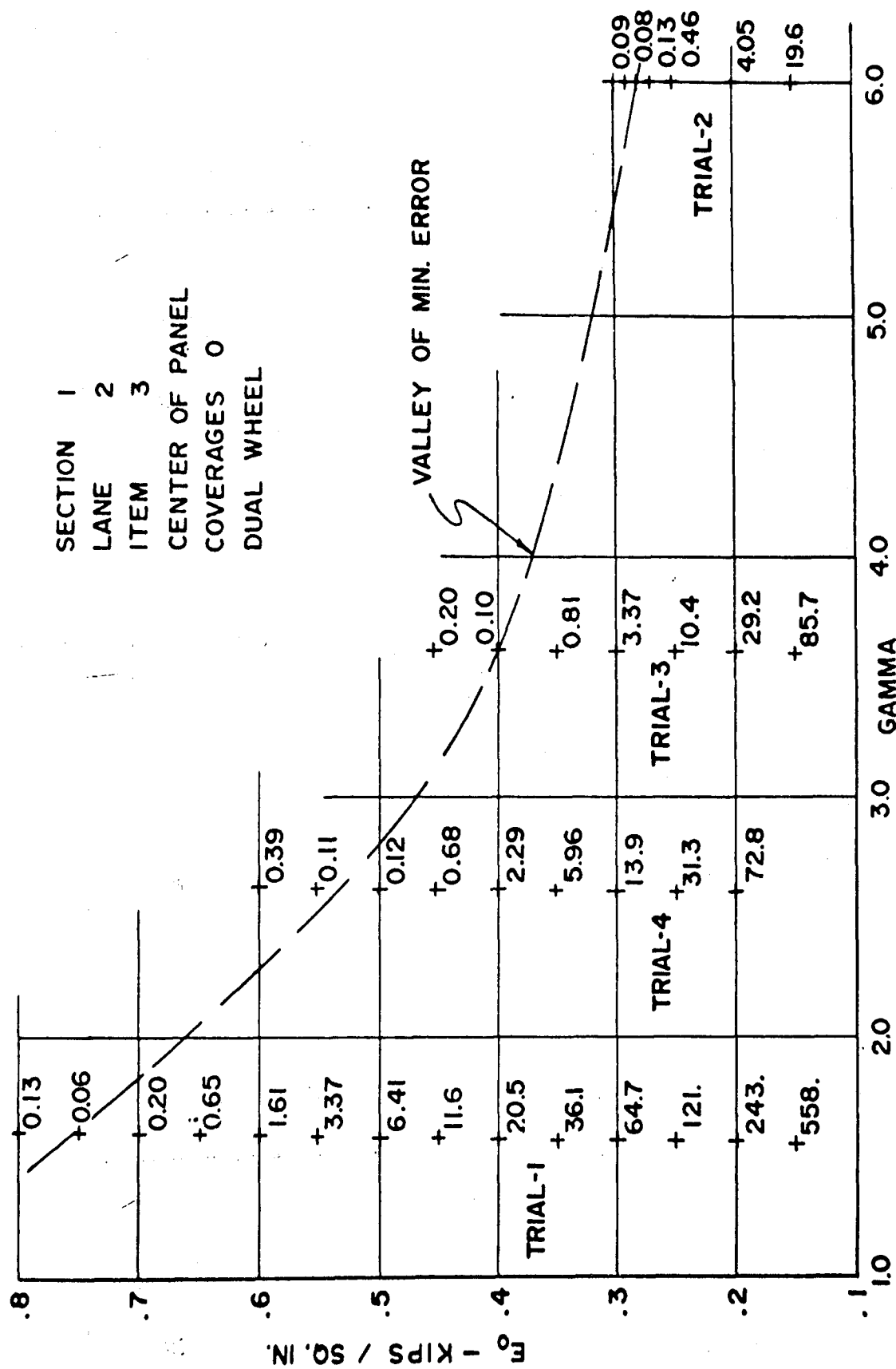
FIGURE 3.  BEHAVIOR OF ERROR FUNCTIONAL
(SECTION I, LANE 2, ITEM 3)

SECTION 9
LANE 22
ITEM 2
CENTER OF PANEL
COVERAGES 0
SINGLE WHEEL

VALLEY OF MIN. ERROR

GAMMA

$E_0$ - KIPS / SQ.IN.

.6
.5
.4
.3
.2
.1
0

1.0   2.0   3.0   4.0   5.0   6.0

1.38
0.67
477
27.9

0.59
0.66
0.96

1.32
0.66
0.72
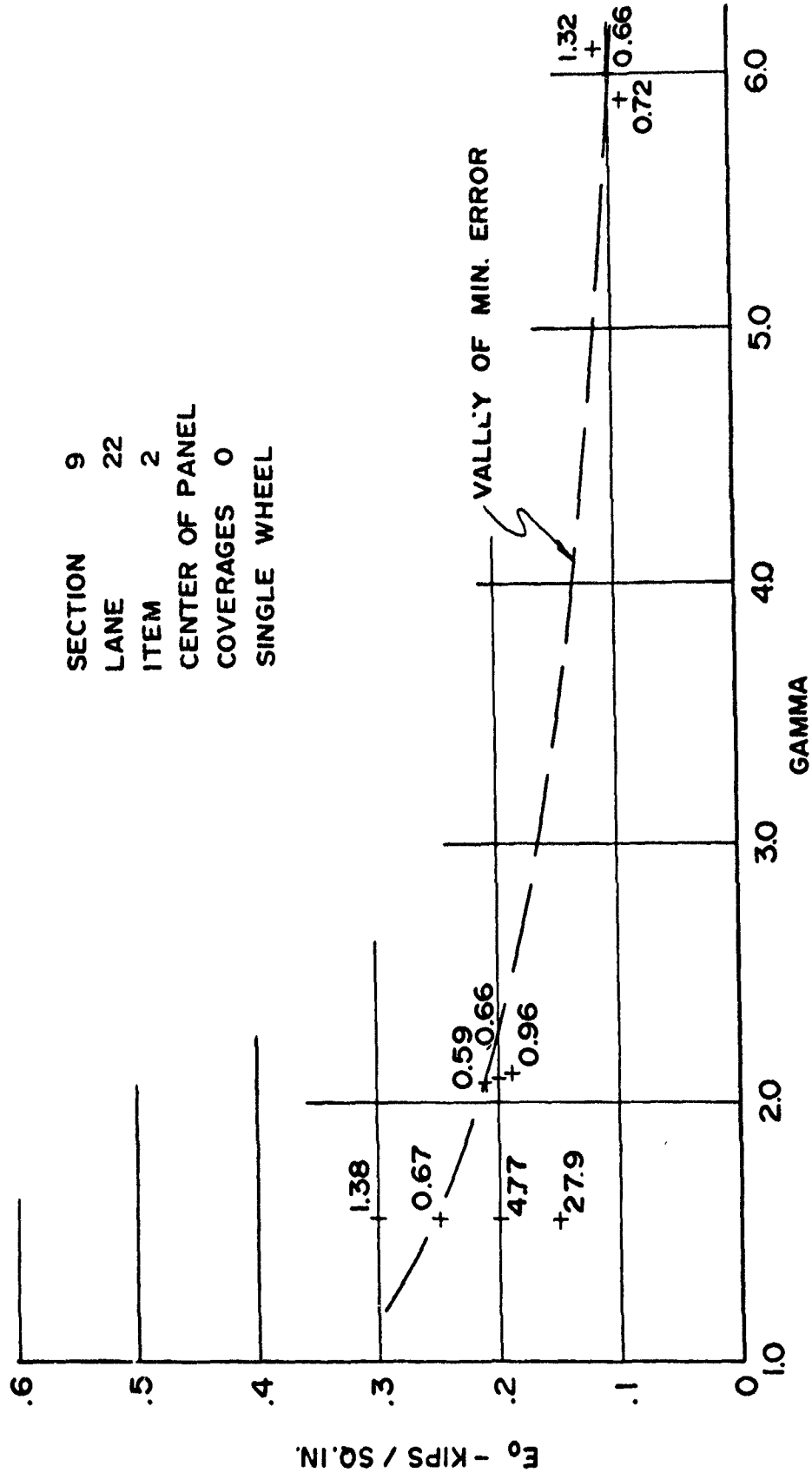
FIGURE 4.  BEHAVIOR OF ERROR FUNCTIONAL
(SECTION 9, LANE 22, ITEM 2)

# Table 2

## Values of k Along the Valley of the Error Functional

| Section 1 $E_o$ | Lane 2 $\gamma$ | Item 3 Error | Zero Coverage k |
|---|---|---|---|
| 750 psi. | 1.598 | 0.060 | 52.5 pci. |
| 530 psi. | 2.620 | 0.095 | 52.4 pci. |
| 400 psi. | 3.608 | 0.100 | 51.0 pci. |
| 280 psi. | 6.006 | 0.079 | 52.8 pci. |

Since the line of steepest descent for all trials, Figures 3 and 4, was essentially parallel to the $E_o$ axis, the identification procedure was modified somewhat. Values of 1.0, 2.5, 4.0, 5.5, 7.0, and 8.5 were assigned to the parameter $\gamma$ and for each of these values $E_o$ was incremented until the error functional was minimized. This procedure was subsequently employed for all relevant test sections and at all coverage levels.

For a few of the coverage levels, where the actual deflection pattern was relatively unsymmetrical, the magnitude of the error functional was found to be greater than 1.0. Nevertheless, the representative value of k was taken as that which existed when the error functional was a minimum for the selected values of $\gamma$.

With the parameter k defined, only one additional parameter had to be identified. As noted in Table 2, the parameter $E_o$ showed considerable variation for the range of values of $\gamma$ investigated. As the parameter $\gamma$ appeared more stable it was selected for identification.

## Identification of the Parameter $\gamma$

Due to the small variation in the error functional for the range of $\gamma$ values investigated, it was concluded that the preceding procedure was not satisfactory for identifying the parameter $\gamma$. The procedure developed for determining $\gamma$ was less direct than that used previously for the parameter k. Preliminary studies, Figure 5, indicated that the value of $\gamma$ did not influence greatly the magnitude of the deflections. However, it was noted that as $\gamma$ increased deflections

25
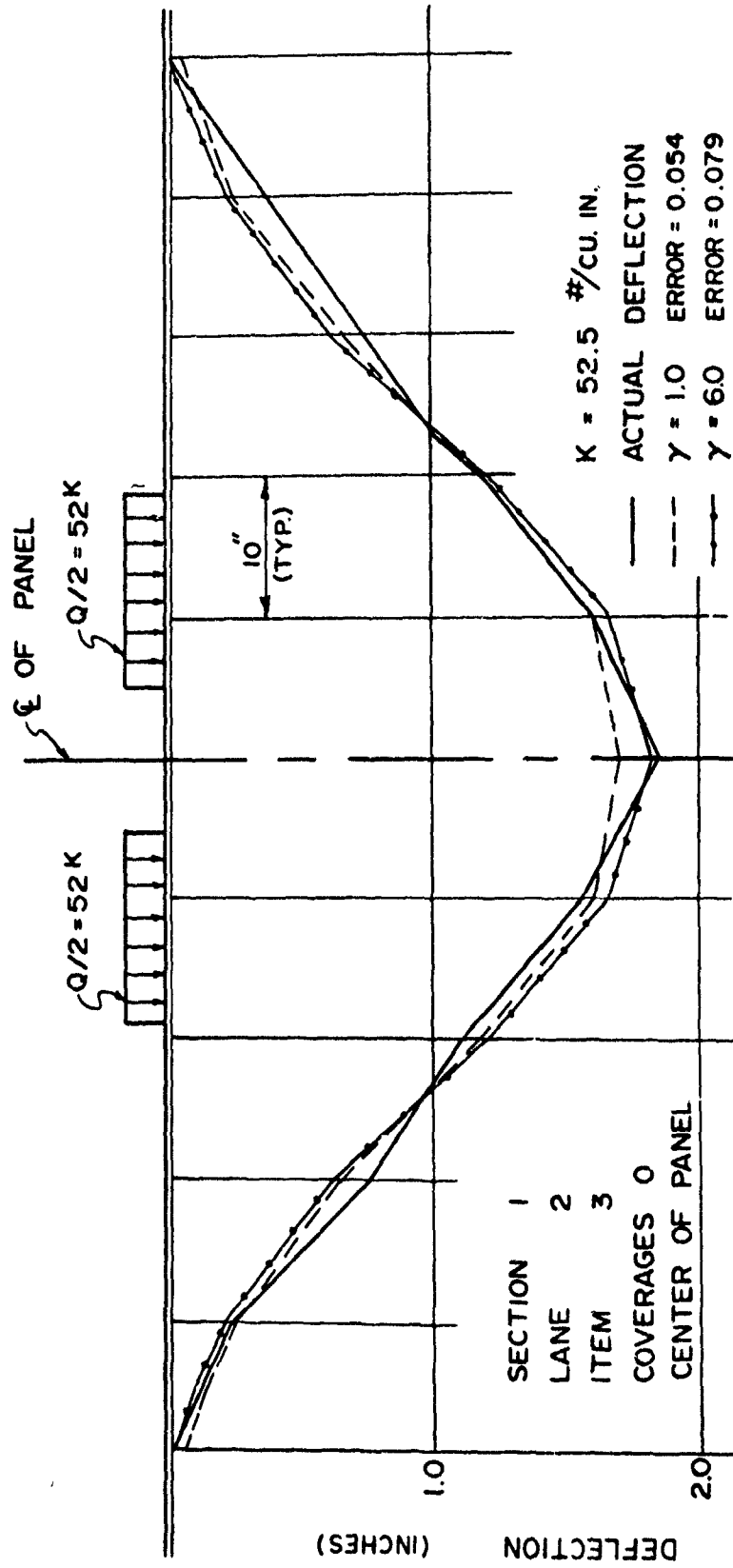
FIGURE 5. INFLUENCE OF THE PARAMETER GAMMA
ON THE DEFLECTION PATTERN

in the vicinity of the loads became larger and were dissipated more rapidly as the distance from the load increased. This indicated that the value of γ was dependent upon the rigidity of the mat; that is, the less rigid the mat, the larger the deflection under the load and the more rapid the dissipation of deflection. From comparison of deflection patterns at identical coverage levels, it was also observed that, in general, the convexity (curvature) of the deflection patterns for the M8 mat was greater than that for the T11 mat. In addition, the subgrade strength, as represented by the CBR values, was higher for the M8 mat tests than that for the T11 mat tests. It was therefore concluded that the difference in the convexity of the deflection patterns resulted primarily from the differences in mat rigidity and could be accounted for in the model by the selection of the parameter γ.

The parameter γ was established by a trial and error procedure utilizing the computed model deflections. The previously determined value of k was maintained constant for each coverage level while different values were assigned to γ. The "correct" value of γ was established by comparing the computed model deflection configuration to the prototype deflection pattern. After the parameter γ had been established slight modifications were made in the value of the parameter k to produce even better correspondence between deflection patterns. This procedure was applied to all tests to provide both γ and k values.


## Correlation of Model Parameters to Mat-Subgrade Properties

From the results of the identification procedure (to be discussed later, see Figures 6 and 7), it was found that the magnitude of k at any coverage level could be established as a function of the initial value. The functional relationship was established as

$$k_N = \frac{k_{INT}}{N^{0.0485}} \tag{13}$$

where $k_{INT}$ is the k value at zero coverage and $k_N$ is the k value after N number of coverages.

In order to determine $k_N$ and the resulting deflections at any coverage, means for obtaining a measure of $k_{INT}$ had to be established. To avoid developing a new soil test which could be both expensive and time consuming to conduct, it was decided to try correlating $k_{INT}$ with the standard soil properties, water content, dry density, CBR, obtained at the test site. Previous work by Black [5] indicated that there exists a strong correlation between soil strength, water content, and dry density. Since $k_{INT}$ is in a sense a measure of soil strength, it was thought that there might exist some correlation between $k_{INT}$, w, and $\gamma_d$. Representative values of the water content and dry density were taken as the average of the respective values given for the top 18 inches of the subgrade. Attempts to develop a relationship among these parameters proved to be fruitless.

The literature [49, 50, 68] also indicated the existence of an empirical relationship between the subgrade modulus and CBR. However, this relation was established for subgrade moduli greater than 100 pci. Extension of these relations to prototype test conditions proved unreliable. Computations did disclose a reasonable correlation among CBR, $w\gamma_d$ (weight of water per unit volume of soil) and the parameter $k$. It was found for these prototype test subgrades that $k_{INT}$ could be reliably established from the relation

$$k_{INT} = 164.0 + 3.0 \text{ CBR} - 5.45 \text{ } w\gamma_d \qquad (14)$$

where CBR is the average CBR for the upper eighteen inches of subgrade and $w\gamma_d$ is in pounds per cubic foot.

Observations of the "average deflection" patterns during the prototype tests indicate that the curvature, in general, increased with increasing number of coverages. Hence, the parameter $\gamma$ must also increase with coverages. The identification procedure demonstrated this response: the value of $\gamma$ did increase with coverages. In addition it became slightly larger with decreasing mat rigidity. The latter was found to be more pronounced for low coverage levels than for high coverage levels. At all coverage levels, the variation with mat rigidity was small. From the simulation of the "average deflection" patterns the relationship for $\gamma_N$ was established as

$$\gamma_N = \sqrt[4]{N} + \frac{(EI)_{T11} - (EI)_{MAT}}{(EI)_{MAT}} \qquad (N \geq 1) \qquad (15)$$

where N is the specific number of coverages, $(EI)_{T11}$ is the rigidity per foot of width of the T11 aluminum mat, and $(EI)_{MAT}$ is the rigidity per foot of width of the mat being investigated. The second term of Eqn. (15) has greater influence on $\gamma$ for low coverages than for high coverages.

With the parameters $k_{INT}$ and $\gamma_N$ defined, respectively, by Eqns. (14) and (15), Eqn. (12a) may be solved for $E_o$ and the characteristic t may be found from Eqn. (12b). Having obtained the characteristics k and t, the mat-soil model may be used to estimate the expected deflections for the mat at different coverage levels.

## Results

### Layer Thickness Investigation

Data from six different test sections [12] were used for this investigation. Identical conditions of wheel load, wheel spacing, width of tire print, and mat rigidity as used in the prototype tests were imposed upon the mat-soil model. The subgrade thickness was varied from 12 in. to an infinite depth. For each layer thickness the simulation of the "average deflection" pattern was achieved by minimizing the error functional, Eqn. (D2). The modified steep descent method was used with the value of 2.50 assigned to the parameter $\gamma$. Values of the error functional and the model characteristic k for the extreme layer thicknesses are given in Table 3.

### Correlation of Model Parameters to Mat-Subgrade Properties

The identification procedure was applied to all test sections. Values of the parameters $\gamma$, $E_o$, k, and the error functional for a few typical test sections are given in Table 4. For the remaining sections, the k values producing the minimum error functional for the selected values of $\gamma$ are given in Table 5.

Plotting the magnitude of k against the number of coverages, Figures 6 and 7, it can be observed that with only rare exception the magnitude of k decreases with coverage

## Table 3

### Comparison of Simulation Error for

### Different Soil Layer Thicknesses

| Sect | Lane | Item | Coverages | H = 12 inches | | H = infinity | |
|------|------|------|-----------|-------|--------|-------|--------|
| | | | | Error | k-pci. | Error | k-pci. |
| 1 | 1 | 3 | 0 | .164 | 51. | .167 | 51. |
| | | | 20 | .182 | 39. | .186 | 39. |
| | | | 200 | .278 | 40. | .281 | 39. |
| | | | 300 | .435 | 45. | .439 | 45. |
| 1 | 2 | 3 | 0 | .072 | 55. | .068 | 54. |
| | | | 20 | .064 | 45. | .062 | 45. |
| | | | 40 | .284 | 41. | .278 | 41. |
| | | | 68 | .286 | 40. | .279 | 40. |
| 3 | 5 | 1 | 0 | .105 | 17. | .122 | 17. |
| | | | 30 | 1.982 | 21. | .758 | 15. |
| 3 | 5 | 2 | 0 | .176 | 23. | .214 | 24. |
| | | | 30 | .347 | 19. | .349 | 19. |
| 6 | 11 | 1 | 0 | .040 | 36. | .040 | 37. |
| | | | 600 | .069 | 28. | .070 | 28. |
| 6 | 11 | 2 | 0 | .020 | 53. | .020 | 53. |
| | | | 600 | .017 | 47. | .017 | 47. |

## Table 4

## Comparison of the Variability of the Characteristic k

| Section 1 | Lane 1 | Item 3 |

### Coverage zero / Coverage 20

| Y | $E_o$-psi. | k-pci. | Error | $E_o$-psi. | k-pci. | Error |
|---|---|---|---|---|---|---|
| 1.0 | 1030. | 50. | 0.218 | 830. | 37. | 0.229 |
| 2.5 | 530. | 51. | 0.167 | 430. | 39. | 0.186 |
| 4.0 | 380. | 53. | 0.161 | 310. | 40. | 0.193 |
| 5.5 | 300. | 53. | 0.157 | 260. | 44. | 0.368 |
| 7.0 | 260. | 56. | 0.181 | 210. | 42. | 0.214 |
| 8.5 | 220. | 54. | 0.156 | 180. | 41. | 0.184 |

### Coverage 200 / Coverage 300

| Y | $E_o$-psi. | k-pci. | Error | $E_o$-psi. | k-pci. | Error |
|---|---|---|---|---|---|---|
| 1.0 | 840. | 38. | 0.334 | 940. | 44. | 0.513 |
| 2.5 | 430. | 39. | 0.281 | 480. | 45. | 0.439 |
| 4.0 | 310. | 40. | 0.271 | 340. | 46. | 0.429 |
| 5.5 | 260. | 43. | 0.404 | 270. | 46. | 0.425 |
| 7.0 | 210. | 42. | 0.278 | 230. | 47. | 0.421 |
| 8.5 | 180. | 41. | 0.265 | 210. | 51. | 0.512 |

| Section 1 | Lane 2 | Item 3 |

### Coverage zero / Coverage 20

| Y | $E_o$-psi. | k-pci. | Error | $E_o$-psi. | k-pci. | Error |
|---|---|---|---|---|---|---|
| 1.0 | 1070. | 52. | 0.052 | 930. | 44. | 0.057 |
| 2.5 | 550. | 54. | 0.068 | 480. | 45. | 0.061 |
| 4.0 | 390. | 55. | 0.075 | 340. | 46. | 0.067 |
| 5.5 | 310. | 55. | 0.077 | 270. | 46. | 0.070 |
| 7.0 | 260. | 56. | 0.079 | 230. | 47. | 0.072 |
| 8.5 | 230. | 57. | 0.079 | 210. | 51. | 0.167 |

Table 4 (Cont'd.)

| Section 1 | | Lane 2 | | Item 3 | |
|---|---|---|---|---|---|

Coverage 40 — Coverage 68

| $\gamma$ | $E_o$-psi | k-pci. | Error | $E_o$-psi. | k-pci. | Error |
|---|---|---|---|---|---|---|
| 1.0 | 870. | 40. | 0.262 | 850. | 39. | 0.242 |
| 2.5 | 450. | 41. | 0.278 | 440. | 40. | 0.279 |
| 4.0 | 320. | 42. | 0.286 | 310. | 40. | 0.294 |
| 5.5 | 260. | 44. | 0.297 | 260. | 44. | 0.369 |
| 7.0 | 220. | 45. | 0.305 | 210. | 42. | 0.299 |
| 8.5 | 210. | 51. | 0.682 | 210. | 51. | 0.971 |

| Section 3 | | Lane 5 | | Item 1 | |
|---|---|---|---|---|---|

Coverage zero — Coverage 30

| $\gamma$ | $E_o$-psi. | k-pci. | Error | $E_o$-psi. | k-pci. | Error |
|---|---|---|---|---|---|---|
| 1.0 | 430. | 16. | 0.116 | 380. | 13. | 0.433 |
| 2.5 | 230. | 17. | 0.122 | 210. | 15. | 0.758 |
| 4.0 | 160. | 17. | 0.135 | 200. | 22. | 1.693 |
| 5.5 | 200. | 31. | 3.189 | 120. | 16. | 0.672 |
| 7.0 | 110. | 18. | 0.107 | 150. | 27. | 1.950 |
| 8.5 | 150. | 32. | 1.453 | 150. | 32. | 6.370 |

| Section 3 | | Lane 5 | | Item 2 | |
|---|---|---|---|---|---|

Coverage zero — Coverage 30

| $\gamma$ | $E_o$-psi. | k-pci. | Error | $E_o$-psi. | k-pci. | Error |
|---|---|---|---|---|---|---|
| 1.0 | 480. | 22. | 0.222 | 410. | 18. | 0.390 |
| 2.5 | 260. | 24. | 0.214 | 220. | 19. | 0.349 |
| 4.0 | 180. | 24. | 0.174 | 160. | 20. | 0.379 |
| 5.5 | 160. | 27. | 0.601 | 150. | 25. | 2.065 |
| 7.0 | 120. | 24. | 0.196 | 110. | 21. | 0.433 |
| 8.5 | 110. | 26. | 0.194 | 150. | 39. | 2.374 |

| Section 6 | | Lane 11 | | Item 1 | |
|---|---|---|---|---|---|

Coverage zero — Coverage 600

| $\gamma$ | $E_o$-psi. | k-pci. | Error | $E_o$-psi. | k-pci. | Error |
|---|---|---|---|---|---|---|
| 1.0 | 770. | 34. | 0.038 | 640. | 26. | 0.077 |
| 2.5 | 410. | 37. | 0.040 | 340. | 28. | 0.070 |
| 4.0 | 290. | 37. | 0.041 | 240. | 29. | 0.069 |
| 5.5 | 230. | 37. | 0.041 | 190. | 29. | 0.069 |
| 7.0 | 190. | 37. | 0.043 | 160. | 29. | 0.069 |
| 8.5 | 170. | 38. | 0.041 | 140. | 30. | 0.069 |

## Table 5

### k Values for Minimum Simulation Error

| Sect | Lane | Item | Coverage | k-pci. | Error |
|------|------|------|----------|--------|-------|
| 2 | 3 | 1 | 0 | 38.4 | 0.102 |
|   |   |   | 200 | 28.8 | 0.023 |
|   |   |   | 600 | 28.7 | 0.040 |
| 2 | 3 | 2 | 0 | 42.6 | 0.172 |
|   |   |   | 66 | 32.2 | 0.872 |
|   |   |   | 120 | 57.4 | 0.086 |
|   |   |   | 200 | 30.3 | 0.144 |
| 2 | 4 | 1 | 0 | 19.9 | 0.177 |
|   |   |   | 20 | 16.5 | 0.373 |
| 2 | 4 | 2 | 0 | 33.0 | 0.130 |
|   |   |   | 20 | 32.2 | 2.836* |
| 3 | 6 | 1 | 0 | 12.3 | 0.174 |
|   |   |   | 20 | 10.5 | 0.211 |
|   |   |   | 76 | 15.0 | 0.661 |
|   |   |   | 156 | 13.9 | 0.298 |
| 3 | 6 | 2 | 0 | 21.8 | 0.308 |
|   |   |   | 20 | 15.9 | 0.841 |
|   |   |   | 76 | 18.4 | 5.818* |
| 6 | 11 | 2 | 0 | 50.2 | 0.014 |
|   |   |   | 600 | 48.5 | 0.016 |
| 6 | 11A | 1 | 0 | 32.1 | 0.137 |
|   |   |   | 20 | 27.0 | 0.259 |
|   |   |   | 130 | 28.4 | 0.168 |
| 6 | 11A | 2 | 0 | 48.8 | 0.425 |
|   |   |   | 20 | 38.0 | 0.623 |
|   |   |   | 130 | 32.6 | 1.951* |
| 6 | 12 | 1 | 0 | 21.6 | 3.689* |
|   |   |   | 20 | 18.5 | 0.646 |
|   |   |   | 90 | 21.6 | 0.203 |
| 6 | 12 | 2 | 0 | 60.0 | 0.152 |
|   |   |   | 20 | 34.1 | 0.253 |
|   |   |   | 44 | 34.3 | 0.669 |

33

Table 5 (Cont'd.)

| Sect | Lane | Item | Coverage | k-pci. | Error |
|------|------|------|----------|--------|-------|
| 9 | 21 | 1 | 0 | 18.9 | 0.070 |
|   |    |   | 20 | 15.6 | 0.159 |
|   |    |   | 200 | 12.6 | 0.131 |
|   |    |   | 300 | 11.3 | 0.541 |
|   |    |   | 600 | 10.4 | 0.868 |
| 9 | 21 | 2 | 0 | 29.1 | 0.053 |
|   |    |   | 20 | 26.7 | 0.041 |
|   |    |   | 200 | 25.9 | 0.500 |
|   |    |   | 300 | 21.8 | 0.126 |
| 9 | 22 | 1 | 0 | 13.9 | 0.511 |
|   |    |   | 20 | 15.3 | 1.266* |
|   |    |   | 400 | 9.6 | 7.937* |
| 9 | 22 | 2 | 0 | 16.8 | 0.573 |
|   |    |   | 20 | 16.8 | 0.425 |
|   |    |   | 100 | 16.8 | 0.927 |
| 10 | 23A | 1 | 0 | 42.9 | 0.222 |
|   |    |   | 32 | 32.9 | 0.160 |
| 10 | 23A | 2 | 2 | 32.2 | 3.825* |
| 10 | 23B | 1 | 4 | 32.1 | 0.586 |
| 13 | 28 | 1 | 0 | 14.0 | 0.687 |
|   |    |   | 200 | 8.9 | 0.992 |
|   |    |   | 550 | 5.6 | 2.890* |
| 13 | 28 | 2 | 0 | 25.3 | 0.145 |
|   |    |   | 200 | 21.1 | 0.336 |
|   |    |   | 550 | 20.5 | 0.579 |
| 13 | 29 | 1 | 0 | 22.7 | 0.395 |
|   |    |   | 42 | 7.8 | 2.204* |
|   |    |   | 140 | 5.6 | 7.704* |
| 13 | 29 | 2 | 0 | 26.1 | 0.384 |
|   |    |   | 42 | 19.9 | 0.542 |
|   |    |   | 140 | 19.9 | 0.432 |
|   |    |   | 200 | 19.9 | 1.714* |

* Indicates that the deflection pattern as given [12] is significantly unsymmetrical.

34
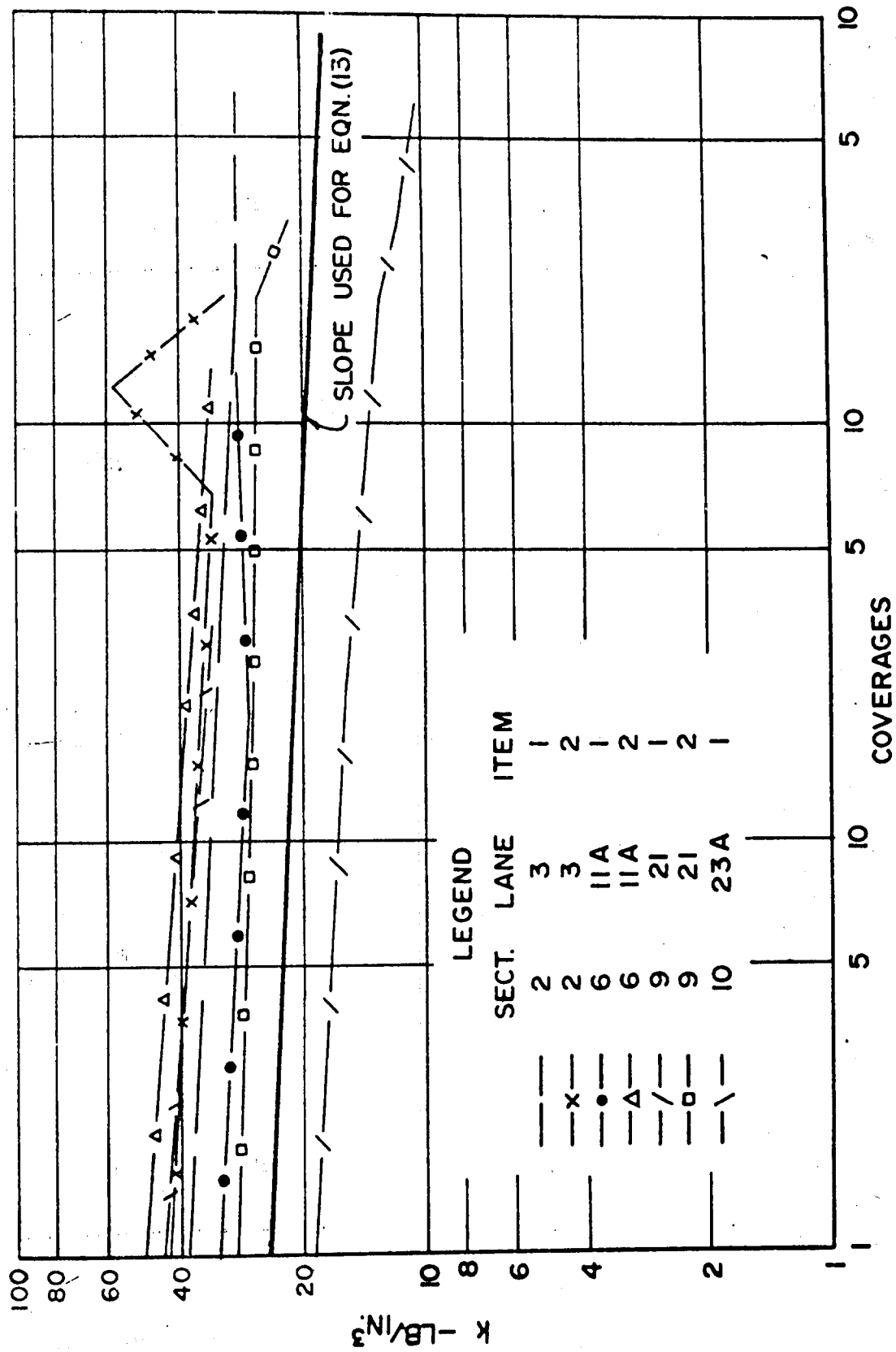
FIGURE 6. VARIATION OF PARAMETER k WITH COVERAGE FOR SINGLE–WHEEL TESTS.
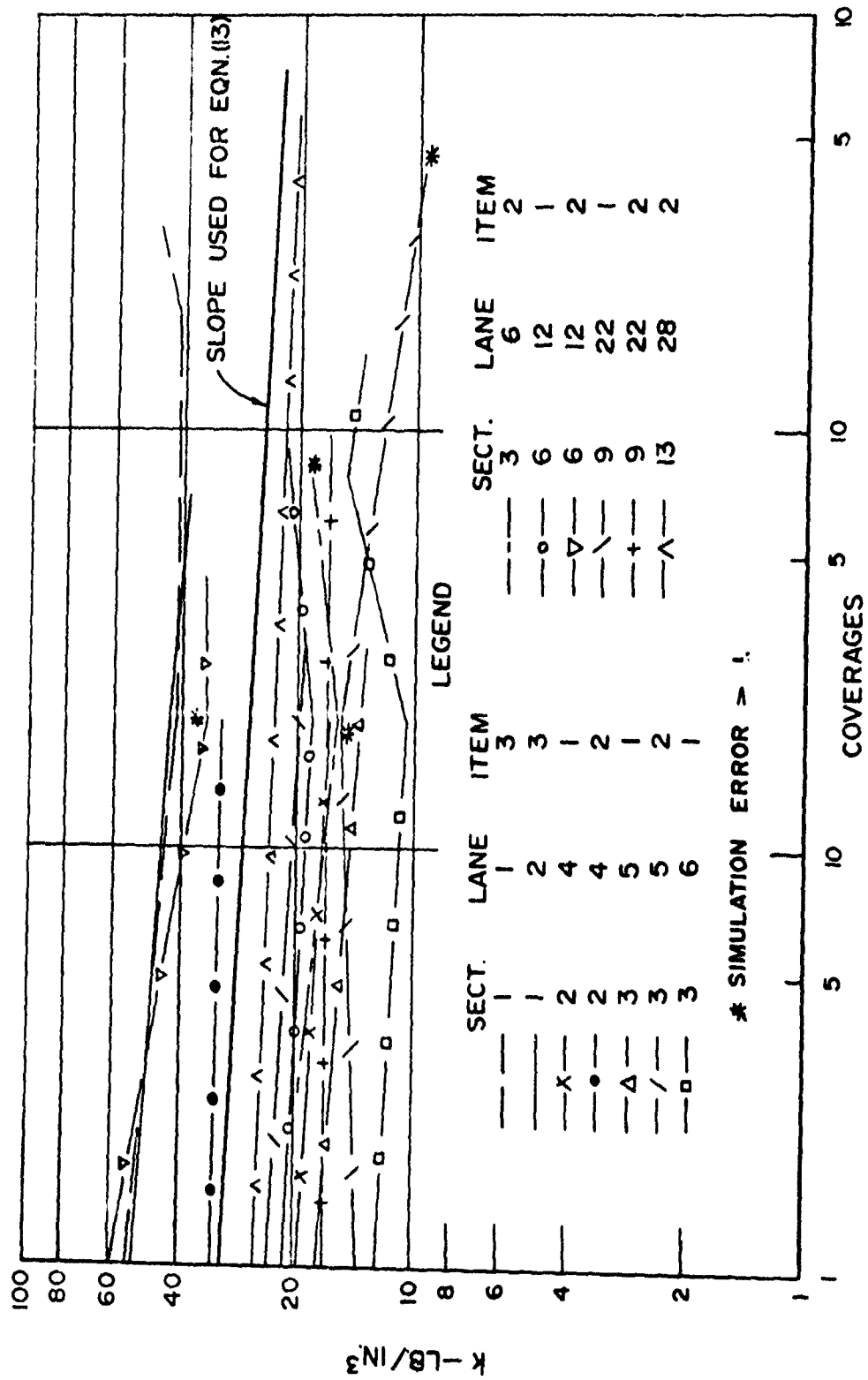
FIGURE 7. VARIATION OF PARAMETER k WITH COVERAGE FOR DUAL-WHEEL TESTS.

for both the single-wheel and dual-wheel tests. In these
illustrations to accommodate the log scale, the value ob-
tained by simulating the "average deflection" pattern for
zero coverages has been plotted as occurring at one coverage.
Also shown, is the slope used for establishing the functional
relationship for $k_{INT}$, Eqn. (13). For clarity of presentation,
results for seven available sections were omitted from these
figures. As can be observed from Table 5, they exhibited
similar behavior to those shown plotted.

Deflection patterns were calculated incorporating the
refined values of $k_{INT}$ and Eqns. (13) and (15). Some typical
deflection patterns are presented in Table 6 along with the
actual deflection patterns. The distances given in this
table are referenced from a point ten feet left of the cen-
terline of the traffic lane.

Table 7 provides a comparison of the initial subgrade
modulus as given by Eqn. (14) with simulated values. It is
noted that the largest discrepancies occur for those sections
where the simulated values are generally high. In Figure 8,
it is observed that small variations in the subgrade strength,
as reflected by the subgrade modulus, have appreciable influ-
ence on the deflection characteristics of the load transfer
element. Consequently, Eqn. (14) was developed with a bias
directed toward the better reproduction of low values of
$k_{INT}$.

## Summary and Discussion of Model

As indicated by the results presented in Table 3, any
choice of layer thickness greater than twelve inches appears
to have negligible effect upon the simulation of the "average
deflection" patterns. Similar behavior was also observed by
Lenczer [36] in his study of the influence of layer thickness.
The assumption of an infinite depth for the subgrade was both
expeditious and justifiable.

Indications were that a Poisson's ratio of 0.4 for the
subgrade material was reasonable; selection of this value
was based upon the work of Pickett [43, 44] and the results
of the preliminary study, Table 1.

# Table 6

## Comparison of Deflection Patterns

### Section 1     Lane 1     Item 3

$k_{INT} = 50.5$pci.    $\gamma_{INT} = 1.00$

**Zero Coverages - Error = 0.059**      **20 Coverages - Error = 0.059**

| Distance (in) | Actual Deflection (in) | Estimated Deflection (in) | Distance (in) | Actual Deflection (in) | Estimated Deflection (in) |
|---|---|---|---|---|---|
| 47. | 0.00 | 0.07 | 44. | 0.00 | 0.01 |
| 51. | 0.10 | 0.14 | 51. | 0.20 | 0.14 |
| 56. | 0.22 | 0.26 | 56. | 0.35 | 0.29 |
| 66. | 0.75 | 0.66 | 66. | 0.80 | 0.78 |
| 76. | 1.10 | 1.22 | 69. | 1.00 | 0.96 |
| 86. | 1.55 | 1.65 | 76. | 1.40 | 1.43 |
| 96. | 1.79 | 1.75 | 86. | 1.85 | 1.94 |
| 106. | 1.59 | 1.65 | 96. | 2.20 | 2.08 |
| 116. | 1.18 | 1.22 | 106. | 1.90 | 1.94 |
| 119. | 1.00 | 1.05 | 116. | 1.30 | 1.43 |
| 126. | 0.75 | 0.66 | 123. | 1.00 | 0.96 |
| 136. | 0.31 | 0.26 | 126. | 0.85 | 0.78 |
| 146. | 0.00 | 0.05 | 136. | 0.31 | 0.29 |
|  |  |  | 148. | 0.00 | 0.01 |

**40 Coverages - Error = 0.313**      **68 Coverages - Error = 0.348**

| Distance (in) | Actual Deflection (in) | Estimated Deflection (in) | Distance (in) | Actual Deflection (in) | Estimated Deflection (in) |
|---|---|---|---|---|---|
| 41. | 0.00 | -0.03 | 49. | 0.00 | 0.10 |
| 51. | 0.31 | 0.15 | 56. | 0.48 | 0.32 |
| 56. | 0.38 | 0.31 | 66. | 1.10 | 0.83 |
| 67. | 1.00 | 0.87 | 76. | 1.40 | 1.52 |
| 76. | 1.50 | 1.48 | 87. | 2.00 | 2.09 |
| 84. | 2.00 | 1.93 | 96. | 2.50 | 2.20 |
| 96. | 2.50 | 2.15 | 109. | 2.00 | 1.94 |
| 106. | 2.00 | 2.01 | 116. | 1.48 | 1.52 |
| 116. | 1.20 | 1.48 | 121. | 1.38 | 1.17 |
| 126. | 0.92 | 0.81 | 126. | 0.90 | 0.83 |
| 131. | 0.50 | 0.53 | 136. | 0.50 | 0.32 |
| 141. | 0.35 | 0.15 | 141. | 0.35 | 0.15 |
| 151. | 0.00 | -0.03 | 151. | 0.00 | -0.03 |

## Table 6 (Cont'd.)

### Section 3    Lane 5    Item 2

$$k_{INT} = 21.0 \text{ pci.} \quad \gamma_{INT} = 1.75$$

Zero Coverages - Error = 0.621          30 Coverages - Error = 0.619

| Distance (in) | Actual Deflection (in) | Estimated Deflection (in) | Distance (in) | Actual Deflection (in) | Estimated Deflection (in) |
|---|---|---|---|---|---|
| 99. | 0.00 | 0.47 | 96. | 0.00 | 0.42 |
| 104. | 0.50 | 0.73 | 104. | 0.79 | 0.88 |
| 109. | 1.00 | 1.04 | 114. | 1.72 | 1.64 |
| 119. | 1.71 | 1.73 | 119. | 2.00 | 2.03 |
| 124. | 2.16 | 2.01 | 124. | 2.66 | 2.35 |
| 134. | 2.10 | 2.20 | 135. | 2.80 | 2.60 |
| 144. | 1.99 | 2.17 | 144. | 2.60 | 2.58 |
| 154. | 2.11 | 2.00 | 154. | 2.60 | 2.60 |
| 166. | 2.00 | 1.91 | 164. | 2.35 | 2.35 |
| 174. | 1.37 | 1.39 | 169. | 1.67 | 2.03 |
| 183. | 0.50 | 0.79 | 174. | 1.60 | 1.64 |
| 190. | 0.00 | 0.42 | 184. | 0.68 | 0.88 |
|  |  |  | 194. | 0.00 | 0.34 |

### Section 13    Lane 28    Item 2

$$k_{INT} = 25.0 \text{ pci.} \quad \gamma_{INT} = 1.75$$

Zero Coverages - Error = 0.157    550 Coverages - Error = 0.788

| Distance (in) | Actual Deflection (in) | Estimated Deflection (in) | Distance (in) | Actual Deflection (in) | Estimated Deflection (in) |
|---|---|---|---|---|---|
| 32. | -0.16 | 0.05 | 32. | -0.16 | 0.09 |
| 36. | 0.00 | 0.10 | 42. | 0.15 | 0.32 |
| 42. | 0.13 | 0.22 | 52. | 0.52 | 0.70 |
| 62. | 1.00 | 0.86 | 57. | 1.00 | 0.92 |
| 72. | 1.00 | 1.06 | 72. | 1.35 | 1.38 |
| 82. | 1.00 | 0.93 | 82. | 1.30 | 1.24 |
| 92. | 0.73 | 0.64 | 94. | 1.00 | 0.88 |
| 102. | 0.51 | 0.52 | 102. | 0.82 | 0.79 |
| 112. | 0.68 | 0.65 | 114. | 1.00 | 0.98 |
| 122. | 1.00 | 0.92 | 122. | 1.00 | 1.23 |
| 132. | 1.02 | 1.06 | 132. | 0.83 | 1.38 |
| 142. | 1.00 | 0.86 | 142. | 0.81 | 1.14 |
| 152. | 0.40 | 0.51 | 152. | 0.30 | 0.70 |
| 162. | 0.12 | 0.22 | 170. | 0.00 | 0.12 |
| 167. | 0.00 | 0.12 |  |  |  |

39

Table 7

Comparison of Simulated to Calculated Values of $k_{INT}$

| | Test | | k pci. | |
| Sect | Lane | Item | Simulated | Calculated |
|------|------|------|-----------|------------|
| 1 | 1 | 3 | 48.5 | 59.3 |
| 1 | 2 | 3 | 50.5 | 66.1 |
| 2 | 3 | 1 | 35.5 | 18.5 |
| 2 | 3 | 2 | 41.0 | 35.1 |
| 2 | 4 | 1 | 19.0 | 15.9 |
| 2 | 4 | 2 | 31.5 | 38.3 |
| 3 | 5 | 1 | 16.0 | 17.0 |
| 3 | 5 | 2 | 21.0 | 32.7 |
| 3 | 6 | 1 | 12.5 | 20.4 |
| 3 | 6 | 2 | 18.0 | 29.2 |
| 6 | 11 | 1 | 34.0 | 20.6 |
| 6 | 11 | 2 | 50.5 | 41.8 |
| 6 | 12 | 1 | 22.0 | 29.4 |
| 6 | 12 | 2 | 36.0 | 36.7 |
| 9 | 21 | 1 | 14.0 | 11.9 |
| 9 | 21 | 2 | 25.5 | 20.2 |
| 9 | 22 | 1 | 10.0 | 11.2 |
| 9 | 22 | 2 | 16.0 | 13.5 |
| 10 | 23A | 1 | 37.5 | 27.1 |
| 10 | 23A | 2 | 27.5 | 31.7 |
| 10 | 23B | 1 | 32.5 | 27.1 |
| 13 | 28 | 1 | 11.0 | 11.6 |
| 13 | 28 | 2 | 25.0 | 25.3 |
| 13 | 29 | 1 | 18.0 | 11.7 |
| 13 | 29 | 2 | 28.0 | 24.2 |
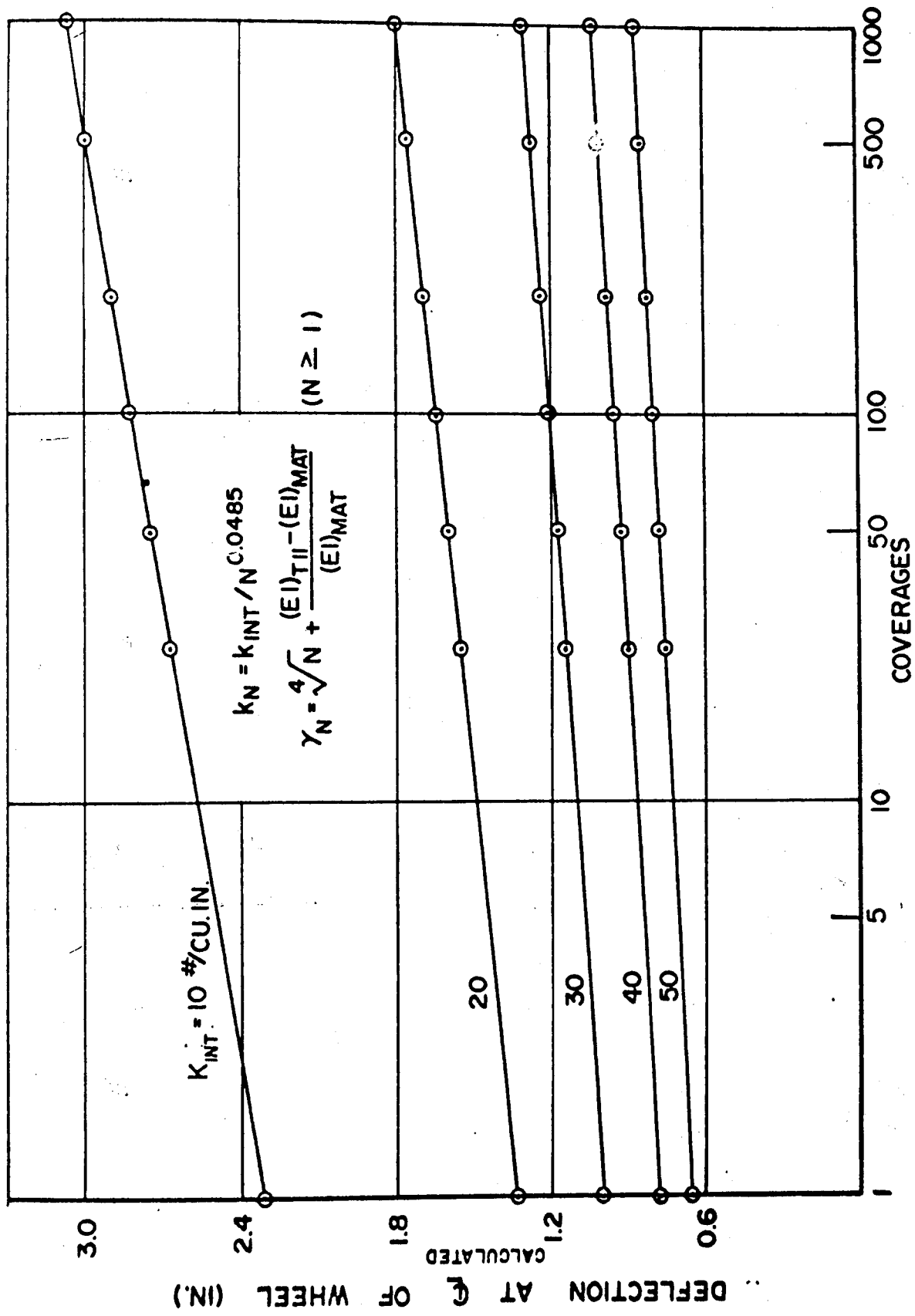
FIGURE 8. INFLUENCE OF $k_{INT}$ ON MAXIMUM DEFLECTION

It is believed that failure of the state variable filter and its modifications to identify the model characteristics $k$ and $t$ was due to the intrinsic representation of the applied loads as step functions. Similar difficulties with step loads had been noted earlier by Kohr [30].

The model characteristics $k$ and $t$, Eqns. (12a) and (12b), are functions of $\gamma$ in addition to the conventional $E_o$ and $\mu$ parameters. The "steep descent" method, in which the deflection difference between the model and the prototype for at least nine discrete points was minimized, also failed to produce unique values of the parameters $E_o$ and $\gamma$, Figures 3 and 4. However, the error functional Eqn. (D2), was found to possess a valley of minimums along which the value of the characteristic $k$ was essentially constant.

The simulation of the "average deflection" patterns, Table 4, indicated that the value of the model parameter $k$ increased slightly with increases in $\gamma$. For a specific value of $\gamma$ (as shown in Table 4) the magnitude of $k$ was found to decrease with the number of coverages. Computations indicated that the magnitude of $k$ was more sensitive to the number of coverages than to the value of the parameter $\gamma$. The evident validity of the developed expression for $k_N$, Eqn. (13) is amply demonstrated in Tables 4 and 5 and Figures 6 and 7.

As noted in Figure 5, variations in the parameter $\gamma$ were reflected primarily as alterations of the deflection pattern curvature. This type of response could not be identified by the selected form of the error functional, Eqn. (D2). The representative value of $\gamma$ was established from the similarity of model deflection curvature for various values of $\gamma$ with prototype deflection curvature. From this comparison it was noted that the curvature, thus $\gamma$, increased with coverages and decreased with increasing mat rigidity. This behavior is expressed by Eqn. (15).

After the parameter $\gamma$ was established (by the above procedure), slight modifications were made in the magnitude of $k$ to provide even better correspondence between the deflection patterns. The simulated values of the characteristic $k$ at zero coverages, Table 7, were found to be less than 51 pci. In this range, the model deflections were found to be quite sensitive to the magnitude of $k_{INT}$. For an incremental change in $k_{INT}$, the difference in deflection characteristics was found to increase as $k_{INT}$ decreased, Figure 8.

42

An empirical relationship, Eqn. (14), was established to relate $k_{INT}$ to the given soil properties of CBR, w, and $\gamma$. Due to the above described model sensitivity, this relationship was developed with a bias toward the smaller values of $k_{INT}$.

In all cases where the "average deflection" patterns were fairly symmetrical, the developed mat-soil model was able to duplicate the mat behavior under static loads with a reasonably low degree of error. The degree of reliability of the simulation of prototype behavior, as reflected by the magnitude of the error functional, can be inferred from Table 6. The magnitude of the error reflects the number of points used for simulation. For example, assuming that the total error is uniformly distributed among all points, errors of 0.5625 and 0.6250 are equivalent to a quarter inch difference at each point on deflection patterns represented by nine and ten points, respectively. It is further noted that only a few deflection patterns were described by the minimum of nine points. The results, Table 5 and particularly Table 6, demonstrate the general reliability of the chosen model and the latter table confirms Eqns. (13) and (15).

For those coverage levels where the resulting error was greater than unity, the prototype deflection pattern was grossly non-symmetrical [12]. Behavior of this type could not be simulated with the chosen mat-soil model because imposed conditions assumed: 1) that the applied load was symmetrical and 2) that the subgrade was homogeneous.

43

# DEVELOPMENT OF FAILURE CRITERION

## Introduction

A failure criterion had to be established to use the developed mat-soil model as a means of predicting mat performance. The search for a failure criterion which would relate well to performance produced many blind alleys. Finally, success was had through an educated "trial and error" procedure. The full chronicle of procedures and methods examined will be given below in the hopes that their display will prove valuable to others on similar expeditions.

Initially, the failure criterion employed was the roughness criterion established by the Corps of Engineers [12]. The basis of this failure criterion was a deviation in the mat surface of 3 inches or more within a 10 feet length in any direction within the traffic lane. Measurements were always made on the unloaded mat and the configuration of the mat surface at intermediate coverage levels and at failure were recorded as "average cross-sectional deformations" [12]. These configurations are referred to as "deformation" patterns in the present study and they represent the residual or irrecoverable displacements of the mat.

The established roughness criterion depended in some complicated way upon the residual deformation of the subgrade and the permanent set that occurred in the mat element. As the selected mat-soil model was capable of estimating deflections only when loads were applied, a fictitious load was assumed to act on the mat. The distribution of this load was taken to be similar to the distribution of the traffic imposed during each test. The magnitude of this fictitious load was selected to be that necessary to simulate the maximum deformation. Investigation of the model deflection curvature revealed that the roughness criterion could not be satisfied at the failure coverage; thus this approach was deemed not successful and another procedure was sought.

A dimensional model was selected as the second means of establishing a failure criterion for the mat or of indicating the dominate factors. Attempts to develop a functional relationship between the failure coverage and the test parameters indicated that the developed functional relationship was not a reliable measure of performance.

Next, the mat-soil model deflection at the indicated failure coverage was expressed as a product function of the failure coverage and test parameters. A stepwise regression analysis of the data in this form was undertaken. The data were divided into two categories: single-wheel tests and dual-wheel tests. Unfortunately, for both categories, the regression analysis indicated that the number of coverages to failure was an insignificant factor.

In light of the above study, various parametric combinations were analyzed in an effort to obtain an ordering which would be more dependent upon the number of coverages to failure, $N_f$. By adjusting the exponents occurring in the product function, a combination was found for the dual-wheel tests which proved reasonably reliable as a failure criterion. Success for the single-wheel tests was limited.

## Residual Load Concept

Comparison of the observed "deformation" patterns with the observed "average deflection" patterns revealed that, although the magnitude of displacements in both patterns were relatively the same, the curvature was much less pronounced in the "deformation" pattern. The primary difference between the "deformation" pattern and the "average deflection" pattern was assumed to be attributed solely to the manner of loading. On this basis the model parameters obtained from simulation of the "average deflection" pattern were equally applicable for the simulation of the "deformation" patterns.

Two types of traffic distribution, uniform and nonuniform, were used during the prototype tests. For the tests with uniform distribution, the fictitious load on the model was applied uniformly over the traffic lane. For the nonuniform traffic distribution, the distribution of the fictitious load, $q_f$, was taken as shown in Figure 9.

45

VARIES | VARIES | VARIES | VARIES | VARIES

100

80                                              80

PERCENT OF $q_f$

20                                              20

TRAFFIC LANE WIDTH
VARIES WITH TESTS
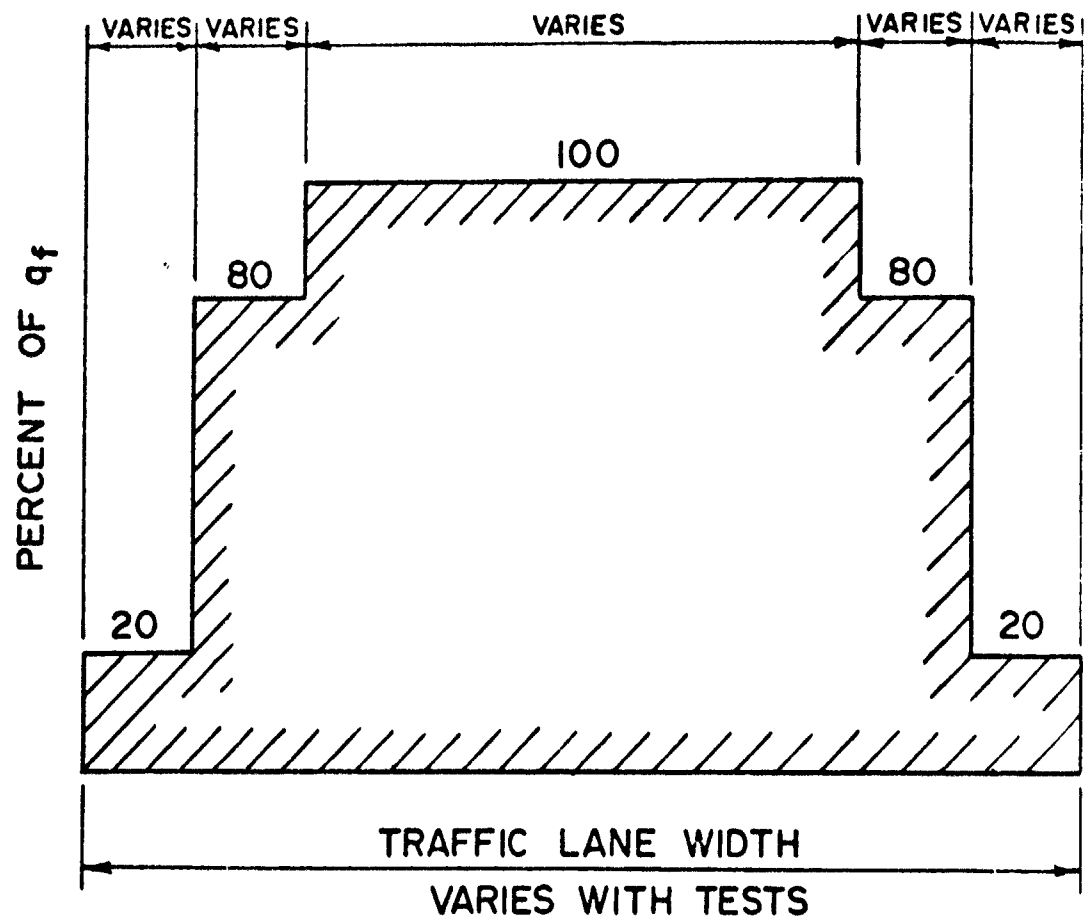
# FIGURE 9. TRAFFIC DISTRIBUTION ACROSS TRAFFIC LANE

The magnitude of $q_f$ was determined by simulating the maximum deformation for each prototype test. The range of values of $q_f$ was found to be large. In addition, as noted previously, the curvature of the deflection patterns, obtained from the model, was much less than that of the "deformation" patterns. This was particularly noted in the lanes which were uniformly loaded. Consequently, the three inch roughness criterion could not be met at a coverage level which could be considered to produce failure. Thus, this approach for establishing a failure criterion was abandoned.

## Dimensional Analysis and Taylor Expansion

Another approach followed to define failure was to obtain a functional relationship among the mat, soil, loading properties, and the number of coverages which caused failure. It was thought that a functional relationship of the form

$$N = f(WL, CA, EI, w\gamma_d, CBR) \tag{16}$$

where     WL is the single wheel load in kips
          CA is the contact area in sq. in.
          and the other symbols are as previously defined

would provide some insight to the development of a failure criterion or could possibly even serve as a means of predicting performance. To reduce the number of variables, the Buckingham Pi theorem [32] was applied to the system, allowing Eqn. (16) to be expressed as

$$N = f(\pi_1, \pi_2, \pi_3) \tag{17}$$

where the $\pi$'s are dimensionless ratios or numbers. Letting $\pi_1$ be a dimensionless ratio of $w\gamma_d$, WL, and EI,

$$\pi_1 = (w\gamma_d)^{C_1} (WL)^{C_2} (EI) \tag{18}$$

where $C_1$ and $C_2$ are constants, it was found that

$$\pi_1 = \frac{(w\gamma_d)^{2/3}\,(EI)}{(WL)^{5/3}} \tag{19}$$

Similarly, letting $\pi_2$ be a dimensionless ratio of $w\gamma_d$, $WL$, and CA,

$$\pi_2 = \frac{(w\gamma_d)^{2/3}\,(CA)}{(WL)^{2/3}} \tag{20}$$

as CBR is a dimensionless quantity,

$$\pi_3 = CBR \tag{21}$$

With the $\pi$ terms so designated, the pursuit of a reasonable functional relationship followed. The function was expanded into a Taylor series about the fixed points $\pi_1^0$, $\pi_2^0$, and $\pi_3^0$, which were assigned typical values for the $\pi_1$, $\pi_2$, and $\pi_3$ factors. The expansion of Eqn. (17) lead to the following relationship

$$
\begin{aligned}
f(\pi_1,\ \pi_2,\ \pi_3) = &\ f(\pi_1^0,\pi_2^0,\pi_3^0) \\
&+\left[(\pi_1-\pi_1^0)\frac{\partial}{\partial\pi_1}+(\pi_2-\pi_2^0)\frac{\partial}{\partial\pi_2}+(\pi_3-\pi_3^0)\frac{\partial}{\partial\pi_3}\right]f(\pi_1,\pi_2,\pi_3)\Big|_{\pi_1^0,\pi_2^0,\pi_3^0} \\
&+\frac{1}{2!}\left[(\pi_1-\pi_1^0)\frac{\partial}{\partial\pi_1}+(\pi_2-\pi_2^0)\frac{\partial}{\partial\pi_2}+(\pi_3-\pi_3^0)\frac{\partial}{\partial\pi_3}\right]^2 f(\pi_1,\pi_2,\pi_3)\Big|_{\pi_1^0,\pi_2^0,\pi_3^0} \\
&+\frac{1}{3!}\left[(\pi_1-\pi_1^0)\frac{\partial}{\partial\pi_1}+(\pi_2-\pi_2^0)\frac{\partial}{\partial\pi_2}+(\pi_3-\pi_3^0)\frac{\partial}{\partial\pi_3}\right]f(\pi_1,\pi_2,\pi_3)\Big|_{\pi_1^0,\pi_2^0,\pi_3^0} \\
&+\ \ldots
\end{aligned}
\tag{22}
$$

where $f(\pi_1^0,\pi_2^0,\pi_3^0)$ represents the value of the function at the fixed points $\pi_1^0$, $\pi_2^0$, and $\pi_3^0$ and hence is a constant.

The expression

$$\frac{\partial}{\partial \pi_i} f(\pi_1, \pi_2, \pi_3) \Big|_{\pi_1^0, \pi_2^0, \pi_3^0} \quad (i = 1, 2, 3)$$

represents the partial derivative of the function with respect to $\pi_i$ evaluated at the fixed points $\pi_1^0$, $\pi_2^0$, and $\pi_3^0$. All of the partial derivatives are unknown but once fixed points are selected they become constants.

Data were used from the prototype tests for the single-wheel load assemblages wherein failure occurred before 700 coverages. In all, a total of 26 different sets of data were utilized. With this amount of available data as many terms of the Taylor series were used as possible. Considering only the first 4 terms of the series, 20 different coefficients or constants had to be evaluated to obtain the required functional relationship. If the functional relationship was to apply, of necessity, it had to satisfy each set of data. Thus in order to determine the coefficients, the data for 20 different tests were used to produce 20 different relationships which were then solved simultaneously to produce the 20 required coefficients.

All of the dual-wheel tests which produced failure were also investigated in the same manner with the inclusion of the wheel spacing, WS, as an additional variable. This additional variable necessitated an additional $\pi$ term. Letting $\pi_4$ be the dimensionless ratio between $w\gamma_d$, WL, and WS, it was found that

$$\pi_4 = \frac{(w\gamma_d)^{1/3}\,(WS)}{(WL)^{1/3}} \tag{23}$$

Hence, for dual-wheel tests the functional relationship becomes

$$N = f(\pi_1, \pi_2, \pi_3, \pi_4) \tag{24}$$

where $\pi_1$, $\pi_2$, and $\pi_3$ are as defined previously. Due to the limited amount of data available, only the first three terms of the series expansion could be considered. This necessitated the evaluation of 15 coefficients.

49

Data from 20 different tests were used to develop the functional relationship for the single-wheel tests, Eqn. (22). The functional relationship obtained from one particular combination of 20 data sets was

$$
\begin{aligned}
N = &- 62.208 && + 0.265(\pi_1 - \pi_1^0) \\
&- 0.154(\pi_2 - \pi_2^0) && - 85.261(\pi_3 - \pi_3^0) \\
&- 0.001(\pi_1 - \pi_1^0)(\pi_2 - \pi_2^0) && + 1.070(\pi_1 - \pi_1^0)(\pi_3 - \pi_3^0) \\
&+ 2.842(\pi_2 - \pi_2^0)(\pi_3 - \pi_3^0) && + 0.002(\pi_1 - \pi_1^0)^2 \\
&+ 0.028(\pi_2 - \pi_2^0)^2 && + 115.730(\pi_3 - \pi_3^0)^2 \\
&- 0.006(\pi_1 - \pi_1^0)(\pi_2 - \pi_2^0)(\pi_3 - \pi_3^0) && - 0.000(\pi_1 - \pi_1^0)^2(\pi_2 - \pi_2^0) \\
&- 0.003(\pi_1 - \pi_1^0)^2(\pi_3 - \pi_3^0) && - 0.000(\pi_1 - \pi_1^0)(\pi_2 - \pi_2^0)^2 \\
&- 0.016(\pi_2 - \pi_2^0)^2(\pi_3 - \pi_3^0) && + 1.036(\pi_1 - \pi_1^0)(\pi_3 - \pi_3^0)^2 \\
&- 3.602(\pi_2 - \pi_2^0)(\pi_3 - \pi_3^0)^2 && - 0.000(\pi_1 - \pi_1^0)^3 \\
&- 0.000(\pi_2 - \pi_2^0)^3 && + 8.466(\pi_3 - \pi_3^0)^3
\end{aligned}
\tag{25}
$$

This relationship was applied to all 26 available field tests. Table 8 gives the results.

As expected, the functional relationship predicted the exact failure coverage for the 20 sets of data used in its development. However, the prediction of the failure coverage was quite poor for the other tests. A total of 100 different combinations of data sets were investigated. The coefficients obtained from the different data combinations were very erratic.

The same procedure was also applied to the dual-wheel test data. Again the developed functional relationship failed to reproduce the failure coverage. Hence this procedure was abandoned.

## Regression Analysis

Actual wheel loadings were applied to the mat-soil model using Eqns. (13), (14), and (15), and the deflection of the mats was computed for the failure coverage. In the single-wheel tests, the deflection of the mats at the center of the

## Table 8

### Results of Dimensional Analysis Study
### of Single-Wheel Tests

| | Test | | Coverages | |
|---|---|---|---|---|
| Sect. | Lane | Item | Actual Failure | Predicted Failure |
| 2 | 3 | 1 * | 600. | 600. |
| 2 | 3 | 2 * | 120. | 120. |
| 9 | 21 | 2 * | 300. | 300. |
| 6 | 11A | 1 * | 130. | 130. |
| 6 | 11A | 2 * | 130. | 130. |
| 10 | 23A | 1 * | 32. | 32. |
| 10 | 23A | 2 * | 2. | 2. |
| 10 | 23B | 1 * | 4. | 4. |
| 10 | 23B | 2 * | 2. | 2. |
| | 7 | ** | 94. | 94. |
| | 8 | ** | 6. | 6. |
| | 9 | ** | 94. | 94. |
| | 36 | ** | 14. | 14. |
| | 37 | ** | 98. | 98. |
| | 38 | ** | 197. | 197. |
| | 39 | ** | 60. | 60. |
| | 40 | ** | 30. | 30. |
| | 41 | ** | 30. | 30. |
| | 71 | ** | 160. | 466. |
| | 72 | ** | 675. | 11384. |
| | 73 | ** | 473. | 5428. |
| | 74 | ** | 74. | 74. |
| | 75 | ** | 360. | 7292. |
| | 76 | ** | 223. | 738. |
| | 92 | ** | 300. | 300. |
| | 93 | ** | 23. | 156. |

*  Reference  12

** Reference  10

wheel was recorded and is presented in Table 9 and Figure 10.
For the dual-wheel test sections, the deflection of the mats
at the centerline of the wheel assembly was recorded and is
presented in Table 10 and Figure 11. It was anticipated
that a failure criterion could be established empirically
provided that the results, as shown in Figures 10 and 11,
could be grouped in some manner. Since the predicted deflec-
tions were themselves functions of other test parameters, in
addition to coverages, the predicted deflections for each
test were taken as a product function of these parameters.
For a single-wheel test, this relation was expressed as

$$\Delta_f = (WL_R)^{C_1} (EI_R)^{C_2} (CA_R)^{C_3} (CBR)^{C_4} N^{C_5} \qquad (26)$$

where     $\Delta_f$ is the predicted deflection at the failure
            coverage in inches
        $WL_R$ is the wheel load relative to 35 kips
        $EI_R$ is the rigidity per foot of width relative to
            13680 kip-in$^2$
        $CA_R$ is the contact area relative to 150 sq. in.
        $N$ is the number of coverages to failure
        $C_1$, $C_2$, $C_3$, $C_4$, $C_5$ are exponents whose values are
                     to be determined.

The parameters of tire inflation pressure and tire ply
rating were not included because their effects were con-
sidered to be reflected by the parameters $WL_R$ and $CA_R$.

The data from each single-wheel test section was
written in the form

$$\log \Delta_f = C_1 \log(WL_R) + C_2 \log(EI_R) + C_3 \log(CA_R) + C_4 \log(CBR) + C_5 \log N$$

$$(27)$$

A multiple stepwise regression analysis of the data was
performed using a computer program [61] to obtain the coef-
ficients, $C_1$, $C_2$, $C_3$, $C_4$, and $C_5$. The failure condition
for all 28 tests are shown in Figure 12. Also indicated
in this figure is the regression line for the failure con-
dition. The results of this analysis indicated that the
factor sought, failure coverage (N), was of only minor
importance.

## Table 9

### Predicted Deflections of the Mat at Failure for Single-Wheel Tests

| Sect. | Lane | Item | Failure Coverage | Deflection in. |
|-------|------|------|------------------|----------------|
| 2 | 3 | 1 | 600 | 2.32 |
| 2 | 3 | 2 | 120 | 1.52 |
| 6 | 11A | 1 | 130 | 2.68 |
| 6 | 11A | 2 | 130 | 1.74 |
| 9 | 21 | 2 | 300 | 1.70 |
| 10 | 23A | 1 | 32 | 2.69 |
| 10 | 23A | 2 | 2 | 2.50 |
| 10 | 23B | 1 | 4 | 4.24 |
| 10 | 23B | 2 | 2 | 4.28 |

| Test | Failure Coverage | Deflection in. |
|------|------------------|----------------|
| 7 | 94 | 1.14 |
| 8 | 6 | 1.74 |
| 9 | 94 | 1.37 |
| 36 | 14 | 1.80 |
| 37 | 98 | 1.56 |
| 38 | 197 | 1.35 |
| 39 | 60 | 1.59 |
| 40 | 30 | 1.49 |
| 41 | 30 | 1.83 |
| 71 | 160 | 1.23 |
| 72 | 675 | 0.95 |
| 73 | 473 | 0.97 |
| 74 | 74 | 1.59 |
| 75 | 360 | 1.18 |
| 76 | 223 | 1.43 |
| 91 | 570 | 0.77 |
| 93 | 23 | 1.75 |
| 108 | 160 | 1.21 |
| 109 | 50 | 1.38 |
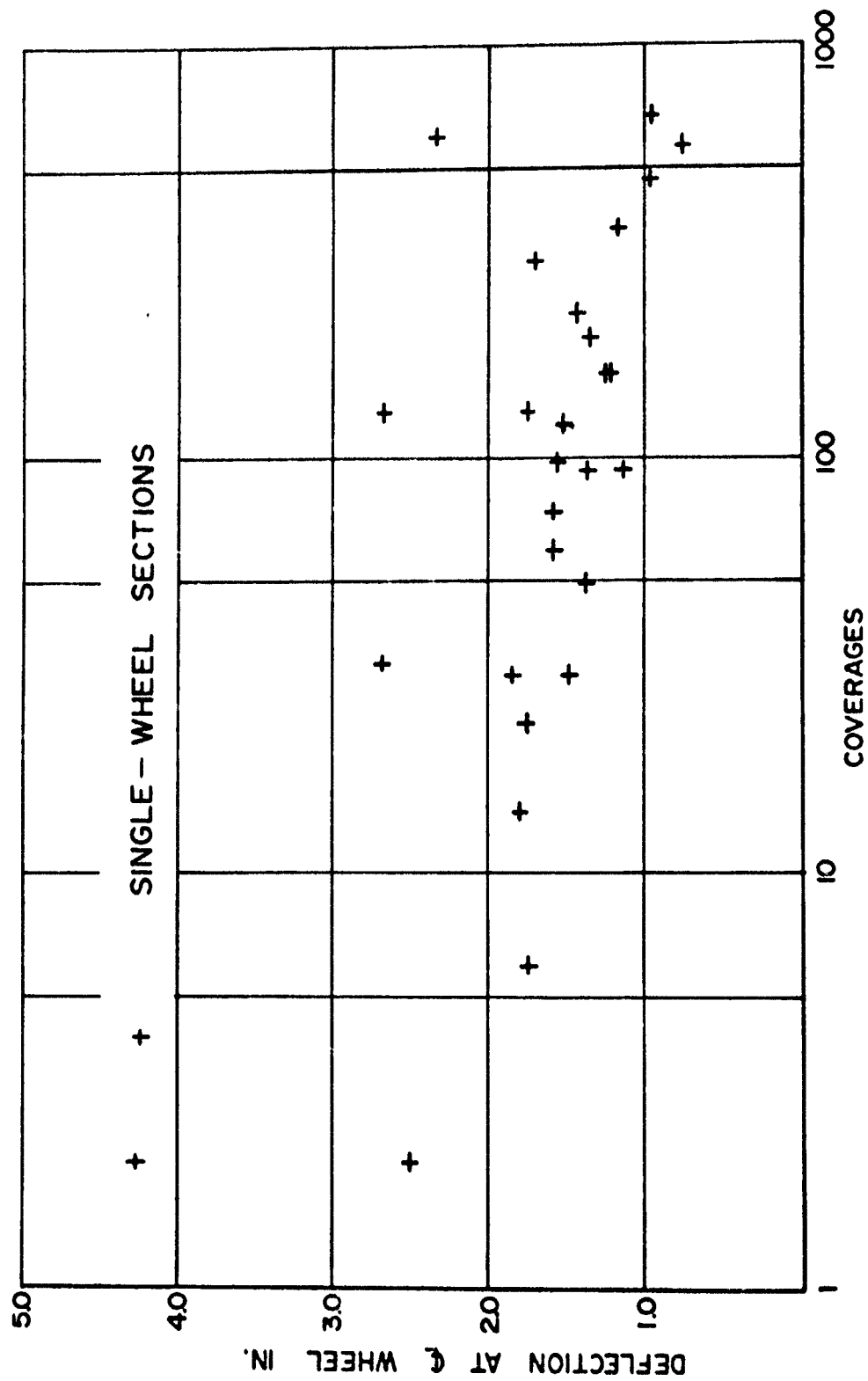
FIGURE 10. DEFLECTION AT CENTER OF WHEEL FROM MODEL AT THE FAILURE COVERAGE.

## Table 10

### Predicted Deflections of the Mat
### at Failure for Dual-Wheel Tests

| Sect. | Lane | Item | Failure Coverage | Deflection in. |
|-------|------|------|------------------|----------------|
| 1 | 1 | 3 | 300. | 1.52 |
| 1 | 2 | 3 | 40. | 1.68 |
| 2 | 4 | 1 | 20. | 3.76 |
| 2 | 4 | 2 | 20. | 1.87 |
| 3 | 5 | 1 | 28. | 3.03 |
| 3 | 5 | 2 | 28. | 1.65 |
| 3 | 6 | 1 | 130. | 2.04 |
| 3 | 6 | 2 | 76. | 1.27 |
| 4 | 8 | 1 | 460. | 0.57 |
| 4 | 8 | 2 | 142. | 0.50 |
| 6 | 12 | 1 | 90. | 1.37 |
| 6 | 12 | 2 | 44. | 0.82 |
| 9 | 22 | 1 | 400. | 3.14 |
| 9 | 22 | 2 | 100. | 2.62 |
| 13 | 28 | 1 | 700. | 2.37 |
| 13 | 28 | 2 | 700. | 0.87 |
| 13 | 29 | 1 | 140. | 3.27 |
| 13 | 29 | 2 | 200. | 1.88 |
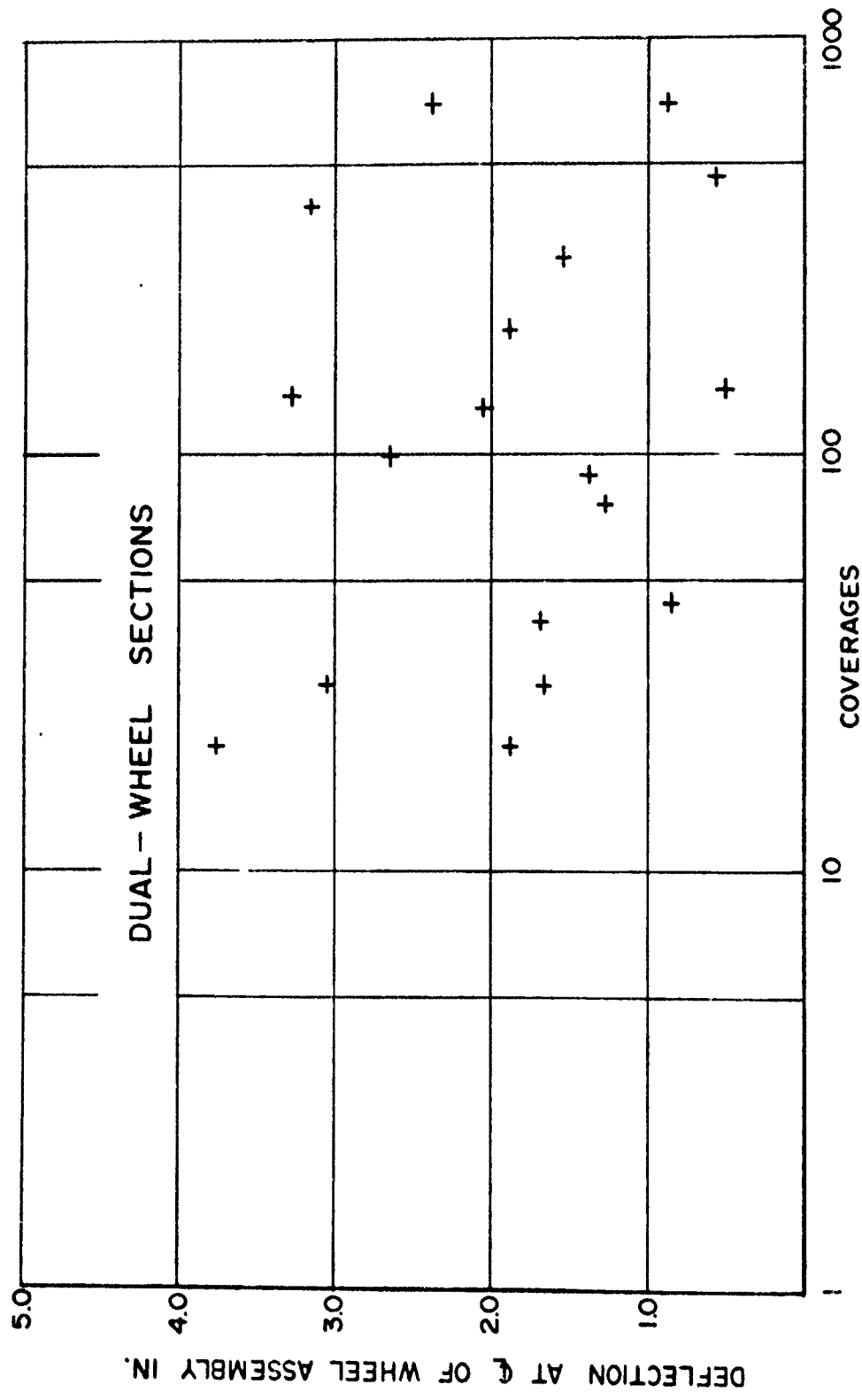
FIGURE 11. DEFLECTION AT CENTERLINE OF WHEEL ASSEMBLY FROM MODEL AT THE FAILURE COVERAGE.

$$\frac{4.83 \, (WL_R)^{C_1} \, N^{C_5}}{(EI_R)^{C_2} (CA_R)^{C_3} (CBR)^{C_4}}$$

$c_1 = 0.998$
$c_2 = 0.188$
$c_3 = 0.518$
$c_4 = 0.596$
$c_5 = 0.002$

TIRE PRESSURE
⊟  50 PSI.
+  100 PSI.
△  200 PSI.
×  250 PSI.
⊙  300 PSI.

DEFLECTION AT ℄ WHEEL IN.
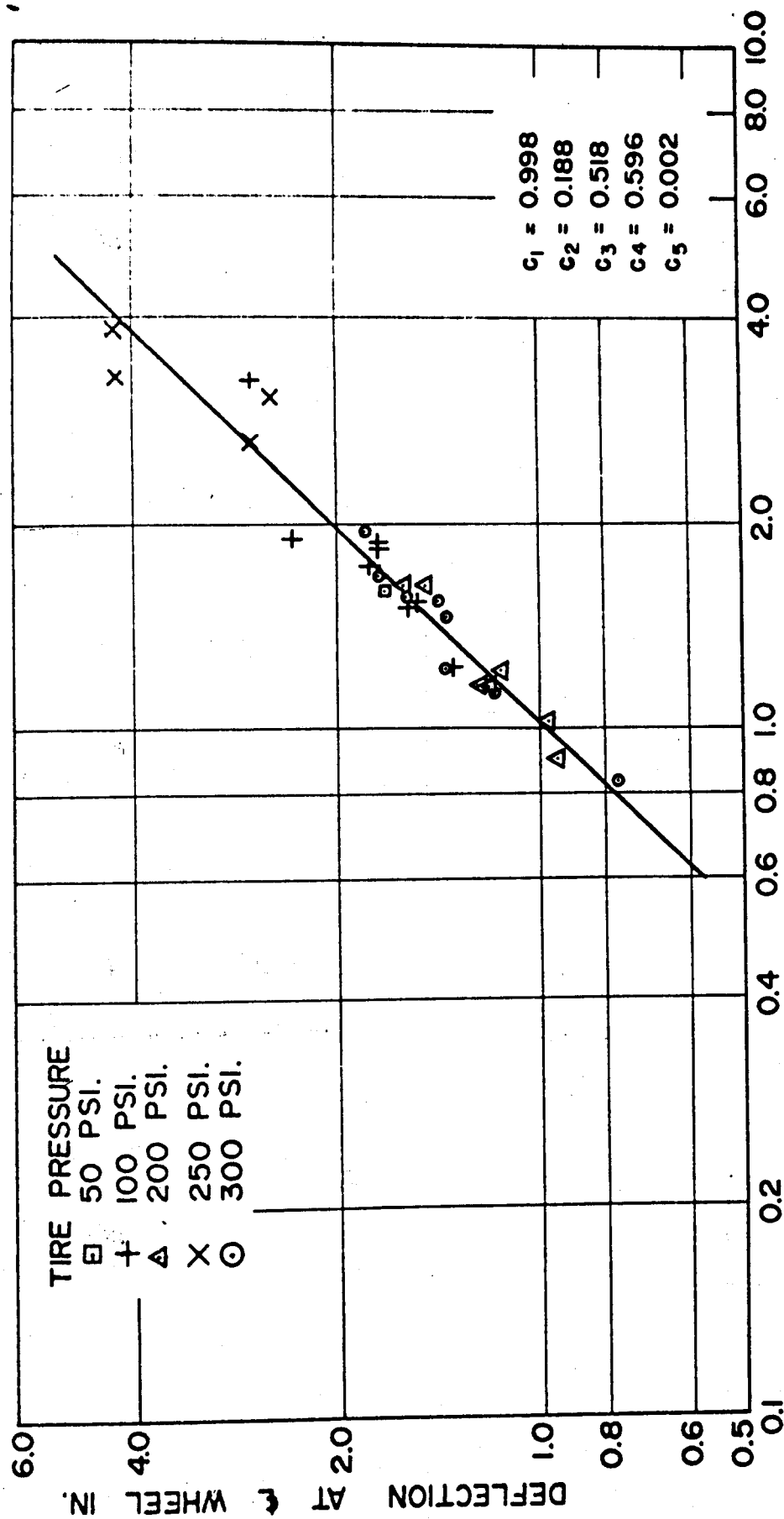
FIGURE 12.   REGRESSION   ANALYSIS   FOR   SINGLE - WHEEL   TESTS.

From the prototype data, it was observed that the same tire ply rating was not used in all tests; thus, the ratio of tire inflation pressure to contact pressure was not a constant. This observation indicated that possibly the tire inflation pressure might indeed be a significant parameter. Thus another regression analysis was performed on the data where each test was expressed as

$$\log \Delta_f = C_1 \log(WL_R) + C_2 \log(EI_R) + C_3 \log(CA_R) + C_4 \log(CBR)$$

$$+ C_5 \log(N) + C_6 \log(TP_R) \tag{28}$$

where $TP_R$ is the tire pressure normalized relative to 100 psi. After obtaining the coefficients, the failure conditions were as shown in Figure 13. This analysis also indicated that the failure coverage was of minor importance.

The dual-wheel test sections were investigated by a similar regression analysis with an additional parameter of wheel spacing. Each dual-wheel data set was expressed as

$$\log \Delta_f = C_1 \log(WL_R) + C_2 \log(EI_R) + C_3 \log(CA_R) + C_4 \log(CBR$$

$$+ C_5 \log(N) + C_6 \log(TP_R) + C_7 \log(WS_R) \tag{29}$$

where $WS_R$ is the wheel spacing normalized relative to 25 in. Surprisingly, the N parameter was again found not to be a significant parameter. In view of the fact that the N parameter is of primary importance to the establishment of a failure criterion, the regression analysis program, as applied to the data in the form of Eqn. (29), was also discarded.

## Educated Trial and Error Procedure

Finally, an educated trial and error procedure was undertaken to achieve the combination of test parameters whose order was more dependent upon the number of coverages,

58
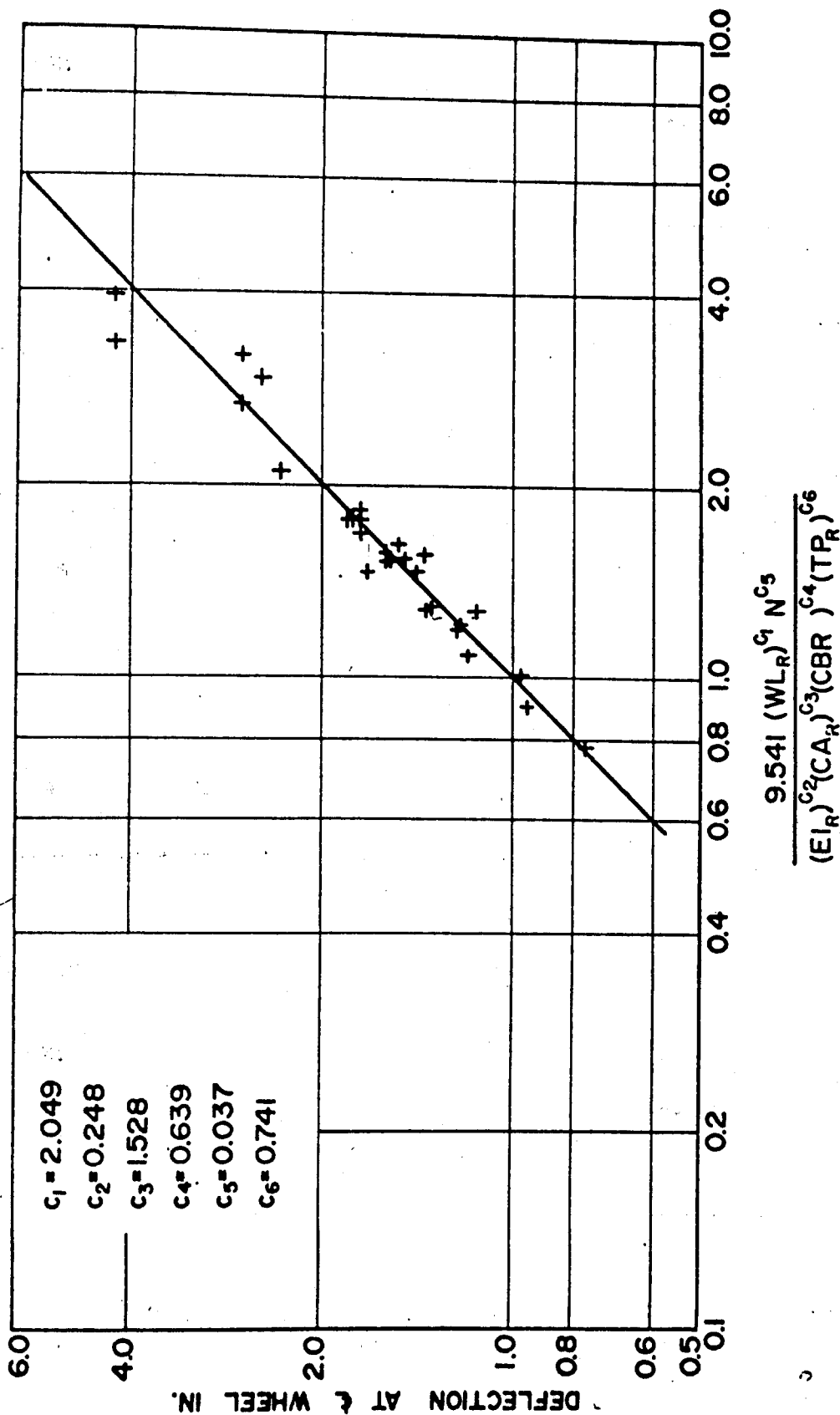
FIGURE 13. REGRESSION ANALYSIS WITH TIRE PRESSURE CONSIDERED.

$$\frac{9.541 \ (WL_R)^{C_1} \ N^{C_5}}{(EI_R)^{C_2}(CA_R)^{C_3}(CBR)^{C_4}(TP_R)^{C_6}}$$

$c_1 = 2.049$
$c_2 = 0.248$
$c_3 = 1.528$
$c_4 = 0.639$
$c_5 = 0.037$
$c_6 = 0.741$

DEFLECTION AT ℄ WHEEL IN.

N.  Combinations of parameters were set up by deleting certain parameters and various forms of the function were obtained by adjusting exponents.  For each combination, computations were directed toward the development of a linear relationship, on a log-log plot, between the predicted failure deflections (Tables 9 and 10), the failure coverages, and the selected test parameters.  Following this procedure a reasonable correlation was eventually achieved for the dual-wheel failure conditions.

A linear approximation of the failure conditions was established as the failure criterion for both the single-wheel and the dual-wheel tests.  A computer program was developed whereby the performance of a mat could be predicted from the parameters of the test section.  This computer program is given in Appendix G.  It requires entries of:  modulus of elasticity of the mat, moment of inertia of the mat per foot of width, the length of a rectangle whose area is equivalent to that of the tire print and whose width is the same as the actual tire print, the number of wheel loads, the weight of water per unit volume of soil, CBR, wheel load, contact area, tire inflation pressure, the distances to the beginning and end of each wheel load from an arbitrarily located origin and the magnitude of the wheel load expressed as a uniform load over the width of the tire print.

The equation of the failure criterion line can be expressed as

$$\Delta_f = C(N)^M \tag{30}$$

where $\Delta_f$ is either the deflection of the center of the wheel for the single-wheel test or the deflection at the centerline of the assembly for the dual-wheel test and C and M are each constants which are dependent on the type of test.  In the computer program, the N parameter is incremented and the deflection at the specified point is computed.  For values of N less than 200 the increment interval is 5 and for values of N greater than 200 the increment interval is 20.

For a single-wheel test as the value of N increases, the deflection as given by the failure criterion will also increase; thus, the deflection will follow the line "C" in Figure 14.  From the simulation model, the deflection of the same point also increases as the value of N increases, line "D", Figure 14.  As N is incremented the model deflection is
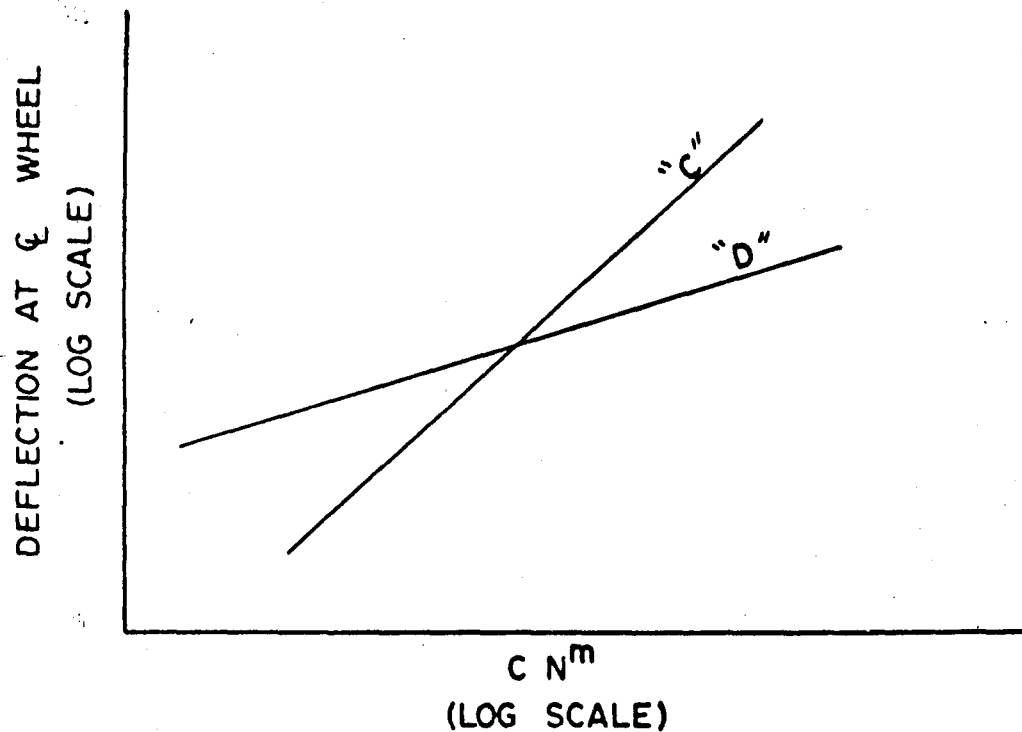
FIGURE 14. PERFORMANCE TEST FOR A
SINGLE WHEEL TEST.
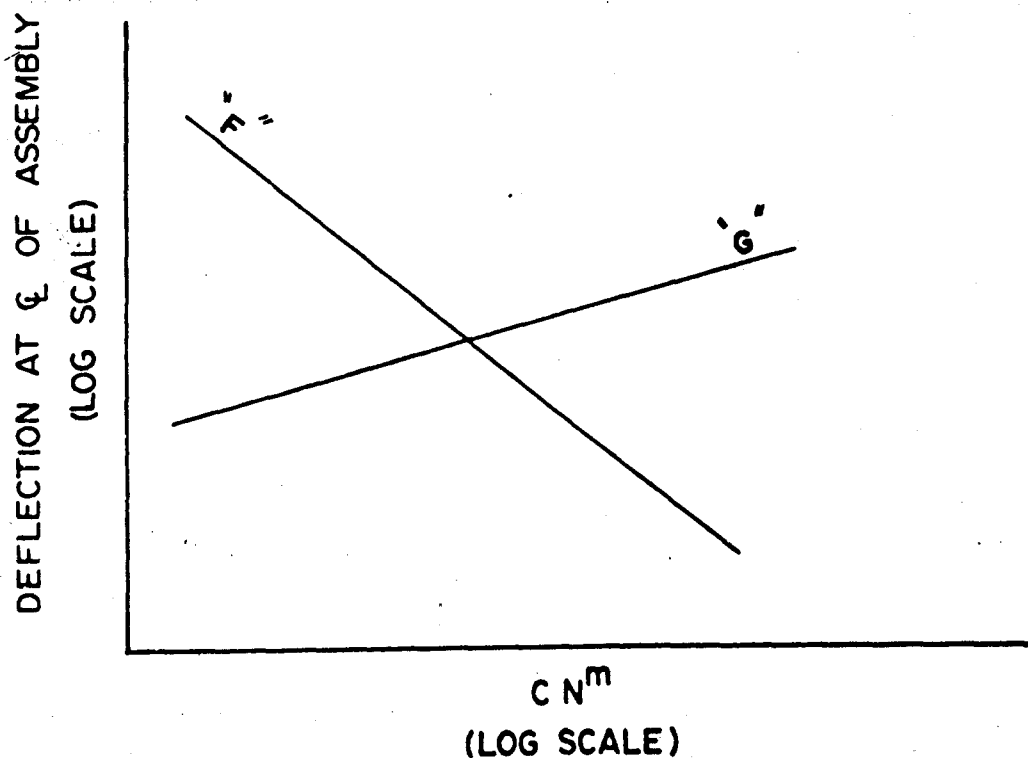


FIGURE 15. PERFORMANCE TEST FOR A DUAL
WHEEL TEST.

computed and compared to the deflection required by the failure criterion. When the latter deflection is just equal to or greater than that of the model, the corresponding value of N is considered the failure coverage.

The procedure given above was also followed for the dual-wheel tests. For this case the failure criterion indicated that the deflections decreased as N increased, line "F", Figure 15. Thus, for small values of N, the deflection as given by the criterion would be larger than the model deflections, line "G", Figure 15. Failure was considered to be imminent when the model deflection became just equal to or greater than the deflection given by the criterion.

## Results

When the trial and error procedure, which was biased toward a significant N parameter, was applied to the dual-wheel test data the "best" ordering of the parameters resulted in a plot of the failure conditions as shown in Figure 16. All data points, except three shown encircled, were fitted with a linear function using a least squares technique. The three points were believed to be in error because.

1) The maximum differential deformation for Section 1, Lane 2, Item 3 at the indicated failure coverage was 2.31 in. This was less than the established criterion for failure. To meet the roughness criterion more actual coverages would be necessary. This indicated that the failure condition should place the point to the left of that shown in Figure 16.

2) The deflection pattern for Section 4, Lane 8, Item 1 was pronouncedly unsymmetrical. This indicated the likelihood that the reported soil properties were not representative of the soil conditions that governed in the process. If this was the case, then the resulting predicted deflection should be larger than shown in Figure 16. In addition, the maximum differential deformation for this section at failure was recorded as 2.63 in. Consideration of these two factors would place the failure condition up and to the left of that shown in Figure 16.

62
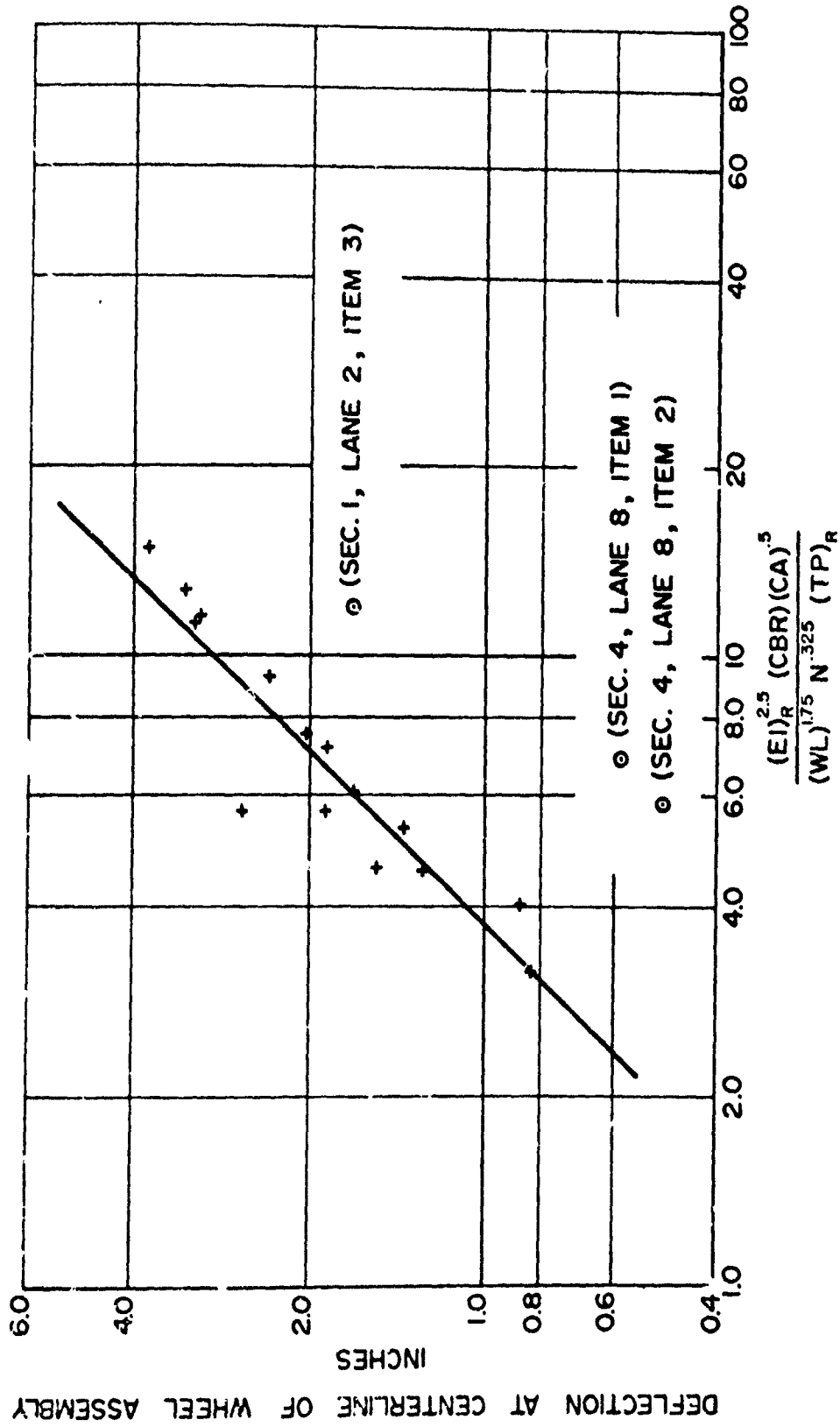
FIGURE 16. CORRELATION OF FAILURE FOR DUAL-WHEEL TESTS.

3) The CBR values reported at the beginning of test, Section 4, Lane 8, Item 2, showed a decrease of strength with depth for the upper 18 in. of soil. For all other dual-wheel test sections the inverse of this condition existed. It appears that the performance of this test section is governed by weaker underlying material. Accounting for the weaker conditions, the predicted deflection at failure would have to be larger than that shown in Figure 16.

The "calculated" trial and error procedure was also applied to the single-wheel test data. The failure conditions for one of the "better" parametric combinations of these is shown in Figure 17. In an attempt to establish a failure criterion for the single-wheel tests, the data shown were fitted by a linear function. The three points indicated by circles in Figure 17 were omitted in the curve fitting procedure. These points represent tests which failed at four or less coverages. In view of the extremely low number of coverages to failure, it was felt that these tests should not be included as they did not represent reasonable engineering solutions for which mats could be employed.

The computer program, Appendix G, developed to predict the performance of a test section, incorporates the linear relationships indicated in Figures 16 and 17. The data for the given prototype tests [10, 12] were processed by this computer program. The predicted failure coverages, along with the actual failure coverages, for the dual-wheel tests are given in Table 11. Similar tabulation for the single-wheel tests is provided in Table 12.

## Summary and Discussion of Failure Criteria

The roughness criterion established by the Corps of Engineers [12] for the prototype tests was based upon the permanent displacements of the unloaded mat. With the developed elastic mat-soil model displacements of the mat could be determined only when the surface was subjected to external loading. Thus in order to use the developed mat-soil model as a means of predicting performance, the behavior of the model, under actual or fictitious loading, had to be related to failure. Initially, a fictitious load with a distribution identical to the traffic distribution

64
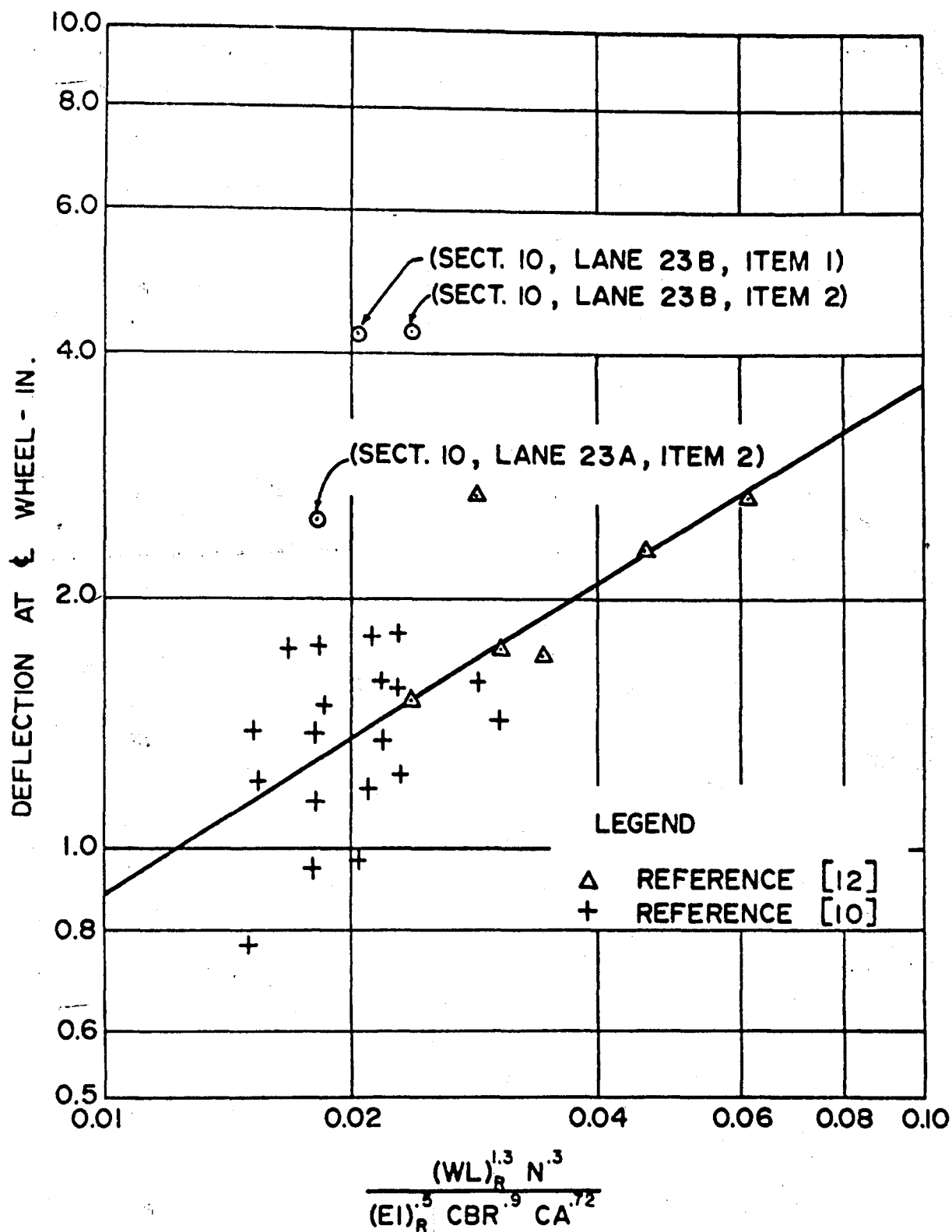
FIGURE 17. CORRELATION OF FAILURE FOR SINGLE - WHEEL TESTS.

# Table 11

## Comparison of Performance
## for Dual-Wheel Tests

| Section | Actual Failure Coverage | Predicted Failure Coverage |
|---------|-------------------------|----------------------------|
| 1-1-3 | 300 | 220 |
| 1-2-3 | 40 (56)* | 260 |
| 2-4-1 | 20 | 25 |
| 2-4-2 | 20 | 25 |
| 3-5-1 | 28 | 35 |
| 3-5-2 | 28 | 35 |
| 3-6-1 | 130 | 150 |
| 3-6-2 | 76 | 85 |
| 6-12-1 | 90 | 120 |
| 6-12-2 | 44 (54)* | 65 |
| 9-22-1 | 400 | 320 |
| 9-22-2 | 100 (56)* | 30 |
| 13-28-1 | 700 (967)* | 880 |
| 13-28-2 | 700 | 1560 |
| 13-29-1 | 140 | 170 |
| 13-29-2 | 200 (145)* | 130 |
| 4-8-1 | 460 | > 5000 |
| 4-8-2 | 142 | 1000 |

* More realistic values, see Summary and Discussion of Failure Criterion.

## Table 12

## Comparison of Performance
## for Single-Wheel Tests

| Test | Actual Failure Coverages | Predicted Failure Coverages |
|------|--------------------------|------------------------------|
| 2-3-1 | 600 | 680 |
| 2-3-2 | 120 | 120 |
| 6-11A-1 | 130 | 125 |
| 6-11A-2 | 130 | 115 |
| 9-21-1 | >600 | 400 |
| 9-21-2 | 300 | 135 |
| 7 | 94 | 40 |
| 8 | 6 | 65 |
| 9 | 94 | 105 |
| 36 | 12-16 | 75 |
| 37 | 70-126 | 140 |
| 38 | 170-224 | 120 |
| 39 | 40-80 | 120 |
| 40 | 20-40 | 75 |
| 41 | 20-40 | 135 |
| 71 | 150-170 | 45 |
| 72 | 650-700 | 80 |
| 73 | 400-546 | 40 |
| 74 | 40-108 | 50 |
| 75 | 350-370 | 110 |
| 76 | 170-276 | 55 |
| 91 | 570 | 35 |
| 92 | 300 | 60 |
| 93 | 23 | 220 |
| 108 | 160 | 195 |
| 109 | 50 | 170 |
| 10-23A-1 | 32 | 580 |
| 10-23A-2 | 2 | 340 |
| 10-23B-1 | 4 | > 5000 |
| 10-23B-2 | 2 | 4940 |

was assumed to act on the mat-soil model. The magnitude of this load was determined from simulation of the maximum deformation. Investigation of the curvature of the resulting model deflection pattern revealed that the roughness criterion could not be satisfied at the defined failure coverage. Comparisons of the magnitude of the fictitious loads to failure coverages was also unsuccessful.

An attempt was made to develop a functional relationship between failure coverages and test parameters by dimensional modeling. The results, Table 8, indicated that a unique relationship could not be established. The inability to develop a satisfactory functional relationship by this procedure was attributed to: 1) consideration of only a limited number of terms in the series expansion, and/or 2) omission of significant factors in the selected dimensional model. For this study more terms were not considered due to the lack of reliable data available. For example, to include the next term in the series for the single-wheel tests would require fifteen additional sets of data. Further examination of Eqn. (25) failed to establish which $\pi$ term was most influential in the functional relationship.

The mat-soil model was subjected to loading identical to that used to obtain the "average deflection" patterns [12]. Under this loading the mat deflection was computed for each specific failure coverage. For consistency, the mat deflection was computed at the center of the wheel and under the centerline of the wheel assembly respectively for the single-wheel and dual-wheel tests. These deflections were then expressed as a product function of the failure coverage and remaining test parameters. A regression analysis of both the single-wheel and dual-wheel test data indicated that the failure coverage was an insignificant parameter, Figures 12 and 13.

An educated trial and error procedure was undertaken to achieve an ordering of the test parameters which was dependent upon the failure coverage. Numerous combinations of the test parameters were investigated. For each combination, computations were directed toward the development of a linear relationship on a log-log plot. A reasonable correlation of the dual-wheel tests was achieved and the results are presented in Figure 16. The results as shown were fitted with a linear function which was established as the failure criterion. Using this criterion the performance of each test

section was predicted with the aid of the computer program, Appendix G. Results from this program may be compared with the actual failure coverage, Table 11. The results indicate that the performance of similar tests may be predicted with reasonable confidence by this procedure. Apparent discrepancies for specific tests may be attributed to the following observations of the prototype data:

1) Section 1, Lane 2, Item 3. This test section was considered to have failed at 40 coverages due to roughness and mat deterioration. However, the maximum differential deformation at this coverage level was 2.31 inches. To meet the established failure criterion for roughness, additional coverages would be necessary. Thus it is believed that the performance of this test was governed by mat deterioration rather than by surface roughness upon which the prediction of performance is based.

2) Section 6, Lane 12, Item 1. The "average deflection" patterns for the various coverages when the load assembly was at the center of the panel are pronouncedly unsymmetrical. In addition the deflection did not increase consistently with the number of coverages. Due to the unsymmetrical characteristic of the deflection patterns, the soil properties reported may not be representative of the governing subgrade conditions.

3) Section 6, Lane 12, Item 2. The maximum differential deformation at failure was reported as 2.63 in. Conformance with the roughness criterion would necessitate more coverages and therefore better agreement with the predicted failure.

4) Section 9, Lane 22, Item 2. The maximum differential deformation at failure was reported as 4.39 in. This indicated that the failure criterion was satisfied at a coverage level less than 100. Applying a linear interpolation between the maximum differential settlement reported for 20 coverages and 100 coverages, the section would have satisfied the failure criterion at 56 coverages.

5) Section 13, Lane 29, Item 2. The maximum differential deformation at failure was 4.00 in. Again applying a linear interpolation for the maximum differential deformations reported for early

coverage levels, failure would have occurred at
145 coverages.

6) Section 4, Lane 8, Item 1. As noted earlier the
deflection pattern was pronouncedly unsymmetrical.
The soil properties reported, which were used for
the mat-soil model, may represent a stronger sub-
grade than actually existed. If there was an
appreciable difference between the worst soil con-
ditions and the conditions as reported, one should
not expect the performance of this section to be
predicted by the developed procedure.

7) Section 4, Lane 8, Item 2. Also, as noted earlier,
the strength of the subgrade as reflected by the
CBR values decreased with depth. The performance
of this section appeared to have been governed by
underlying weaker material.

8) Section 13, Lane 28, Item 1. This section failed
at 700 coverages due to elastic deflections; that
is, excessive displacements were in evidence under
the wheel loads. This failure, therefore, could
not be attributed to roughness. Extrapolation of
the given deformation data indicated that the sec-
tion would satisfy the roughness criterion at 967
coverages.

9) Section 13, Lane 28, Item 2. No apparent reason
can be found from the available data for the dis-
crepancy shown for this section between observed
and predicted performance.

Apparently as indicated in Table 12 and again in Figure
17, the developed procedure demonstrated less success when
predicting the performance of single-wheel tests. The
paucity of available information and test results for the
sections showing the poorest comparison of performance
(sections reported in reference [10]) render the correlation
for the single-wheel tests academic. This is particularly
true since the three inch roughness criterion was not specif-
ically employed; further, the magnitudes of the differential
deformations and the "deformation" patterns were also lack-
ing. If one can speculate, a prime factor which might
effect this correlation is the variability of the number of
passes necessary to complete one coverage. For the tests

70

reported in reference [10] these ranged from a minimum of 7 to a maximum of 29 passes. Thus the input energy level per coverage could be quite different for seemingly similar situations. Hence, it was thought advisable to turn to an improved model whereby actual loadings could be simulated.

# ASYMMETRIC LOAD MODEL

## Introduction

The "deformation" patterns of the prototype landing mat tests conducted by the Corps of Engineers [12] indicate that the time rate of deformation decreases with coverages. Typical mat deformations at the centerline of the traffic lane when plotted as a function of coverages, shown by the circles in Figure 18, suggest that a continuous plot of this relationship might follow the dash-line. Larew and Leonards [ 33] obtained the same general shape in their study of the deformation characteristics of fine-grained soils subject to repetitive loads. They concluded that for repetitive loads, wherein the ratio of the repeatedly applied deviator stress to the static deviator stress causing shear failure was in excess of 0.91, the behavior might best be represented by a viscoelastic model.

Most works to date which employ viscoelastic models assume for mathematical expediency, the existence of a continuously applied constant load or a single step load in time [ 20, 55 ]. Generally, the first type of load is utilized in the study of creep phenomena while the latter is employed in the study of stress relaxation.

The time-dependent response of a soil may assume a variety of forms depending on such factors as soil type, soil structure, stress history, type of loading, and other factors [58 ]. In most studies these factors are classified into two groups of effects: a creep effect and a relaxation effect. It has been shown, Singh and Mitchell [58] and Konder and Krizek [31], that in general soils exhibit both linear and non-linear behavior. It is also commonly assumed that the magnitude of the strain is stress dependent. Thus any strain-time function which is to describe the response of such materials must: 1) be applicable to the range of stress levels encountered; 2) account for both linear and non-linear relationships between strain and time; and 3) be relatively simple in form for ease of application and determination of parameters.

72
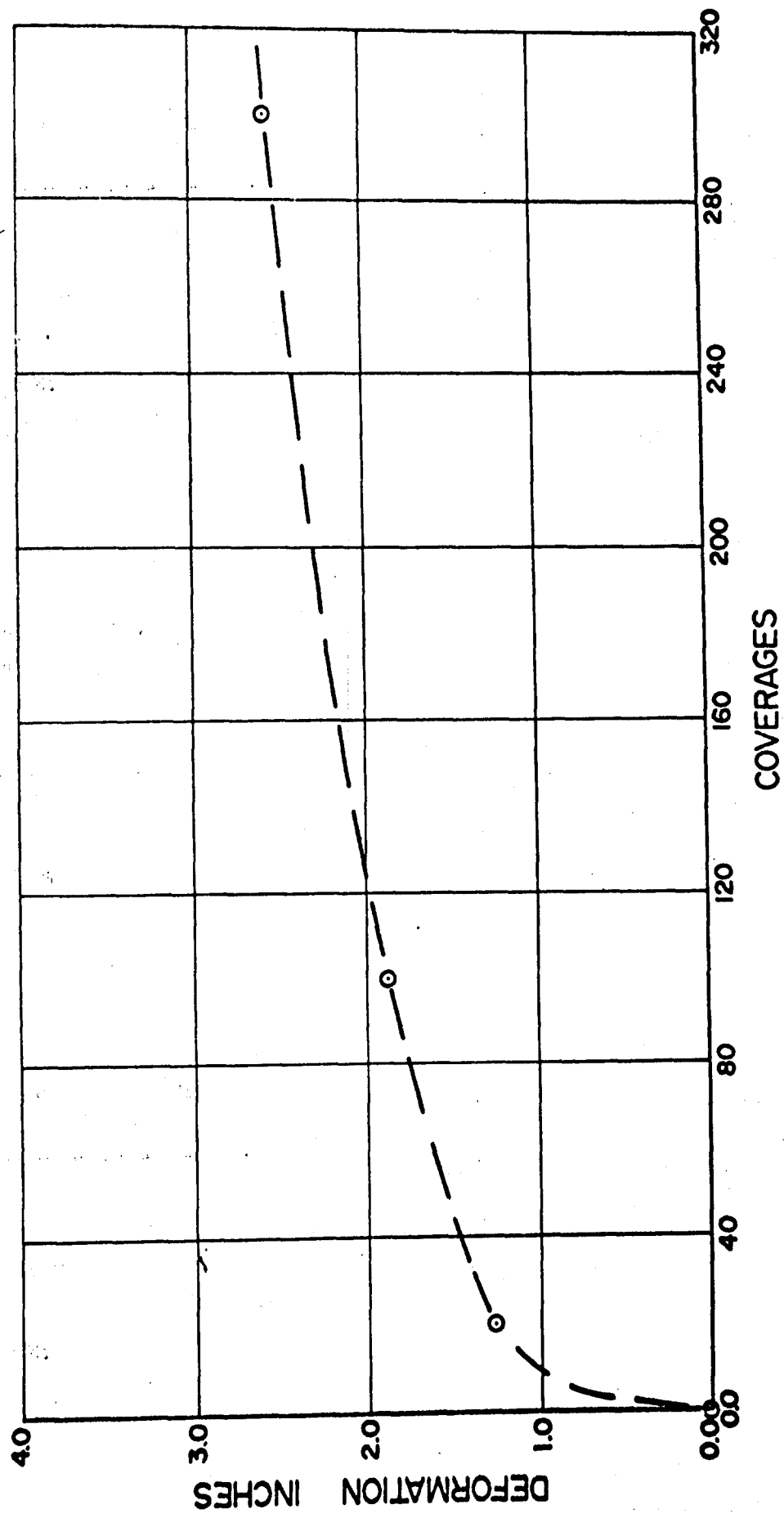
FIGURE 18. TYPICAL DEFORMATION AT THE CENTERLINE OF TRAFFIC LANE.

In this section a viscoelastic model is developed for predicting the response of landing mats to a simulation of the actual sequence of traffic loads. Although only the subgrade will be taken to possess viscoelastic properties, the model parameters which are established from the response of actual tests will also indirectly reflect the viscoelastic behavior of the landing mats.

### Analysis of Model Behavior

Assume that a load applied to a mat-soil system produces a constant stress $\sigma_1$, as shown in Figure 19(a). The response of the system due to this stress will be as shown in Figure 19(b) wherein $\epsilon_0$ represents the immediate elastic strain and $\epsilon(t)$ represents the strain for times $t > 0$. If transient effects are considered negligible in the elastic range, $\epsilon_0$ will be a constant and $\epsilon(t)$ may be expressed as

$$\epsilon(t) = \epsilon_0 + \Delta\epsilon(t) \tag{31}$$

where $\Delta\epsilon(t)$ contains all the time effects, Figure 19(b). An increase in the magnitude of the constant stress will simply displace the response curve upward, Figure 19(c). Assuming strain is time dependent and stress is independent of time, an associated stress-strain relationship will take the form

$$\epsilon(t) = D_u(t)\sigma \tag{32}$$

where $\sigma$ represents the magnitude of the (constant) stress and $D_u(t)$ is a "compliance" function. According to Schapery [55] this function can be expressed as

$$D_u(t) = D_0 + D(t) \tag{33}$$

where $D_0$ is a test dependent constant
$D(t)$ is a function of time so defined that $D(0) = 0$.

The assumption is commonly made [55, 58] that time effects can be expressed by a power law of the form

$$D(t) = D_1\left(\frac{t}{a_D}\right)^n \qquad (0 < n \leq 1) \tag{34}$$

74
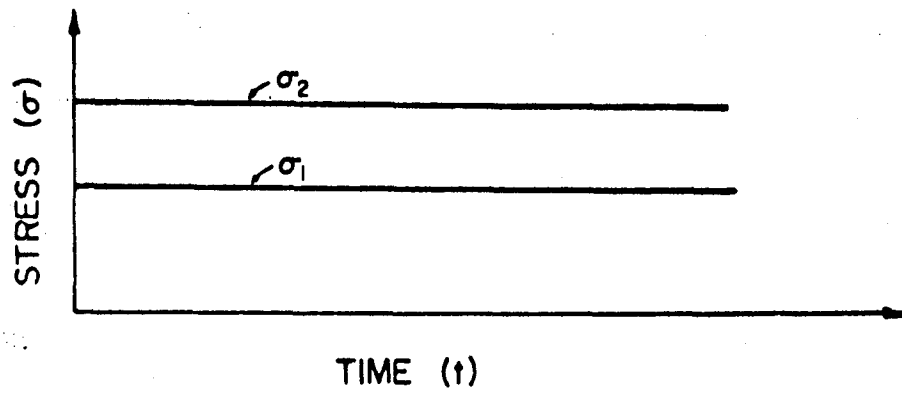
a) APPLIED STRESS
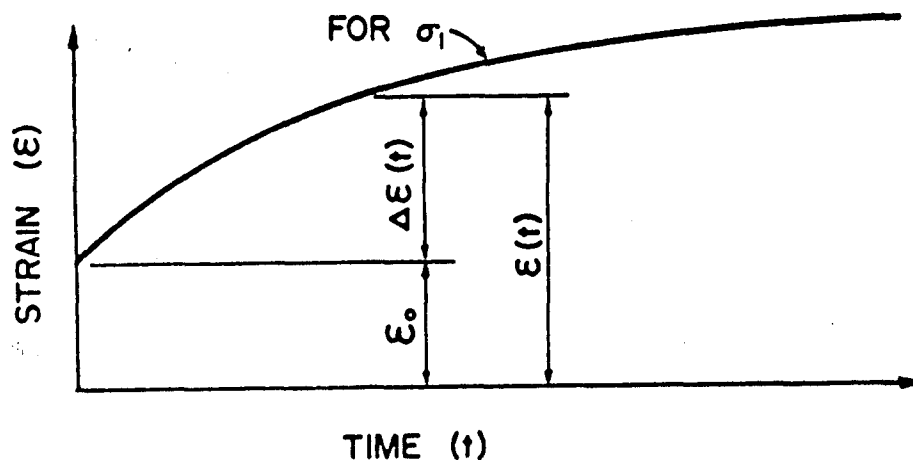
b) RESPONSE DUE TO $\sigma_1$
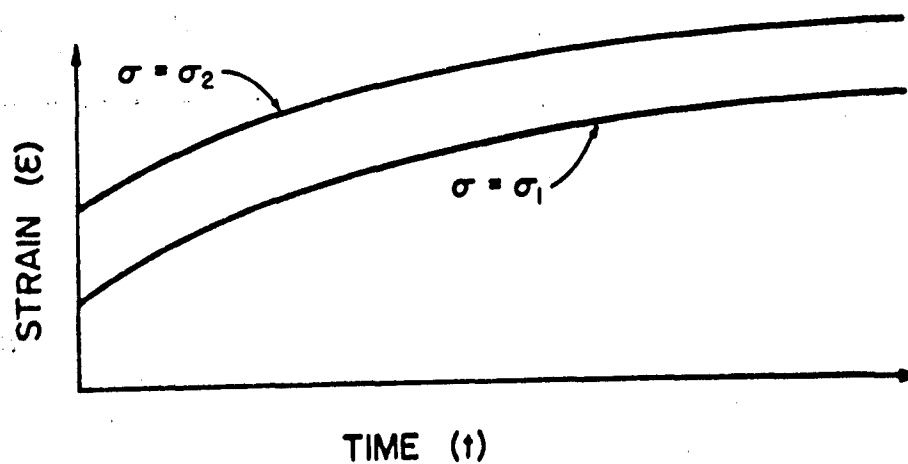
c) EFFECT OF STRESS LEVEL

FIGURE 19. STRESS - STRAIN - TIME BEHAVIOR.

where $D_1$ and n are parameters to be determined from response curves; $a_D$ is the shift factor which is stress dependent and expressed as

$$a_D = a_D(\sigma) = \left| \frac{\sigma/\sigma_j}{\sinh \sigma/\sigma_j} \right|^{1/n} \qquad (35)$$

and $\sigma_j$ is a constant. For constant stress conditions $a_D$ is seen to be equal to unity. Hence from Eqns. (32) and (33), the strain at any time $t > 0$ under a constant stress will be given by

$$\epsilon(t) = (D_0 + D_1 t^n)\sigma \qquad (36)$$

If a step stress of time duration $t_1$ is applied, the corresponding strain will be as shown in Figure 20. For any time $t < t_1$ the strain will be defined by Eqn. (36). For times $t > t_1$ the residual strain in the system can be expressed by

$$\epsilon_r(t) = [D_0 + D_1 (t)^n]\sigma - [D_0 + D_1 (t - t_1)^n]\sigma$$

or $\qquad\qquad\qquad\qquad\qquad\qquad\qquad\qquad\qquad (37)$

$$\epsilon_r(t) = [D_1 t^n - D_1 (t - t_1)^n]\sigma$$


## Development of Landing Mat-Soil Model

Under the action of a single pass of a load vehicle, a point on the surface of the subgrade experiences a normal stress variation similar to that shown in Figure 21. This stress variation can be represented by a step stress provided that the time duration for stress build-up and release is small. The effective time duration of the step stress, say $t_1 = t_{i+1} - t_i$, will be a fraction of the time required to complete one pass.

It will be assumed that trafficking of the section was continuous and performed at uniform speed. The actual time to complete one pass will then be a constant and one pass may serve as a basic time unit. Also, the duration $t_1$ of the step stress will be a constant independent of pass. The magnitude of the step stress will be dependent upon the assembly load and the position of the point under consideration relative to the path followed during the pass.

76
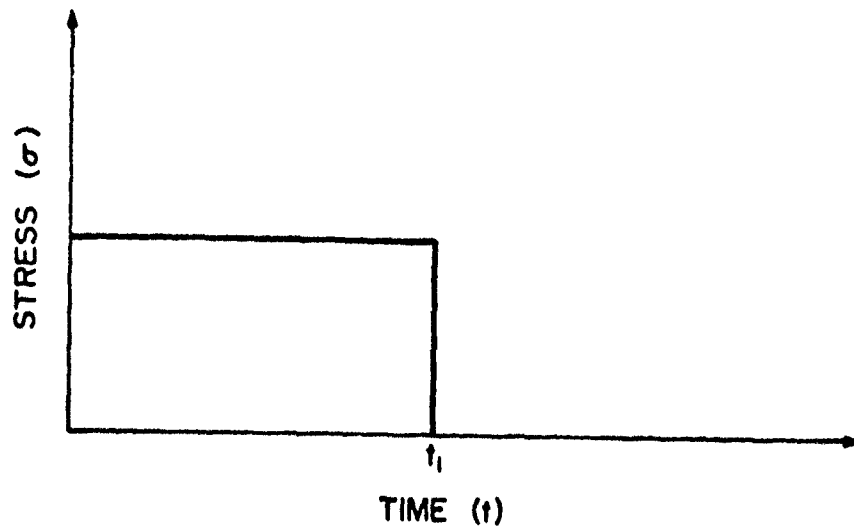
a) APPLIED STEP STRESS
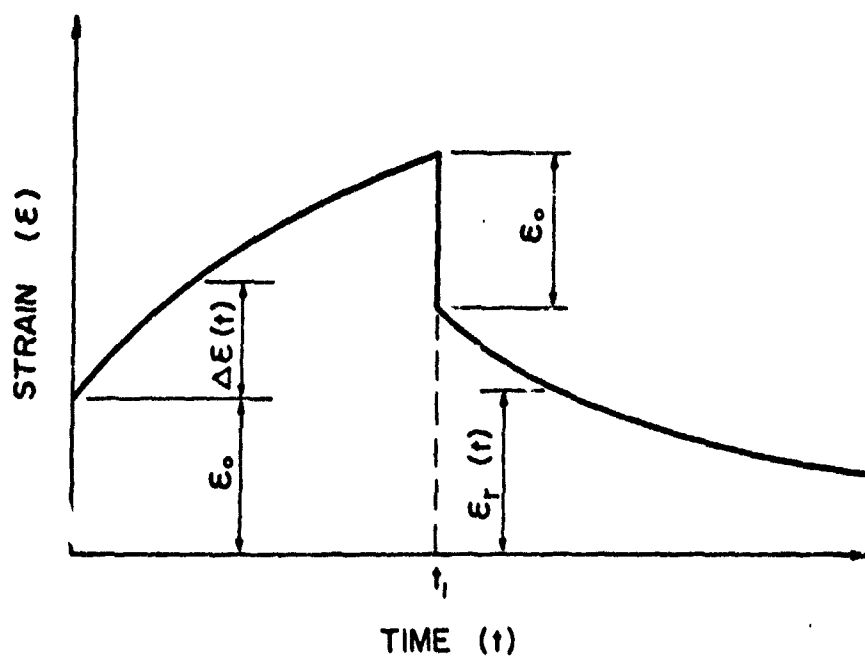


b) RESPONSE DUE TO STEP STRESS

FIGURE 20. BEHAVIOR OF SYSTEM TO APPLIED
STEP STRESS.
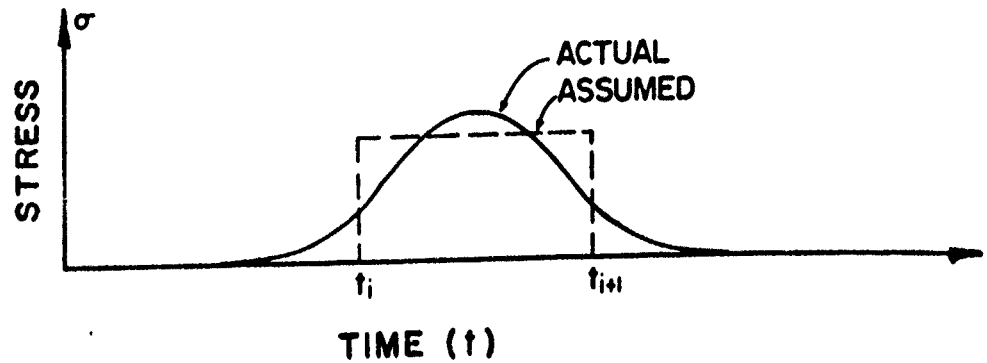
FIGURE 21. LOAD DISTRIBUTION AT A POINT DURING A SINGLE PASS.
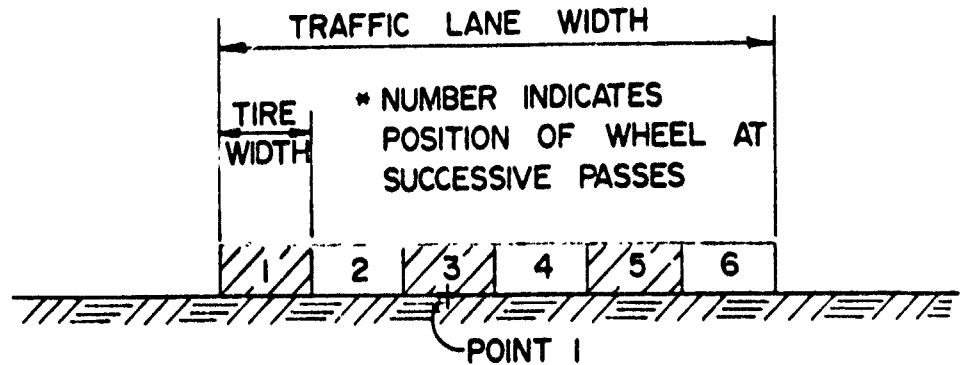


a) LOADING SEQUENCE
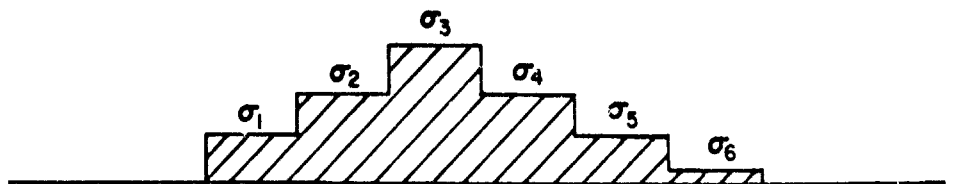


b) MAXIMUM STRESS AT POINT I

FIGURE 22. VARIATION OF STRESS WITH LOAD POSITION.

Assuming the surface displacement of the subgrade for time $t < t_1$ can be expressed by Ecn. (36), the residual displacement at the end of one pass will be given by

$$\Delta_r(1) = [D_1(1)^n - D_1(1-t_1)^n]\sigma \qquad (1 > t_1) \qquad (38)$$

where
$t_1$ is the time duration of the step stress
$\sigma$ is the magnitude of the step stress
$D_1$ and $n$ are constants.

The superposition principle may be used to extend the applicability of Ecn. (38) to more than one pass of the load vehicle. For example, if two passes of the load vehicle are made along the same path, the residual deformation at the end of the second pass will be

$$\Delta_r(2) = [D_1(2)^n - D_1(2-t_1)^n + D_1(1)^n - D_1(1-t_1)^n]\sigma \qquad (39)$$

Generalizing Eqn. (39) for any number of passes N, along the same path, one obtains

$$\Delta_r(N) = D_1\,\sigma\sum_{m=1}^{m=N}[m^n - (m-t_1)^n] \qquad (40)$$

Under normal traffic conditions the path of the load vehicle changes with passes. Thus, the magnitude of the step stress is also altered as the path of the load vehicle changes, see Figure 22. Therefore the stress is space dependent and must remain in the summation operation, Eqn. (40). The residual deformation at any number of passes regardless of the path followed would then be given by

$$\Delta_r(N) = D_1\sum_{m=1}^{m=N}[m^n - (m-t_1)^n]\sigma_m \qquad (41)^*$$

where $\sigma_m$ is the magnitude of the stress at the point for the specific position of the load vehicle.

---

* It is noted that $D_1\displaystyle\sum_{m=1}^{m=N}[m^n-(m-t_1)^n]$ is analogous to the reciprocal of the subgrade modulus used in the Winkler hypothesis assuming it to be time dependent.

A quasi-elastic analysis was developed to predict the residual deformation of a landing mat-subgrade system (computer program given in Appendix H). The model consisted of an infinite beam with rigidity identical to that of the mat and continuously supported by a subgrade whose response to loading could be expressed by Eqn. (41). The loading on the beam was designed to approximate the loading sequence employed in the prototype tests (from reference [12]) where uniform distribution of traffic was applied. The loading was made both time and space dependent. The sequence of loading for a single-wheel test is given in Figure 23 and for a dual-wheel test in Figure 24.

To be consistent with the prototype tests, the basic time unit was taken as one coverage. Due to lack of information as to the actual time to conduct the prototype tests, the duration of load application was assumed equal to one-half the time required to make one pass. This assumption may be unrealistic but lacking more information it was expedient and in addition it does not effect the validity of the model or the method of application. Only the numerical values of the parameters $D_1$ and n are influenced by this assumption. Not having adequate test information available, these parameters could only be roughly approximated.

## Results

The developed model was applied to a dual wheel test. The values of the parameters, $D_1$ and n, were obtained by comparing the model response for a point located on the centerline of the traffic lane to the actual response of the same point during the prototype test. In Figure 25, the fitted model deformation of a point on the centerline is indicated by the curve labeled "theoretical" and the actual deformation is given (by crosses) at three coverage levels. The actual deformations shown are the average of the centerline deformations at three coverage levels obtained from the two "deformation" patterns given in reference [12]. Some predicted deformation patterns at various coverage levels are shown in Figure 26.

The model was also employed for a single wheel test. Some results are given in Figure 27 and Figure 28.
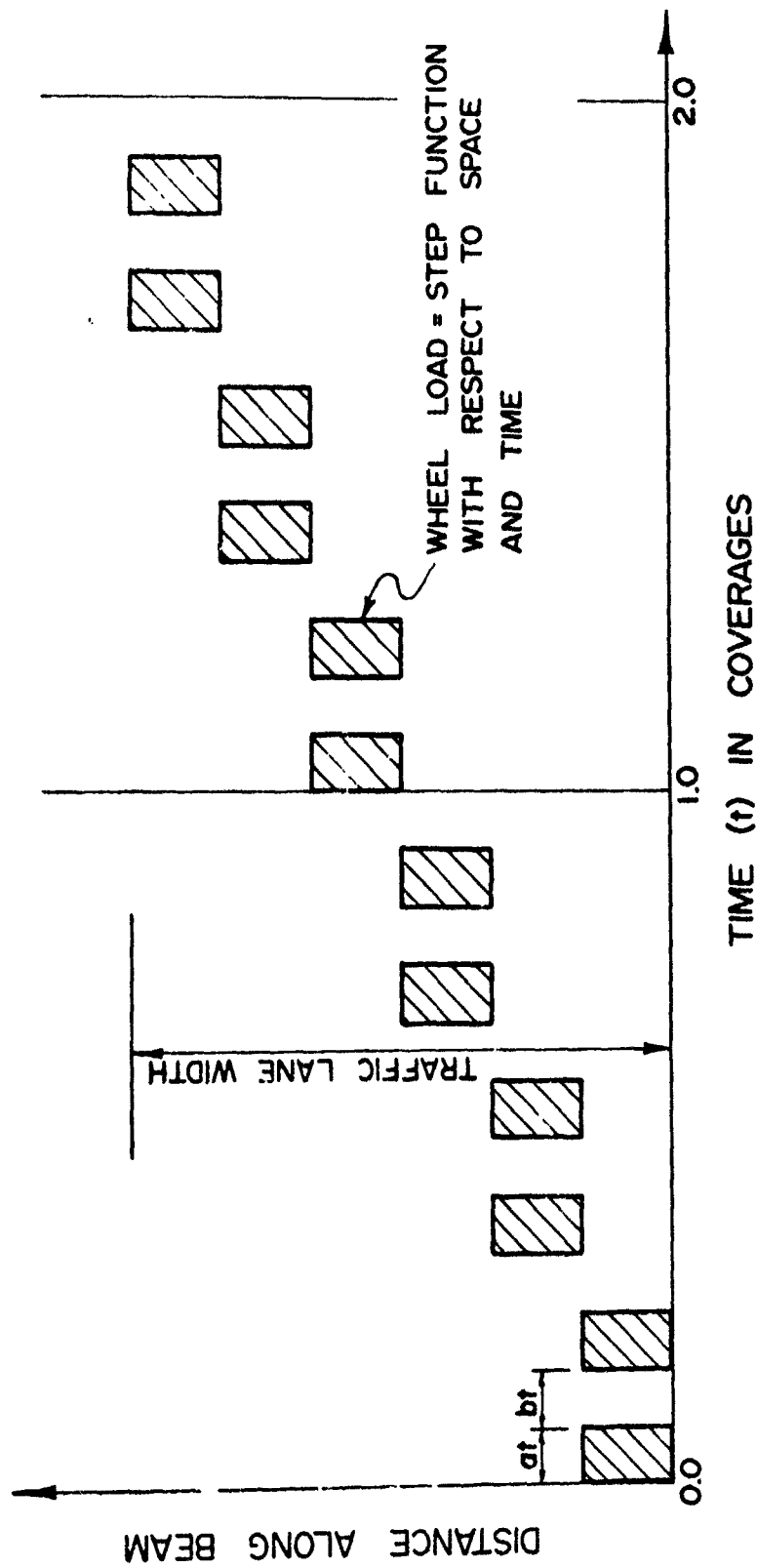
NOTE: $af = bf = 0.5./$NUMBER OF PASSES/COVERAG

FIGURE 23. LOADING ARRANGEMENT AND SEQUENCE FOR SINGLE - WHEEL TEST.
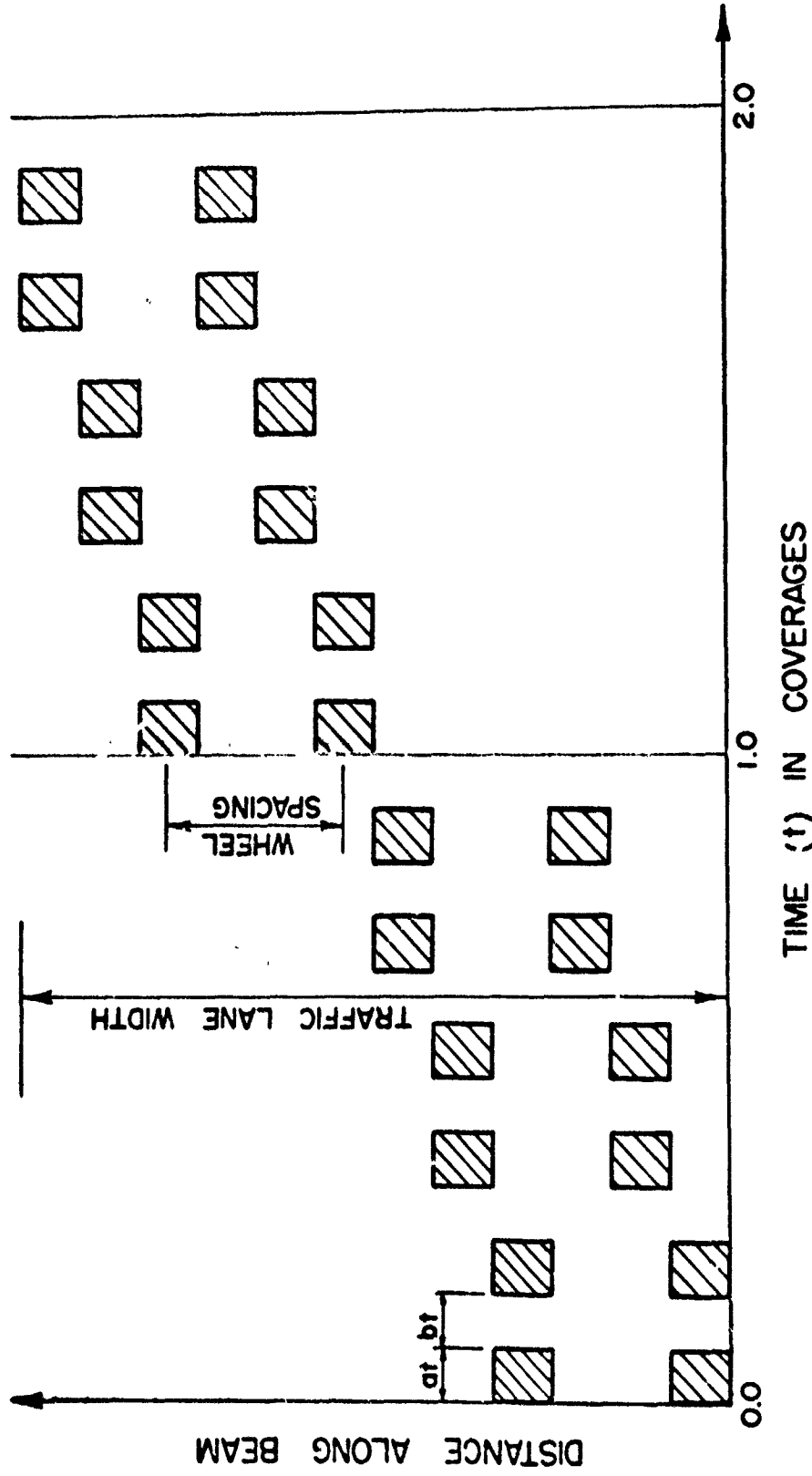
NOTE: af = bf = 0.5/NUMBER OF PASSES/COVERAGE

FIGURE 24. LOADING ARRANGEMENT AND SEQUENCE FOR DUAL - WHEEL TEST.

FIGURE 24. LOADING ARRANGEMENT AND SEQUENCE FOR LOADING TEST.



SECTION: I LANE I ITEM 3

POINT ON CENTERLINE OF TRAFFIC LANE

$D_1 = 90.0$
$n = 0.175$

THEORETICAL

+ INDICATES AVERAGE OF ACTUAL DEFORMATION AT CENTERLINE OF TRAFFIC LANE

COVERAGES
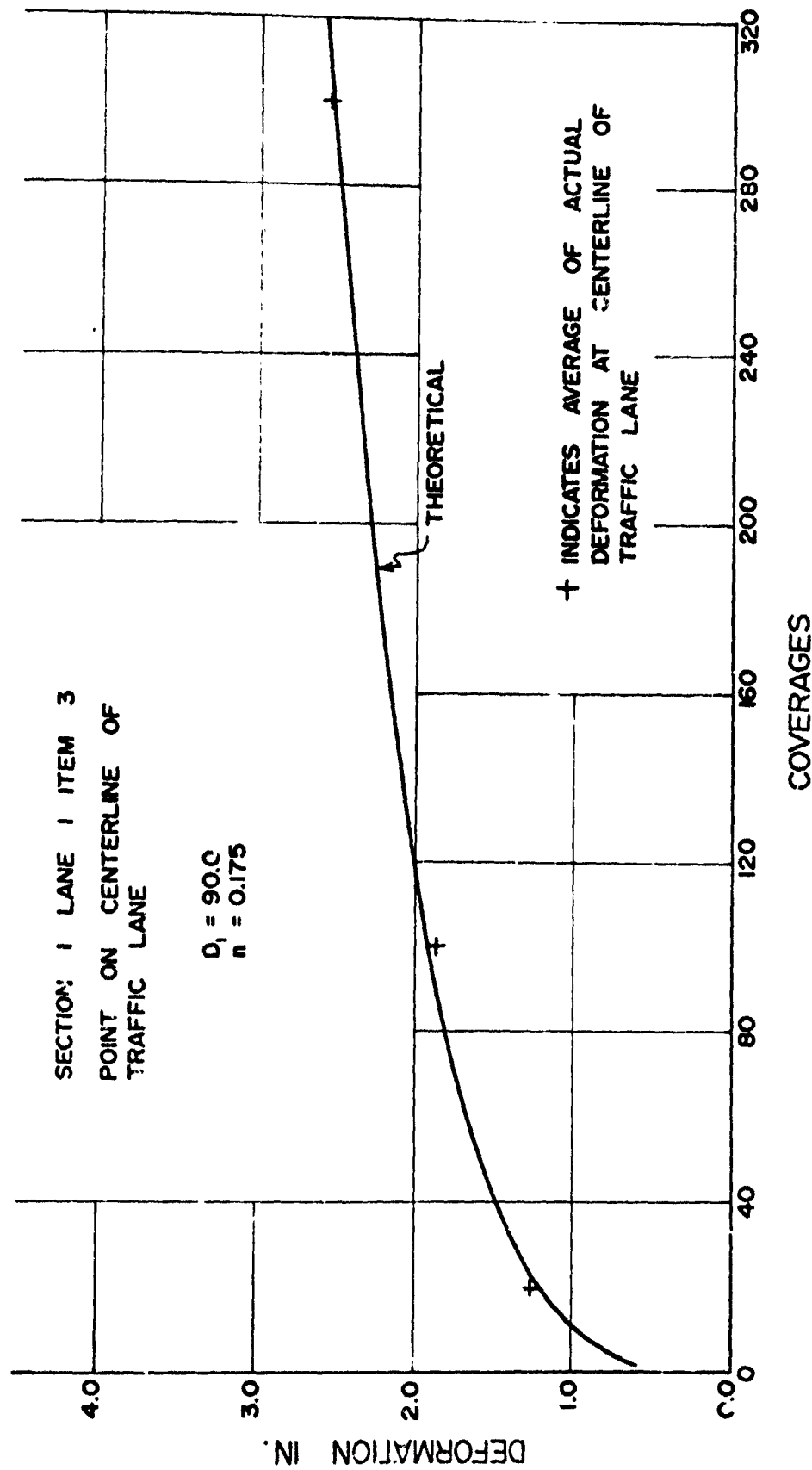
DEFORMATION IN.

FIGURE 25. COMPARISON OF DEFORMATIONS (SECTION I, LANE I, ITEM 3).

TRAFFIC LANE WIDTH = 12'

DUAL - WHEEL
ASSEMBLY LOAD = 104$^K$
AVE. INITIAL CBR = 6.75

NOTE: NUMBER ON CURVE = NUMBER OF COVERAGES
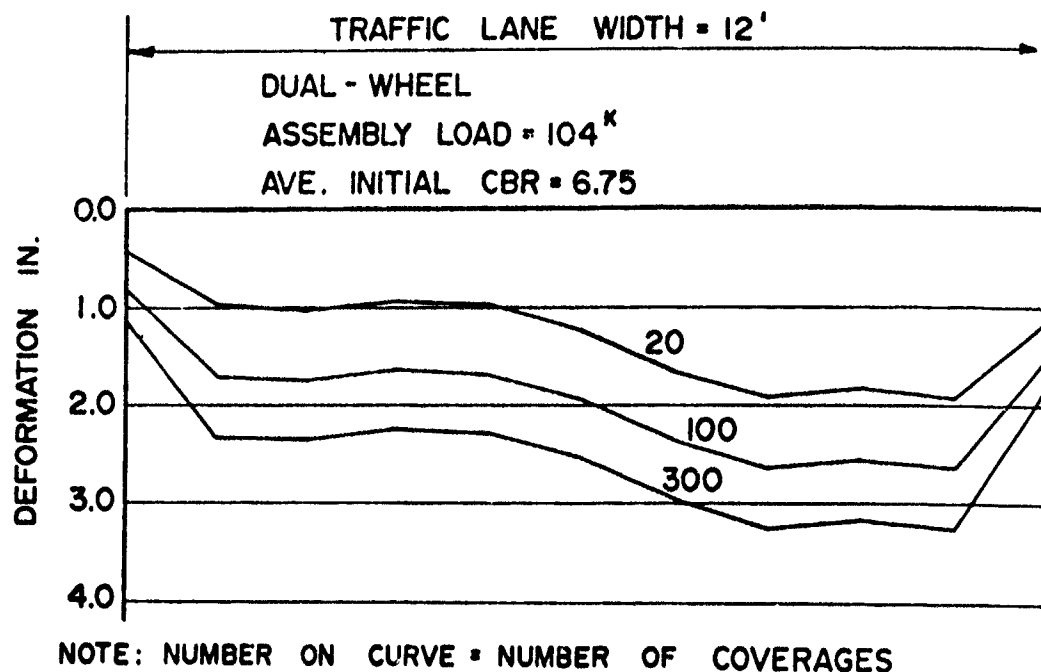
FIGURE 26. PREDICTED DEFORMATION PATTERNS
FOR SECTION 1, LANE 1, ITEM 3.



TRAFFIC LANE WIDTH = 12'

SINGLE - WHEEL
ASSEMBLY LOAD = 35$^K$
AVE. INITIAL CBR = 2.53

NOTE: NUMBER ON CURVE = NUMBER OF COVERAGES
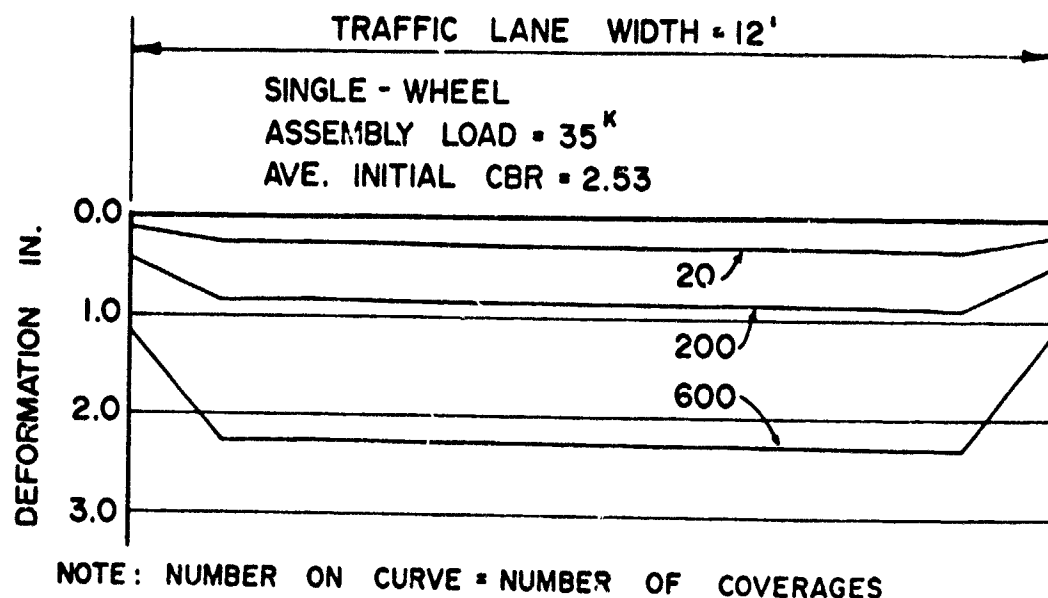
FIGURE 27. PREDICTED DEFORMATION PATTERNS
FOR SECTION 2, LANE 3, ITEM 1.

SECTION 2   LANE 3   ITEM 1

$D_i = 2.4$
$n = 0.82$

+ INDICATES AVERAGE OF ACTUAL
DEFORMATION AT CENTERLINE OF
TRAFFIC LANE

COVERAGES
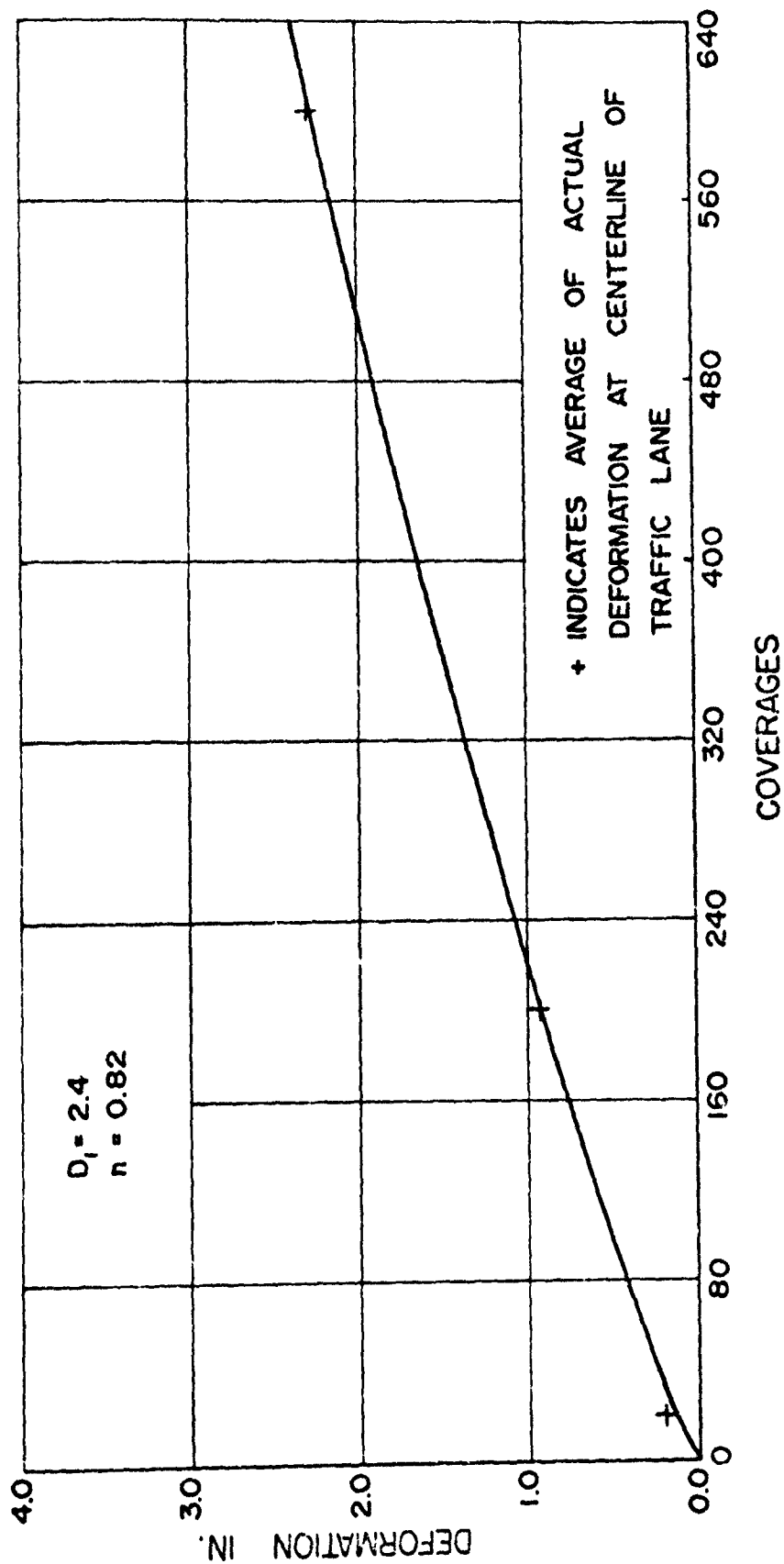
DEFORMATION   IN.

FIGURE 28.   COMPARISON OF DEFORMATIONS   (SECTION 2, LANE 3, ITEM 1).

## Discussion

It should be recalled that the parameters, $D_1$ and n shown in Figures 25 and 28, were selected so as to provide the simulation of the deformation at a single point. No attempt has been made to attach any physical significance to the values of these parameters. In addition to the usual test variables, wheel load, number of wheels, wheel spacing, contact area, mat rigidity, and soil conditions, these parameters are influenced by the width of the traffic lane and the number of positions of the load vehicle required to complete one coverage. More detailed information of the deformation-coverage response of sections and loading sequences are necessary to develop a procedure of identifying these parameters with conditions of either past or contemplated future tests.

It is noted that the shape of the deflection pattern for the dual-wheel test, Figure 26, is very different than that for the single-wheel test, Figure 27. This is due primarily to the assemblages used and the magnitude of the total load applied to the subgrade. Another contributing factor is the test procedure itself. For the dual-wheel test six different assembly locations were used to complete one coverage; whereas, for the single-wheel test, eleven assembly locations were necessary to complete one coverage. To maintain a correspondence between coverages, it was assumed that the load for the dual-wheel test was applied for a time 1.835 longer than that for the single-wheel test. For these conditions, the effect of the preceding position of loading is more pronounced for the dual-wheel test than for the single-wheel test.

Equation (41) may be generalized further. Under the assumption of a steady, continuous trafficking, the value of $t_1$ may be taken as a constant and Eqn. (41) can be expressed as the difference equation

$$\frac{\Delta_r(N)}{t_1} = D_i \sum_{m=1}^{m=N} \left[ \frac{f(m) - f(m-t_1)}{t_1} \right] \sigma_m \qquad (42)$$

Recognizing that the value of $t_1$ is small in comparison to the time required to complete one pass, the terms in the brackets may be taken as the derivative of the $f(m)$ with respect to $t_1$. The summation of this quantity approximates the integral of the derivative which is the function itself, $f(m)$. Under an average stress condition Eqn. (42) may be expressed as

$$\frac{\Delta_r(N)}{t_i} = D_1 \sigma_{ave} f(N) \qquad (43)$$

If the residual deformation at a point k can be measured at two specific number of passes, $N_i$ and $N_j$, the function $f(N)$ may be established by

$$\frac{\Delta_r(N_i)}{\Delta_r(N_j)} = \frac{f(N_i)}{f(N_j)} \qquad (44)$$

Thus the function $f(N)$ could be taken as any form which satisfies Eqn. (44).

In summary, a mechanistic model has been developed which is capable of simulating the actual loading sequence and which also provides a means whereby residual deformations of the mat surface may be predicted. The potentialities of this model have been demonstrated for a single-wheel and dual-wheel prototype test. To fruitfully pursue the capabilities of this model, more detailed test data are necessary to identify or attach physical significance to the model parameters. A continuous record of the deflection as a function of the number of passes is necessary along with a record of the position of the load vehicle during each pass. Also, information concerning the speed of the load vehicle and the time interval (expressed as a function of the time required to complete one pass) required to shift the position of the load vehicle is necessary. With this additional data and by selecting a single pass rather than a single coverage as the basic time unit, better correspondence between deformation patterns can be achieved thus allowing the possible establishment of a limiting deformation as the failure criterion.

# MOMENT TRANSFER INVESTIGATION

In most of the test sections reported in the Corps of Engineer's report [12] it was observed that the distress in the traffic lane was quite pronounced in the vicinity of the end joints of the mat elements. This is why in all simulations the load was laced in the center of the mat element. In view of this observation, a study was undertaken to investigate the effectiveness of the end joints to transfer moment from one mat element to another under simulated test conditions.

Due to the masonry type of placement of the mats, Figure 29, it was not possible to determine the amount of moment transferred solely across the end joints. A significant amount of moment could be transferred around the end joint between mat elements A and B, Figure 29, due to the transfer of shear across the transverse joints. An investigation that considers the presence of elements C and D under field conditions is further complicate, by the contact length of the tires under test loading being greater than the width of the mat element. Thus it was decided in this study to restrict the investigation to the overall influence that the presence of an end joint has on the transverse continuity of the traffic lane. Emphasis will be placed upon the performance of the T11 aluminum and the M8 steel mats as reported by the Corps of Engineers[ 10, 12].

The type of end connector employed for the T11 mat was described in some detail in the Corps of Engineer's report [11]. The method of connecting the M8 mat, which is a self-locking mat, was also described. A modified or strengthened joint connection was given in a later report [9]. An examination of the performance of these connectors suggested efficient shear transfer across the end joints; however, the capacity of the end joint to transfer moment appeared to be less than that of the mat itself. The latter is attested to by the end joints shown in the photographs, Figure 22, Part III and Figure 8, Part XI of [12]. As a consequence of the above, the assumption was made that in the simulation model there exists complete transfer of shear across the end joint.

TRANSVERSE JOINTS

ELEMENT C

ELEMENT A          ELEMENT B

ELEMENT D

END JOINT
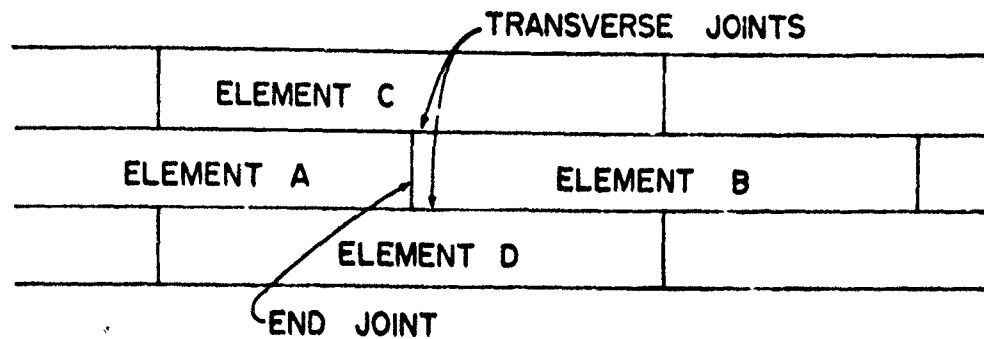
FIGURE 29. ARRANGEMENT OF MAT ELEMENTS
WITHIN THE TRAFFIC LANE.

JOINT LOCATION
WHEEL LOADS

$\infty$    $\infty$ =
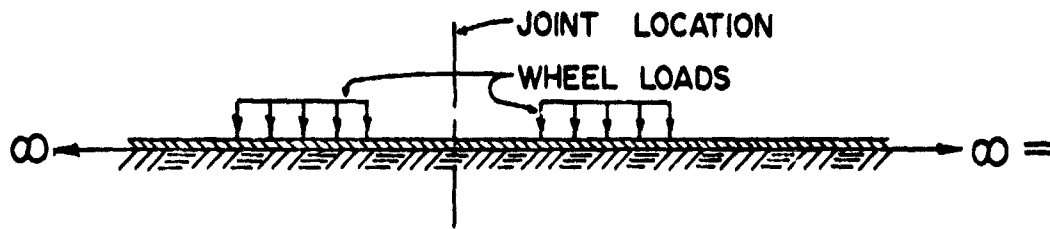
a) ACTUAL FIELD CONDITION

WHEEL LOADS

$\infty$    $\infty$ +
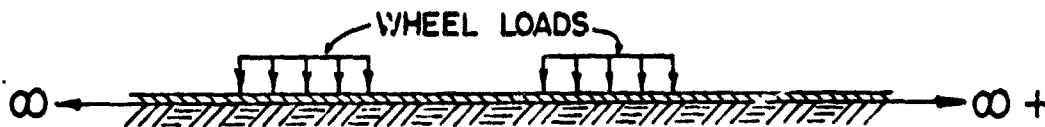
b) WHEEL LOADS ON INFINITE BEAM

HINGE LOCATION

M    M

$\infty$    $\infty$
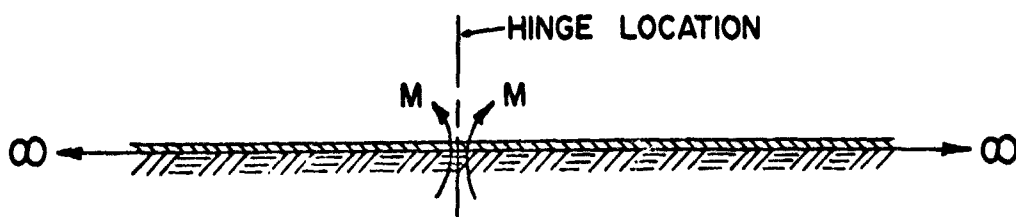
c) CONCENTRATED MOMENT APPLIED TO JOINT

FIGURE 30. SUPERPOSITION OF LOAD CONDITIONS

Since the subgrade in the prototype tests was con-
structed under tight control, it was further assumed that
the strength of the subgrade, as expressed by the k param-
eter, was uniform throughout the traffic lane. In line
with this assumption, any variation in the "average deflec-
tion" patterns (between that at the end joint and that at
the center of panel) might then be taken as a measure of
the degree to which the end joint provided moment transfer.

The mat-soil model developed earlier was employed to
simulate the "average deflection" patterns at the end joints.
The k parameter was assigned the values, Table 13, Column 5,
which resulted in a minimum of the error functional for the
previous simulation of the "average deflection" patterns at
the center of the panel. These k values were used to exclude
any inherent errors in Eqns. (13) and (14). The parameter $\gamma$
was permitted to vary with coverages in accordance with
Eqn. (15).

Postulating the validity of superposition, Figure 30,
two distinct steps were followed to simulate the "average
deflection" pattern reported in the vicinity of an end joint.
Initially, the mat was considered to be of infinite extent
and devoid of any joints. Actual wheel loads were applied
symmetrically about what would be the location of an end
joint. The moment developed in the mat at the location of
the fictitious end joint was then computed in addition to
the deflections of the nine or more discrete points used to
characterize the "average deflection" pattern. Next, the
mat was considered to be hinged and a concentrated moment
was applied at the end joint, Figure 30(c). The mathematical
development for this condition is given in Appendix E. The
deflections of the mat under the action of the concentrated
moment loading were determined and algebraically added to
the deflections of the mat wherein complete continuity was
assumed. Simulation of the "average deflection" pattern
was achieved by increasing incrementally the magnitude of
the concentrated moment until the error functional, Eqn.
(D2), was a minimum. The increment size was taken as one
percent of the moment which existed at the fictitious joint
in the infinite beam. The deficiency of moment transfer
across the end joint was taken as the ratio of the magnitude
of the concentrated moment to the moment in the assumed
infinite beam. These deficiency percentages are listed in
the last column of Table 13.

## Table 13

### End Joint Moment Transfer Deficiency Based
### Upon Uniform Subgrade Conditions

| Sect. | Lane | Item | Cov. | k-pci | Deficiency % |
|-------|------|------|------|-------|--------------|
| 1 | 1 | 3 | 0 | 54.1 | 1. |
|   |   |   | 20 | 41.4 | 1. |
|   |   |   | 200 | 41.4 | 1. |
|   |   |   | 300 | 46.0 | 1. |
| 1 | 2 | 3 | 0 | 52.5 | 337. |
|   |   |   | 20 | 43.5 | 158. |
|   |   |   | 40 | 39.8 | 197. |
| 2 | 3 | 1 | 0 | 38.4 | 107. |
|   |   |   | 200 | 28.8 | 187. |
|   |   |   | 600 | 28.7 | 271. |
| 2 | 3 | 2 | 0 | 42.6 | 531. |
|   |   |   | 120 | 57.4 | 2896. |
|   |   |   | 200 | 30.3 | 711. |
| 2 | 4 | 1 | 0 | 19.9 | 72. |
|   |   |   | 20 | 16.5 | 122. |
| 2 | 4 | 2 | 0 | 33.0 | 246. |
|   |   |   | 20 | 32.2 | 155. |
| 3 | 5 | 1 | 0 | 17.7 | 1427. |
|   |   |   | 30 | 13.2 | 504. |
| 3 | 5 | 2 | 0 | 23.5 | 104. |
|   |   |   | 30 | 19.2 | 1. |
| 3 | 6 | 1 | 0 | 12.3 | 1. |
|   |   |   | 20 | 10.5 | 1. |
|   |   |   | 76 | 15.0 | 1. |
|   |   |   | 156 | 13.9 | 1. |
| 3 | 6 | 2 | 0 | 21.8 | 78. |
|   |   |   | 20 | 15.9 | 32. |
|   |   |   | 76 | 18.4 | 41. |
| 6 | 11A | 1 | 0 | 32.1 | 73. |
|   |   |   | 20 | 27.0 | 59. |
|   |   |   | 130 | 28.4 | 64. |

91

Table 13 (cont'd.)

| Sect. | Lane | Item | Cov. | k-pci | Deficiency % |
|-------|------|------|------|-------|--------------|
| 6 | 11A | 2 | 0 | 46.8 | 1. |
|   |     |   | 20 | 38.0 | 68. |
|   |     |   | 130 | 32.6 | 47. |
| 6 | 12 | 1 | 0 | 21.6 | 48. |
|   |    |   | 20 | 18.5 | 28. |
|   |    |   | 90 | 21.6 | 1. |
| 6 | 12 | 2 | 0 | 60.0 | 134. |
|   |    |   | 20 | 34.1 | 53. |
|   |    |   | 44 | 34.3 | 79. |
| 9 | 21 | 1 | 0 | 18.9 | 85. |
|   |    |   | 20 | 15.6 | 16. |
|   |    |   | 200 | 12.6 | 8. |
|   |    |   | 300 | 11.3 | 16. |
| 9 | 21 | 2 | 0 | 29.1 | 61. |
|   |    |   | 20 | 26.7 | 106. |
|   |    |   | 200 | 25.9 | 175. |
|   |    |   | 300 | 21.8 | 186. |
| 9 | 22 | 1 | 0 | 13.9 | 1. |
|   |    |   | 20 | 15.3 | 1. |
|   |    |   | 400 | 9.6 | 1310. |
| 9 | 22 | 2 | 0 | 16.8 | 105. |
|   |    |   | 20 | 16.8 | 71. |
|   |    |   | 100 | 16.8 | 1. |
| 10 | 23A | 1 | 0 | 42.9 | 1. |
|    |     |   | 32 | 32.9 | 1376. |
| 10 | 23B | 1 | 4 | 32.1 | 1. |

For many coverage levels the percentage of moment deficiency was found to be greater than 100; obviously, the selected assumptions were in error. It was apparent for these cases that even a perfect hinge could not account mathematically for variations in the "average deflection" patterns.

To examine the assumption of uniform support (as expressed by a unique $k$ parameter), the "average deflection" patterns for the end joints were again simulated by the mat-soil model assuming an infinite beam and that no joints existed. A new value of the $k$ parameter was obtained from this simulation. A comparison of these $k$ values, denoted by $k_e$, with those obtained from the simulation of the "average deflection" patterns at the center of the mat element can be had from Table 14, Columns 5 and 7. It may be observed that, in general, the difference in the $k$ values is not large; however, they are large enough to influence the magnitude of deflections because of the great sensitivity of the model to this parameter, particularly at relatively low values of $k$. The respective simulation errors for the continuous mat analysis are also given in Table 14. A comparison of these errors indicates that considerably better simulation of the end joint "average deflection" patterns were achieved by using $k_e$.

Values of $k_e$, like those of $k$, were found to decrease with the number of coverages. More importantly, the value of $k_e$ at any coverage level was found, with only very few exceptions, to be less than that of the corresponding $k$. This tends to indicate, as was noted previously in Eqn. (13), that the mat and subgrade in the vicinity of the end joints effectively experienced more coverages (in the sense that more energy was applied).

One might speculate on the nature of the behavior at a joint. The difference in the values of $k$ and $k_e$ at zero coverages could be attributed, in part, to the inherent slack generally found in end joint connections necessary to permit such connections to be made under field conditions. Also, high stress concentrations are undoubtedly developed in the connectors which could produce local yielding of the material. A strong case can be made for the latter point by examining the distress exhibited by the end joints in the photographs accompanying the Corps of Engineer's reports [9, 10, 12].

## Table 14

## Comparison of k Values

| Sect. | Lane | Item | Cov. | k-pci | Error in./pt. | $k_e$-pci | Error in./pt. |
|-------|------|------|------|-------|---------------|-----------|---------------|
| 1 | 1 | 3 | 0 | 54.1 | .103 | 48.1 | .072 |
|   |   |   | 20 | 41.4 | .150 | 37.4 | .085 |
|   |   |   | 200 | 41.4 | .340 | 32.4 | .133 |
|   |   |   | 300 | 46.0 | .231 | 40.0 | .151 |
| 1 | 2 | 3 | 0 | 52.5 | .157 | 47.5 | .114 |
|   |   |   | 20 | 43.5 | .266 | 37.5 | .184 |
|   |   |   | 40 | 39.8 | .440 | 31.8 | .287 |
| 2 | 3 | 1 | 0 | 38.4 | .158 | 33.4 | .137 |
|   |   |   | 200 | 28.8 | .338 | 20.8 | .204 |
|   |   |   | 600 | 28.7 | .539 | 15.7 | .196 |
| 2 | 3 | 2 | 0 | 42.6 | .214 | 41.6 | .214 |
|   |   |   | 120 | 57.4 | .342 | 37.4 | .245 |
|   |   |   | 200 | 30.3 | .507 | 24.3 | .466 |
| 2 | 4 | 1 | 0 | 19.9 | .200 | 19.9 | .200 |
|   |   |   | 20 | 16.5 | .591 | 14.5 | .525 |
| 2 | 4 | 2 | 0 | 33.0 | .244 | 29.0 | .164 |
|   |   |   | 20 | 32.2 | .552 | 30.2 | .543 |
| 3 | 5 | 1 | 0 | 17.7 | .640 | 13.7 | .227 |
|   |   |   | 30 | 13.2 | 1.030 | 9.2 | .482 |
| 3 | 5 | 2 | 0 | 23.5 | .206 | 22.5 | .180 |
|   |   |   | 30 | 19.2 | .252 | 17.2 | .157 |
| 3 | 6 | 1 | 0 | 12.3 | .225 | 11.3 | .168 |
|   |   |   | 20 | 10.5 | .116 | 10.5 | .116 |
|   |   |   | 76 | 15.0 | .758 | 11.0 | .400 |
|   |   |   | 156 | 13.9 | .690 | 10.9 | .254 |
| 3 | 6 | 2 | 0 | 21.8 | .225 | 20.8 | .211 |
|   |   |   | 20 | 15.9 | .324 | 15.9 | .324 |
|   |   |   | 76 | 18.4 | .873 | 14.4 | .709 |

# Table 14 (Cont'd.)

| Sect. | Lane | Item | Cov. | k-pci | Error in./pt. | $k_e$-pci | Error in./pt. |
|-------|------|------|------|-------|---------------|-----------|---------------|
| 6 | 11A | 1 | 0 | 32.1 | .211 | 27.1 | .152 |
|   |     |   | 20 | 27.0 | .210 | 24.0 | .181 |
|   |     |   | 130 | 28.4 | .261 | 23.4 | .175 |
| 6 | 11A | 2 | 0 | 48.8 | .167 | 48.8 | .167 |
|   |     |   | 20 | 38.0 | .273 | 38.0 | .273 |
|   |     |   | 130 | 32.6 | .210 | 32.6 | .210 |
| 6 | 12 | 1 | 0 | 21.6 | .427 | 21.6 | .427 |
|   |     |   | 20 | 18.5 | .395 | 18.5 | .395 |
|   |     |   | 90 | 21.6 | .362 | 17.6 | .137 |
| 6 | 12 | 2 | 0 | 60.0 | .216 | 53.0 | .202 |
|   |     |   | 20 | 34.1 | .240 | 30.1 | .204 |
|   |     |   | 44 | 34.3 | .232 | 34.3 | .232 |
| 9 | 21 | 1 | 0 | 18.9 | .259 | 13.9 | .089 |
|   |     |   | 20 | 15.6 | .085 | 14.6 | .059 |
|   |     |   | 200 | 12.6 | .152 | 12.6 | .152 |
|   |     |   | 300 | 11.3 | .201 | 11.3 | .201 |
| 9 | 21 | 2 | 0 | 29.1 | .119 | 25.1 | .096 |
|   |     |   | 20 | 26.7 | .223 | 23.7 | .211 |
|   |     |   | 200 | 25.9 | .411 | 18.9 | .348 |
|   |     |   | 300 | 21.8 | .422 | 18.8 | .409 |
| 9 | 22 | 1 | 0 | 13.9 | .439 | 10.9 | .199 |
|   |     |   | 20 | 15.3 | 1.034 | 8.3 | .290 |
|   |     |   | 400 | 9.6 | 2.160 | 4.6 | .734 |
| 9 | 22 | 2 | 0 | 16.8 | .213 | 15.8 | .200 |
|   |     |   | 20 | 16.8 | .190 | 15.8 | .172 |
|   |     |   | 100 | 16.8 | .395 | 12.8 | .173 |
| 10 | 23A | 1 | 0 | 42.9 | .252 | 36.9 | .206 |
|    |     |   | 32 | 32.9 | .850 | 24.9 | .761 |
| 10 | 23B | 1 | 4 | 32.1 | .668 | 32.1 | .668 |

95

In general, $k_e$ decreased more rapidly with coverages than $k$ (Table 15, Columns 5 and 6). This behavior is not surprising since in all test sections the mats in the vicinity of the end joint experienced progressive deterioration due to a concentration of mat breaks (rivet failure, cracking, and curling) [12]. The weakened mat evidently losses its effectiveness and the underlying subgrade is subjected to higher energy levels. Thus in the vicinity of the end joint, the subgrade experiences larger shear deformations and considerably more remolding than in other locations.

Regardless of the exact nature of the behavior of the end joints, a measure of their effectiveness might follow from an examination of the ratios of $k_e$ to $k$. Table 15, Column 7, provides a listing of these ratios. Discounting the differences in the error functionals, average values for these ratios are 0.84 and 0.90 for the T11 and M8 mats respectively. If credence can be placed upon the above supposition, it appears that the effectiveness of the end joint connections is approximately 10 to 16 percent less than that of the mat elements. The foregoing results are not in conflict with the observations of the Corps of Engineers noted earlier [9]. Indications suggest that some increase in serviceability can be achieved by further strengthening of the end joint connector.

# Table 15

## Ratio of k Values

| Sect. | Lane | Item | Cov. | $k_N/k_{INT}$ | $(k_e)_N/(k_e)_{INT}$ | $(k_e)_N/k_N$ |
|-------|------|------|------|---------------|-----------------------|----------------|
| 1 | 1 | 3 | 0 | 1.00 | 1.00 | .89 |
|   |   |   | 20 | .77 | .78 | .91 |
|   |   |   | 200 | .77 | .67 | .79 |
|   |   |   | 300 | .85 | .83 | .87 |
| 1 | 2 | 3 | 0 | 1.00 | 1.00 | .91 |
|   |   |   | 20 | .83 | .79 | .86 |
|   |   |   | 40 | .76 | .67 | .80 |
| 2 | 3 | 1 | 0 | 1.00 | 1.00 | .87 |
|   |   |   | 200 | .75 | .62 | .73 |
|   |   |   | 600 | .75 | .47 | .55 |
| 2 | 3 | 2 | 0 | 1.00 | 1.00 | .98 |
|   |   |   | 120 | 1.35 | .90 | .65 |
|   |   |   | 200 | .71 | .59 | .80 |
| 2 | 4 | 1 | 0 | 1.00 | 1.00 | 1.00 |
|   |   |   | 20 | .83 | .73 | .88 |
| 2 | 4 | 2 | 0 | 1.00 | 1.00 | .88 |
|   |   |   | 20 | .95 | 1.07 | .94 |
| 3 | 5 | 1 | 0 | 1.00 | 1.00 | .78 |
|   |   |   | 30 | .75 | .67 | .70 |
| 3 | 5 | 2 | 0 | 1.00 | 1.00 | .96 |
|   |   |   | 30 | .82 | .76 | .90 |
| 3 | 6 | 1 | 0 | 1.00 | 1.00 | .92 |
|   |   |   | 20 | .65 | .93 | 1.00 |
|   |   |   | 76 | 1.22 | .97 | .74 |
|   |   |   | 156 | 1.13 | .96 | .79 |
| 3 | 6 | 2 | 0 | 1.00 | 1.00 | .96 |
|   |   |   | 20 | .73 | .76 | 1.00 |
|   |   |   | 76 | .84 | .69 | .79 |

Table 15 (Cont'd.)

| Sect. | Lane | Item | Cov. | $k_N/k_{INT}$ | $(k_e)_N/(k_e)_{INT}$ | $(k_e)_N/k_N$ |
|-------|------|------|------|------|------|------|
| 6 | 11A | 1 | 0 | 1.00 | 1.00 | .85 |
|   |     |   | 20 | .84 | .89 | .89 |
|   |     |   | 130 | .89 | .86 | .83 |
| 6 | 11A | 2 | 0 | 1.00 | 1.00 | 1.00 |
|   |     |   | 20 | .78 | .78 | 1.00 |
|   |     |   | 130 | .67 | .67 | 1.00 |
| 6 | 12 | 1 | 0 | 1.00 | 1.00 | 1.00 |
|   |    |   | 20 | .86 | .86 | 1.00 |
|   |    |   | 90 | 1.00 | .82 | .82 |
| 6 | 12 | 2 | 0 | 1.00 | 1.00 | .89 |
|   |    |   | 20 | .57 | .57 | .89 |
|   |    |   | 44 | .57 | .65 | 1.00 |
| 9 | 21 | 1 | 0 | 1.00 | 1.00 | .74 |
|   |    |   | 20 | .83 | 1.05 | .94 |
|   |    |   | 200 | .67 | .91 | 1.00 |
|   |    |   | 300 | .60 | .81 | 1.00 |
| 9 | 21 | 2 | 0 | 1.00 | 1.00 | .86 |
|   |    |   | 20 | .92 | .95 | .89 |
|   |    |   | 200 | .89 | .75 | .73 |
|   |    |   | 300 | .75 | .75 | .86 |
| 9 | 22 | 1 | 0 | 1.00 | 1.00 | .79 |
|   |    |   | 20 | 1.10 | .76 | .54 |
|   |    |   | 400 | .69 | .42 | .48 |
| 9 | 22 | 2 | 0 | 1.00 | 1.00 | .94 |
|   |    |   | 20 | 1.00 | 1.00 | .94 |
|   |    |   | 100 | 1.00 | .81 | .76 |
| 10 | 23A | 1 | 0 | 1.00 | 1.00 | .86 |
|    |     |   | 32 | .77 | .68 | .76 |
| 10 | 23B | 1 | 4 | 1.00 | 1.00 | 1.00 |

# SUGGESTIONS FOR FUTHER RESEARCH

Based upon the results of this study, the following suggestions for future study are presented:

1.  A study should be undertaken to establish a basic unit for defining a single coverage: one which is not test dependent.

2.  It is urged that a comprehensive study be conducted to investigate the full capabilities of the asymmetric load model described herein. Although laboratory testing of isolated subgrade samples subjected to repetitive loads would be of value for such a study, a test series, smaller in size than the conventional prototype tests, could provide meaningful data for the determination of the model parameters. Necessary information to establish the time duration for the applied load, could be obtained by installing a continuously monitored load cell at the subgrade surface of a conventional prototype test.

# SUMMARY AND CONCLUSIONS

Two mechanistic models have been developed to simulate the behavior of landing mat systems. The first model, which is based upon elastic theory, was shown to be capable of duplicating the action of such systems under static loads with a reasonably low degree of error. Numerical values for parameters entering the model were obtained from the simulation of prototype deflection patterns. Values of the k parameter, the subgrade modulus, were found to be less than 51 pci. at the start of the prototype tests. The magnitude of this parameter was then found to decrease as trafficking progressed. It is particularly noteworthy that contrary to prevailing opinion, model behavior is extremely sensitive to the magnitude of the subgrade modulus.

Empirical relationships were developed which related test properties to all model parameters. Use of these relationships along with the failure criterion established herein indicated that the performance of dual-wheel tests can be predicted with a reasonable degree of confidence. Apparently, the developed procedure is less satisfactory when employed for the prediction of single-wheel tests. There is a strong indication that the variability of the number of passes necessary to complete one coverage in the latter case may be a prime factor influencing performance. This is particularly true as input energy level per coverage can be quite different for seemingly similar situations.

It appears that the effectiveness of the end joint connections is approximately 10 to 16 percent less than that of the mat elements. Indications suggest that some increase in the serviceability of a landing mat system can be achieved by strengthening the end joint connectors.

The second mechanistic model developed is capable cf simulating actual loading sequences and can also provide a means of estimating residual deformations of the mat surface. The potentialities of this model were demonstrated for both single-wheel and dual-wheel prototype tests. Lacking adequate experimental information the full capabilities of this model could not be examined in this study.

# LIST OF REFERENCES

1. Barden, L., "Distribution of Contact Pressure under Foundations," _Geotechnique_, Vol. 12, No. 3, September, 1962, pp. 181-198.

2. Barden, L., "Approximate Solution for Finite Beams Resting on Elastic Soil," _Civil Engineering and Public Works Review_, Vol. 57, No. 676, November, 1962, pp. 1429-1433.

3. Barksdale, R. D., "Elastic and Viscoelastic Analysis of Layered Pavement Systems," _Ph.D. Thesis_, Purdue University, Lafayette, Indiana, 1966.

4. Biot, M. A., "Bending of an Infinite Beam on an Elastic Foundation," _Journal of Applied Mechanics_, Transactions of the ASME, Vol. 59, 1937, pp. A1-A7.

5. Black, W. P. M., "The Calculation of Laboratory and In-Situ Values of California Bearing Ratio from Bearing Capacity Data," _Geotechnique_, Vol. 11, No. 1, March, 1961, pp. 14-21.

6. Burmister, D. M., "The Theory of Stresses and Displacements in Layered Systems and Applications to the Design of Airport Runways," _Proceedings of the Highway Research Board_, Vol. 23, 1943, pp. 126-144.

7. Cheung, Y. K., Discussion of Paper by L. Barden, "Distribution of Contact Pressure under Foundations," _Geotechnique_, Vol. 13, No. 1, March, 1963, pp. 14-21.

8. Corps of Engineers, U. S. Army, "Development of Tentative CBR Design Curves for Landing Mats," _Miscellaneous Paper No. 4-29_, Waterways Experiment Station, Vicksburg, Miss., December, 1952.

9. Corps of Engineers, U. S. Army, "Theoretical Landing Mat Studies," _Technical Memorandum No. 3-418_, Waterways Experiment Station, Vicksburg, Miss., October, 1955.

10. Corps of Engineers, U. S. Army, "Criteria for Designing Runways to be Surfaced with Landing Mat and Membrane-Type Materials," Technical Report No. 3-539, Waterways Experiment Station, Vicksburg, Miss., April, 1960.

11. Corps of Engineers, U. S. Army, "Engineering Tests of Experimental T11 Aluminum Airplane Landing Mat," Technical Report No. 3-634, Waterways Experiment Station, Vicksburg, Miss., September, 1963.

12. Corps of Engineers, U. S. Army, "Aircraft Ground-Floatation Investigation," Technical Documentary Report AFFDL-TDR-66-43, Part I, II, III, IV, V, VII, X, XI, XIII, Air Force Flight Dynamics Laboratory, Wright-Patterson Air Force Base, Ohio, 1966.

13. Davis, E. H., and Taylor, H., "The Surface Displacement of an Elastic Layer due to Horizontal and Vertical Surface Loading," Proceedings, Fifth International Conference on Soil Mechanics and Foundation Engineering, Vol. 1, Paris, 1961, pp. 621-627.

14. DeBeer, E. E., "Computation of Beams Resting on Soil," Proceedings, Second International Conference on Soil Mechanics and Foundation Engineering, Vol. 1, Rotterdam, 1948, pp. 119-121.

15. DeBeer, E. H., "Tests for the Determination of the Distribution of Soil Reactions underneath Beams Resting on Soil," Proceedings, Second International Conference on Soil Mechanics and Foundation Engineering, Vol. 2,

16. Drapkin, B., "Grillage Beams on Elastic Foundation," Proceedings of the ASCE, Vol. 81, No. 771, August, 1955, pp. 771:1-771:19.

17. Filonenko-Borodich, M. M., "Some Approximate Theories of the Elastic Foundation," Uchenyie Zapiski Moskovskogo Gosudarstvennogo Universiteta Mekhanica, No. 46, 1940, pp. 3-18, (In Russian).

18. Florin, V. A., "Analyses of Foundations for Hydro-Engineering Structures," Raschety Osnovanii Gidrotekhnicheskikh Sooruzhenii, Stroiizdat, 1948.

19. Foppl, A., Vorlesungen uber technische Mechanik, Vol. 5, B. G. Teuber, Leipzig, 1922, pp. 20-22.

20. Freudenthal, A. M., and Lorsch, H. G., "The Infinite Elastic Beam on a Linear Viscoelastic Foundation," Journal of the Engineering Mechanics Division, Proceedings of the ASCE, Vol. 83, No. EM1, January, 1957, pp. 1158:1-1158:22.

21. Gazis, D. C., "Analysis of Finite Beams on Elastic Foundations," Journal of the Structural Division, Proceedings of the ASCE, Vol. 84, No. ST4, July, 1958, pp. 1722:1-1722:18.

22. Gorbunov-Posadov, M. I., Beams and Plates on an Elastic Base, Stroiizdat, Moscow, 1949.

23. Gorbunov-Posadov, M. I., and Serebrjanyi, R. V., "Design of Structures on Elastic Foundations," Proceedings, Fifth International Conference on Soil Mechanics and Foundation Engineering, Vol. 1, Paris, 1961, pp. 643-648.

24. Harr, M. E., and Leonards, G. A., "Analysis of Concrete Slabs on Ground," Journal of the Soil Mechanics and Foundations Division, Proceedings of the ASCE, Vol. 85, No. SM 3, June, 1959, pp. 35-58.

25. Hayashi, K., Theorie des Tragers auf elastischer Unterlage, J. Springer, Berlin, 1921, pp. 31-33.

26. Hetenyi, M., Beams on Elastic Foundations, The University of Michigan Press, Ann Arbor, 1946.

27. Hoskin, B. C., and Lee, E. H., "Flexible Surfaces on Viscoelastic Subgrades," Journal of the Engineering Mechanics Division, Proceedings of the ASCE, Vol. 85, No. EM4, October, 1959, pp. 11-30.

28. Kerr, A. D., "Viscoelastic Winkler Foundation with Shear Interaction," Journal of the Engineering Mechanics Division, Proceedings of the ASCE, Vol. 87, No. EM 3, June, 1961, pp. 13-30.

29. Klepikov, S. N., "Calculation of Beams on an Elastic Foundation with a Variable Modulus of Subgrade Reaction," Soil Mechanics and Foundation Engineering, No. 5, September-October, 1965, Consultants Bureau, New York, pp. 296-299.

30. Kohr, R. H., "On the Identification of Linear and Nonlinear Systems," Simulation, Vol. 8, No. 3, March, 1967, pp. 165-174.

31. Konder, R. L., and Krizek, R. J., "Creep Compliance Response of a Cohesive Soil," *Journal of the Franklin Institute*, Vol. 279, No. 5, May, 1965, pp. 366-373.

32. Langhaar, H. L., *Dimensional Analysis and Theory of Models*, Wiley, New York, 1951.

33. Larew, H. G., and Leonards, G. A., "A Strength Criterion for Repeated Loads," *Proceedings of the Highway Research Board*, Vol. 41, 1962, pp. 529-556.

34. Lee, I. K., "Elastic Settlements of Footing with Rough Interface," *Proceedings, Fourth Australia-New Zealand Conference on Soil Mechanics and Foundation Engineering*, August, 1963, pp. 225-232.

35. Lemcoe, M. M., "Stresses in Layered Elastic Solids," *Journal of the Engineering Mechanics Division*, Proceedings of the ASCE, Vol. 86, No. EM4, August, 1960, pp. 1-22.

36. Lenczner, D., "Variation of Subgrade Modulus with Depth of Sand," *Civil Engineering and Public Works Review*, Vol. 57, No. 667, February, 1962, pp. 210-212.

37. Leonov, M. Ia, "Consideration of Horizontal Forces in the Analysis of an Infinite Plate on the Elastic Half-Space," *Prikl. Mat. Mekh.*, Vol. 3, No. 3, 1949.

38. Malter, H., "Numerical Solutions for Beams on Elastic Foundations," *Transactions of the ASCE*, Vol. 125, 1960, pp. 757-791.

39. Murphy, G., *Stresses and Deflections in Loaded Rectangular Plates on Elastic Foundations*, Bulletin 135, Iowa Engineering Experiment Station, Ames, 1937.

40. Noble, B., "The Exploration of Functional Relationships - An Aspect of Optimization," *Applications of Undergraduate Mathematics in Engineering*, MacMillan, New York, 1967.

41. Panchanathan, S., and Chandrasekaran, V. S., "Study of Contact Pressure Distribution below Symmetrically Loaded Rectangular Footings," *Journal of Scientific and Industrial Research*, Vol. 21D, No. 10, October, 1962, pp. 356-361.

42. Pasternak, P. L., "On a Method of Analysis of an Elastic Foundation by Means of Two Foundation Constants," _Gosuedarstvennoe Izadatelstvo Literaturi po Stroitelstvu i Arkhitekture_, Moscow, 1954, (In Russian).

43. Pickett, G., et al., "Deflections, Moments, and Reactive Pressures for Concrete Pavements," _Kansas State College Bulletin No. 65_, Manhattan, Kansas, October, 1951.

44. Pickett, G., "Analytical Studies of Landing Mats for Forward Airfields," _Final Report to Corps of Engineers_, Waterways Experiment Station, Vicksburg, Miss., December, 1951.

45. Pickett, G., "Analytical Studies of Orthotropic Landing Mats for Forward Airfields," _Miscellaneous Paper No. 4-113_, Corps of Engineers, Waterways Experiment Station, Vicksburg, Miss., February, 1955.

46. Pister, K. S., "Viscoelastic Plate on a Viscoelastic Foundation," _Journal of the Engineering Mechanics Division_, Proceedings of the ASCE, Vol. 87, No. EM1, February, 1961, pp. 43-54.

47. Pister, K. S., and Williams, M. L., "Bending of Plates on a Viscoelastic Foundation," _Journal of the Engineering Mechanics Division_, Proceedings of the ASCE, Vol. 86, No. EM5, October, 1960, pp. 31-44.

48. Popov, E. P., "Successive Approximation for Beams on an Elastic Foundation," _Proceedings of the ASCE_, Vol. 76, No. 18, May, 1950, pp. 18:1-18:13.

49. Portland Cement Association, _Concrete Pavement Design_, Portland Cement Association, Chicago, Ill., 1951, p. 11.

50. Portland Cement Association, _PCA Soil Primer_, Portland Cement Association, Chicago, Ill., 1962, p. 36.

51. Ray, K. C., "Influence Lines for Pressure Distribution under a Finite Beam on Elastic Foundations," _Journal of American Concrete Institute_, Vol. 30, No. 6, December, 1958, pp. 729-740.

52. Reissner, E., "A Note on Deflections of Plates on a Viscoelastic Foundation," _Transactions of the ASME_, Vol. 25, No. 1, March, 1958, pp. 144-145.

53. Schapery, R. A., "A Method of Viscoelastic Stress Analysis Using Elastic Solutions," Journal of the Franklin Institute, Vol. 279, No. 4, April, 1965, pp. 268-289.

54. Schapery, R. A., "Stress Analysis of Viscoelastic Composite Materials," Journal of Composite Materials, Vol. 1, No. 3, July, 1967, pp. 228-267.

55. Schapery, R. A., "On the Application of a Thermodynamic Constitutive Equation to Various Nonlinear Materials," Report AA and ES 68-4, Purdue Research Foundation, West Lafayette, Indiana, June, 1968.

56. Schiel, F., "Der Schwimmende Balken," Zeitschrift fur angewandte Mathematik und Mechanik, Vol. 22, 1942.

57. Schultze, E., "Distribution of Stress Beneath a Rigid Foundation," Proceedings, Fifth International Conference on Soil Mechanics and Foundation Engineering, Vol. 1, Paris, 1961, pp. 807-813.

58. Singh, A. and Mitchell, J. K., "General Stress-Strain-Time Function for Soils," Journal of the Soil Mechanics and Foundations Division, Proceedings of the ASCE, Vol. 94, No. SM1, January, 1968, pp. 21-46.

59. Sinitsyn, A. P., Computations of Beams and Plates on Elastic Bases for Limiting Elasticity, Stroiizdat, Moscow, 1964, (In Russian).

60. Sovinc, I., "Stresses and Displacements in a Limited Layer of Uniform Thickness, Resting on a Rigid Base, and Subjected to an Uniformly Distributed Flexible Load of Rectangular Shape," Proceedings, Fifth International Conference on Soil Mechanics and Foundation Engineering, Vol. 1, Paris, 1961, pp. 823-827.

61. Stepwise Regression, BMD2R, Computer Science Center, Purdue University, Lafayette, Indiana, December, 1965.

62. Terzaghi, K., "Evaluation of Coefficients of Subgrade Reaction," Geotechnique, Vol. 5, No. 4, December, 1955, pp. 297-326.

63. Vlasov, V. Z., and Leont'ev, N. N., Beams, Plates, and Shells on an Elastic Foundation, (Translated from Russian), Israel Program for Scientific Translations, Jerusalem, 1966.

64. Westergaard, H. M., "Stresses in Concrete Pavements Computed by Theoretical Analysis," Journal of Public Roads, Vol. 7, No. 2, 1926, pp. 25-35.

65. Westergaard, H. M., "New Formulas for Stresses in Concrete Pavements of Airfields," Proceedings of the ASCE, Vol. 73, 1947, pp. 687-701.

66. Wilde, D. J. and Beighter, C. S., "Direct Climbing," Foundations of Optimization, Prentice-Hall, New Jersey, 1967, pp. 288-313.

67. Winkler, E., Die Lehre von der Elasticitaet and Festigkeit, Dominicus, Prag., 1867.

68. Yoder, E. J., Principles of Pavement Design, Wiley, New York, 1964.

69. Zhemochkin, B. N., Practical Method of Calculating Foundations, Beams, and Plates on Elastic Bases, Gos. Izd. Lit. Stroit., Arkh. i Stroit. Mater., Moscow, 1962, (In Russian).

70. Zimmermann, H., Die Berechnung des Eisenbahnoberbaues, Berlin, 1888.

# APPENDIX A

## VARIATIONAL METHOD OF ANALYSIS FOR ELASTIC FOUNDATIONS

The variational method of analysis for elastic foundations presented here was developed originally by Vlasov and Leont'ev [63]. Due to the limited circulation of this important publication, a detailed formulation is given for a single-layer foundation under plane strain conditions.

Consider a homogeneous, elastic compressible layer of soil of thickness H resting on a rigid base subjected to imposed loadings which produce conditions of plane strain, Figure Al(a). Under such conditions if the horizontal and vertical displacements, respectively, u(x,y) and v(x,y), at all points are known, the stresses and strains in the soil layer may be obtained from established stress-strain relationships. Following Vlasov and Leont'ev, the unknown displacements will be taken as the finite series

$$u(x,y) = \sum_{i=1}^{m} U_i(x)\, \phi_i(y) \qquad (i = 1, 2, 3,\ldots m) \quad \text{(Ala)}$$

$$v(x,y) = \sum_{k=1}^{n} V_k(x)\, \psi_k(y) \qquad (k = 1, 2, 3,\ldots n) \quad \text{(Alb)}$$

Here it is assumed that the functions $\phi_i(y)$ and $\psi_k(y)$, which represent, respectively, the distribution of the displacements u(x,y) and v(x,y) over any section x = constant, are either known or may be assigned. With $\phi_i(y)$ and $\psi_k(y)$ established as dimensionless functions, the functions $U_i^k(x)$ and $V_k(x)$ will have dimensions of length. The latter are seen to represent the magnitude of the displacements u(x,y) and v(x,y) at the section x = constant.

Once the form of the functions $\phi_i(y)$ and $\psi_k(y)$ are established for a given physical problem the functions $U_i(x)$ and $V_k(x)$ can be determined from equilibrium conditions relative to a differential strip of length dx, Figure Al(b), and the stress-strain relationships developed from the conventional theory of elasticity.
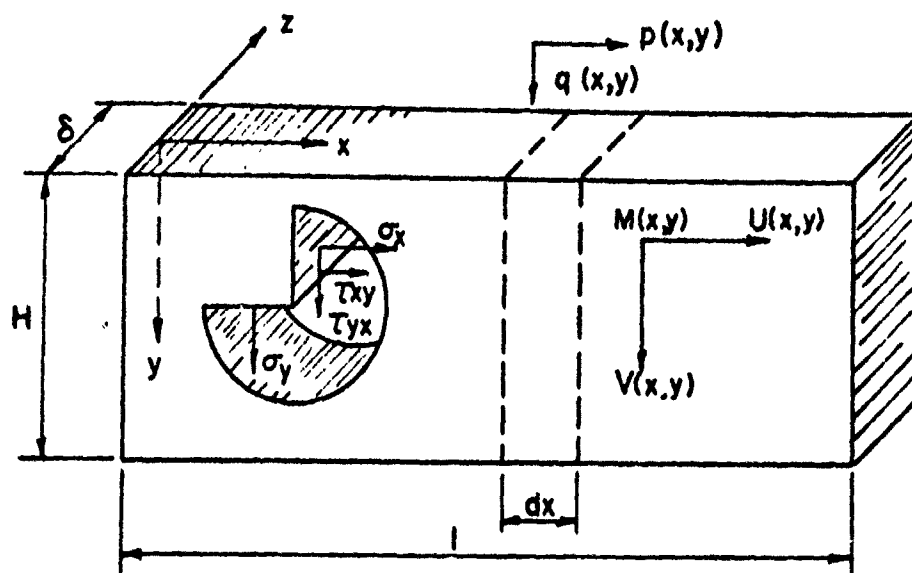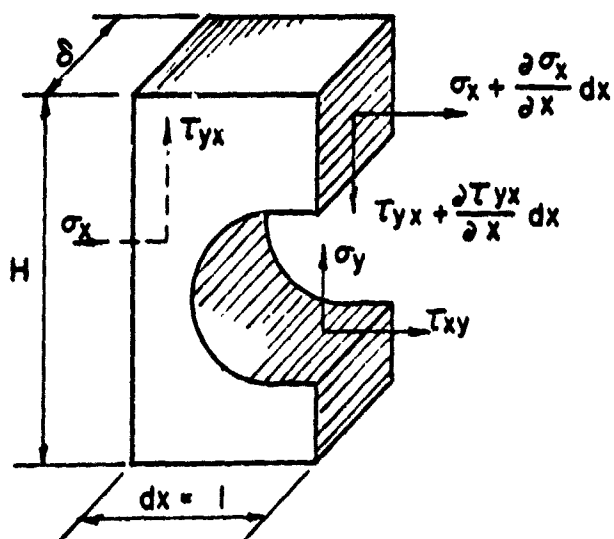
FIGURE AI.  STRESS  STATE  IN  SOIL  MASS.

From the Hookean stress-strain relationship, the stresses may be expressed as

$$\sigma_x = \frac{E_0}{1-\mu_0^2}\left[\sum_{i=1}^{m} U_i'\phi_i + \mu_0 \sum_{k=1}^{n} V_k\psi_k'\right] \qquad (A2a)$$

$$\sigma_y = \frac{E_0}{1-\mu_0^2}\left[\sum_{k=1}^{n} V_k\psi_k' + \mu_0 \sum_{i=1}^{m} U_i'\phi_i\right] \qquad (A2b)$$

$$\tau_{xy} = \frac{E_0}{2(1+\mu_0)}\left[\sum_{i=1}^{m} U_i\phi_i' + \sum_{k=1}^{n} V_k'\psi_k\right] \qquad (A3b)$$

The equilibrium conditions are obtained by equating the work of all internal forces to the work of all external forces acting on the strip under any virtual displacement.

Consider the differential strip when given a virtual displacement in the x direction, $\bar{u}_i = \phi(y)$ for $U_i = 1$ where i can have m different values, and a virtual displacement in the y direction, $\bar{v}_k = \psi_k(y)$ for $V_k = 1$ where k can be any of n virtual displacements. The differential strip thus possesses (m + n) degrees of freedom in the xy plane. The external forces acting on this strip result from the normal stresses, $\sigma_x$, $\sigma_x + \frac{\partial\sigma_x}{\partial x} dx$, the shearing stresses, $\tau_{yx}$, $\tau_{yx} + \frac{\partial\tau_{yx}}{\partial x} dx$, and from the distributed applied load whose x and y components (per unit of length) are $\bar{p}(x,y)$ and $\bar{q}(x,y)$, respectively. The internal forces are caused by the normal stresses $\sigma_y$ and the shearing stresses $\tau_{xy}$. An examination of Figures A2(a) and A2(b) provides the following relationships:

in the x direction, Figure A2(a),

$$\int_0^Y \tau_{xy}\phi_i' \,\delta dy = \int_0^Y \frac{\delta\sigma_x}{\delta x}\phi_i\,\delta dy + \int_0^Y \bar{p}(x,y)\phi_i\,dy \qquad (A3)$$

$$(i = 1, 2, 3,\ldots m)$$

110

in the y direction, Figure A2(b),

$$\int_0^Y \sigma_y \psi_k \delta dy = \int_0^Y \frac{\partial \tau_{yx}}{\partial x} \psi_k \delta dy + \int_0^Y \bar{q}(x,y) \psi_k dy \qquad (A4)$$

$$(k = 1, 2, 3, \ldots n)$$

Substitution of Eqns. (A2) into Eqns. (A3) and (A4) leads to a system of ordinary differential equations in $U_i(x)$ and $V_k(x)$. This system consists of $(m + n)$ equations and can be expressed as

$$\sum_{i=1}^m a_{ij} U_i'' - \frac{(1-\mu_0)}{2} \sum_{i=1}^m b_{ij} U_i + \sum_{k=1}^n \left(\mu_0 t_{jk} - \frac{1-\mu_0}{2} c_{jk}\right) V_k' + \frac{1-\mu_0}{E_0} q_h = 0$$

$$(A5a)$$

$$(j = 1, 2, 3, \ldots m)$$

$$-\sum_{i=1}^n \left(\mu_0 t_{hi} - \frac{(1-\mu_0)}{2} c_{hi}\right) U_i' + \frac{(1-\mu_0)}{2} \sum_{k=1}^n r_{hk} V''_{hk} - \sum_{k=1}^n s_{hk} U_k + \frac{(1-\mu^2)}{E_0} q_h = 0$$

$$(A5b)$$

$$(h = 1, 2, 3, \ldots n)$$

where the coefficients are obtained from the following

$$a_{ij} = \int \phi_i \phi_j \delta dy \; ; \; r_{hk} = \int \psi_h \psi_k \delta dy \qquad (A6a)$$

$$b_{ij} = \int \phi_i' \phi_j' \delta dy \; ; \; s_{hk} = \int \psi_h' \psi_k' \delta dy \qquad (A6b)$$

$$c_{ij} = \int \phi_i' \psi_j \delta dy \; ; \; c_{hi} = \int \psi_h \phi_i' \delta dy \qquad (A6c)$$

$$t_{jk} = \int \phi_j \psi_k' \delta dy \; ; \; t_{hi} = \int \psi_h' \phi_k \delta dy \qquad (A6d)$$

$$p_j = \int \bar{p}(x,y) \phi_j dy \; ; \; q_h = \int \bar{q}(x,y) \psi_h dy \qquad (A6e)$$

where the loads $\bar{p}(x,y)$ and $\bar{q}(x,y)$ are taken as positive when acting in the positive direction of the coordinate axis.
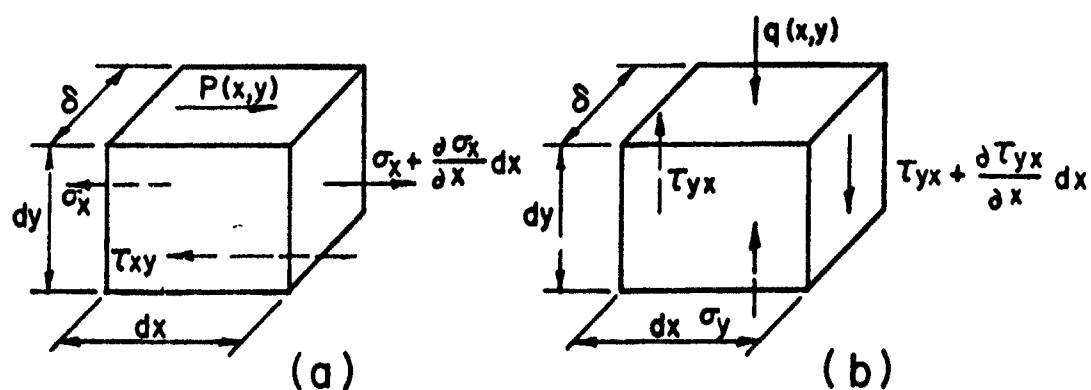
FIGURE A2.  DIFFERENTIAL ELEMENTS
OF SOIL MASS.
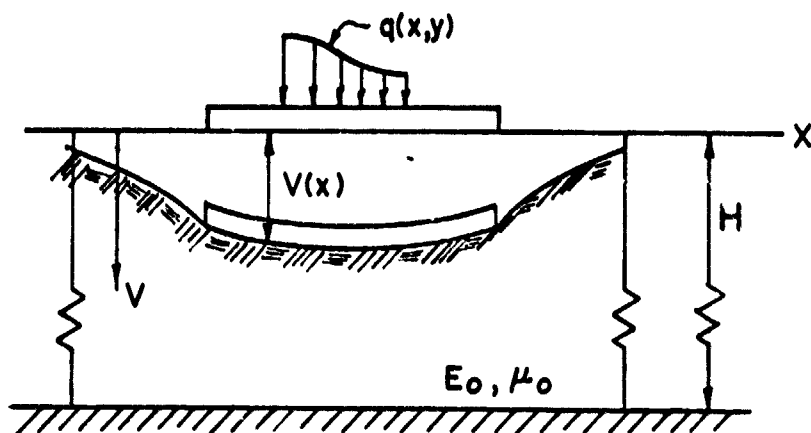


FIGURE A3. DISPLACEMENT  OF  SOIL
SURFACE.

The applied loads $\bar{p}(x,y)$ and $\bar{q}(x,y)$ are assumed to be distributed over the plate height as arbitrary functions of $y$. However, if only external normal and shearing forces, $\bar{q}(x,0)$ and $\bar{p}(x,0)$, act on the upper surface of the layer, the coefficients $p_j$ and $q_h$ become

$$p_j = p(x)\phi_j(0) \; ; \; q_h = q(x)\psi_h(0) \tag{A7}$$

The system of ordinary differential equations in $U_i(x)$ and $V_r(x)$ obtained from Eqns. (A5) can be solved to obtain the unknown displacements for the plane strain problem.

If it is assumed that the horizontal displacements in the compressible layer are either zero or are negligible $\phi_i(y) = 0$, the displacements $u(x,y)$ and $v(x,y)$ can be expressed as

$$u(x,y) = 0 \tag{A8a}$$

$$v(x,y) = \sum_{k=1}^{n} V_k(x)\,\psi_k(y) \tag{A8b}$$

The system of Eqns. (A5) reduces to

$$\frac{1-\mu_0}{2} \sum_{k=1}^{n} r_{hk}V_k''(x) - \sum_{k=1}^{n} s_{hk}V_k(x) + \frac{1-\mu_0^2}{E_0} q_h = 0 \tag{A9}$$

where

$$r_{hk} = \int_0^H \psi_h \psi_k \delta\, dy \; ; \; s_{hk} = \int_0^H \psi_h' \psi_k' \delta\, dy \tag{A10}$$

Also assuming that the base of the elastic layer is fixed to the rigid base; that is, there is no slip at the interface, the displacement function $v(x,y)$ becomes

$$v(x,y) = V_1(x)\,\psi_1(y) \tag{A11}$$

113

and the function $V_1(x)$ represents the deflection of the foundation layer surface as illustrated in Figure A3. This last assumption does not produce a model with a unique solution as the dimensionless function $\psi_1(y)$ may be selected in any arbitrary manner provided that $\psi_1^1(H) = 0$.

Applying the previous assumption of a fixed base, Eqn. (A9) reduces to the single differential equation

$$\frac{1-\mu_0}{2} r_{11} V_1''(x) - s_{11} V_1(x) + \frac{1-\mu_0^2}{E_0} q = 0 \qquad (A12)$$

where

$$r_{11} = \int_0^H \psi_1^2 \, dy \; ; \; s_{11} = \int_0^H \psi_1'^2 \, dy \qquad (A13)$$

Eqn. (A12) may be further simplified by multiplying each term by $\dfrac{E_0}{(1-\mu_0^2)}$ to yield,

$$2tV_1''(x) - kV_1(x) + q(x) = 0 \qquad (A14)$$

where

$$t = \frac{E_0 r_{11}}{4(1+\mu_0)} \; ; \; k = \frac{E_0 s_{11}}{1-\mu_0^2} \qquad (A15)$$

and $r_{11}$ and $s_{11}$ are defined by Eqns. (A13).

Differential equation (A14) defines a model whereby the vertical displacements of the surface of the soil are related to the load applied on the surface. This model not only considers the compressive strains in the elastic foundation but also the shearing strains within the foundations.

With the displacements of all points expressed by Eqn. (A11) and employing the stress-strain relationships of the classical theory of elasticity the normal and shearing stresses may be obtained from Eqns. (A5) as

$$\sigma_x = \frac{E_0 \mu_0}{1-\mu_0^2} V_1(x) \psi_1'(y) \qquad (A16a)$$

114

$$\sigma_y = \frac{E_0}{1-\mu_0^2}\, V_1(x)\, \psi_1'(y) \qquad\qquad \text{(A16b)}$$

$$\tau_{yx} = \frac{E_0}{2(1+\mu_0)}\, V_1'(x)\psi_1(y) \qquad\qquad \text{(A16c)}$$

Selecting any section $x$ = constant, the total force T in the x direction is given by $T_i = \int_0^H \sigma_x \phi_i \,\delta dy$ $(i = 1, 2, 3,\ldots m)$ and the total force in the y direction is given by

$s_h = \int_0^H \tau_{yx} \psi_h \,\delta dy$ $(h = 1, 2, 3,\ldots n)$. Pleading the assumption of negligible horizontal displacements and applying Eqn. (A16c) there results

$$T_1 = \int_0^H \sigma_x \phi_i \,\delta dy = 0 \qquad\qquad \text{(A17a)}$$

$$s_1 = \int \tau_{yx} \psi_1 \,\delta dy = \frac{E_0 \delta}{2(1+\mu_0)}\, V_1'(x) \int_0^H \psi_1^2(y) dy = 2tV_1'(x) \quad \text{(A17b)}$$

The foundation model is now completely defined once the dimensionless function $\psi_1(y)$ has been established.

# APPENDIX B

## INFINITE BEAM ON AN ELASTIC FOUNDATION

Superimpose on the surface of the soil model, as defined in Appendix A, an infinitely long beam which obeys Eulerian conditions. Let p(x) represent the applied normal load on the beam, q(x) represent the reaction due to the elastic foundation and V(x) represent the beam deflection. The bending of the beam will be described by [63]

$$EI \frac{d^4 V(x)}{dx^4} = p(x) - q(x) \qquad (B1)$$

In Appendix A the relationship

$$-2t \frac{d^4 V(x)}{dx^2} + kV(x) = q(x) \qquad (B2)$$

was developed to relate surface deflections of the soil to superficial loads. Assuming that the beam and the soil are always in contact, Eqns. (B1) and (B2) can be combined by elimination of the interfacial normal force σ(x), to yield

$$EI \frac{d^4 V(x)}{dx^4} - 2t \frac{d^2 V(x)}{dx^2} + kV(x) = p(x) \qquad (B3)$$

Implicitly, this last assumption requires the development of normal tensile stresses across the beam-soil interface. Fortunately, any development of these stresses generally will occur in a region somewhat removed from the load and will be of small magnitude.

For computational expediency, Vlasov and Leont'ev defined a non-dimensional coordinate, $\eta = \frac{x}{L}$, as

$$L = \sqrt[3]{\frac{2EI(1-\mu_0^2)}{E_0 \delta}} \qquad (B4)$$

116

## APPENDIX B

## INFINITE BEAM ON AN ELASTIC FOUNDATION

Superimpose on the surface of the soil model, as defined in Appendix A, an infinitely long beam which obeys Eulerian conditions. Let $p(x)$ represent the applied normal load on the beam, $q(x)$ represent the reaction due to the elastic foundation and $V(x)$ represent the beam deflection. The bending of the beam will be described by [63]

$$EI \ \frac{d^4 V(x)}{dx^4} = p(x) - q(x) \tag{B1}$$

In Appendix A the relationship

$$- 2t \ \frac{d^4 V(x)}{dx^2} + kV(x) = q(x) \tag{B2}$$

was developed to relate surface deflections of the soil to superficial loads. Assuming that the beam and the soil are always in contact, Eqns. (B1) and (B2) can be combined by elimination of the interfacial normal force $\sigma(x)$, to yield

$$EI \ \frac{d^4 V(x)}{dx^4} - 2t \ \frac{d^2 V(x)}{dx^2} + kV(x) = p(x) \tag{B3}$$

Implicitly, this last assumption requires the development of normal tensile stresses across the beam-soil interface. Fortunately, any development of these stresses generally will occur in a region somewhat removed from the load and will be of small magnitude.

For computational expediency, Vlasov and Leont'ev defined a non-dimensional coordinate, $\eta = \frac{x}{L}$, as

$$L = \sqrt[3]{\frac{2EI(1- \mu_0^2)}{E_0 \delta}} \tag{B4}$$

where           E is Young's modulus of the beam
                   I is the moment of inertia of the beam
                   $E_0$ is Young's modulus of the soil
                   $\mu_0$ is Poisson's ratio of the soil
                   $\delta$ is the width of the beam

Employing the nondimensional coordinate and dividing Eqn. (B3) by the beam rigidity, the governing differential equation is established as

$$\frac{d^4 V(\eta)}{d\eta^4} - 2r^2 \frac{d^2 V(\eta)}{d\eta^2} + s^4 V(\eta) = \frac{p(x)L^4}{EI} \qquad (B5)$$

where

$$r^2 = \frac{tL^2}{EI} = \frac{1-\mu_0}{2L} \int_0^H \psi_1^2 \, dy \qquad (B6a)$$

$$s^2 = \frac{kL^4}{EI} = 2L \int_0^H \psi_1' \, dy \qquad (B6b)$$

If a concentrated force P, Figure B1, acts at the origin of coordinates, the following homogeneous differential equation is applicable for all points except the origin

$$\frac{d^4 V(\eta)}{d\eta^4} - 2r^2 \frac{d^2 V(\eta)}{d\eta^2} + s^4 V(\eta) = 0 \qquad (B7)$$

The corresponding characteristic equation is

$$m^4 - 2r^2 m^2 + s^4 = 0 \qquad (B8)$$

As r and s are positive, the ratio $\frac{r}{s}$ must be positive and the solution of the characteristic equation may take one of three forms depending on the relative magnitudes of r and s. The solution of prime importance for the present study is obtained for the condition when s > r. Physically, this condition implies that the majority of the supporting capacity of the soil is developed by normal stresses rather than by the shearing stresses within the foundation. Close investigation of Eqn. (B7) reveals that for the condition r = 0, the model becomes identical to the one which employs the Winkler hypothesis. At the other extreme as s approaches

117
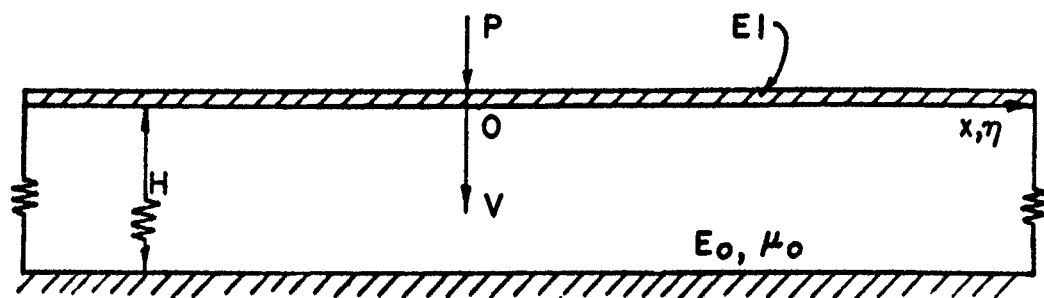
FIGURE BI. CONCENTRATED LOAD ON MODEL.
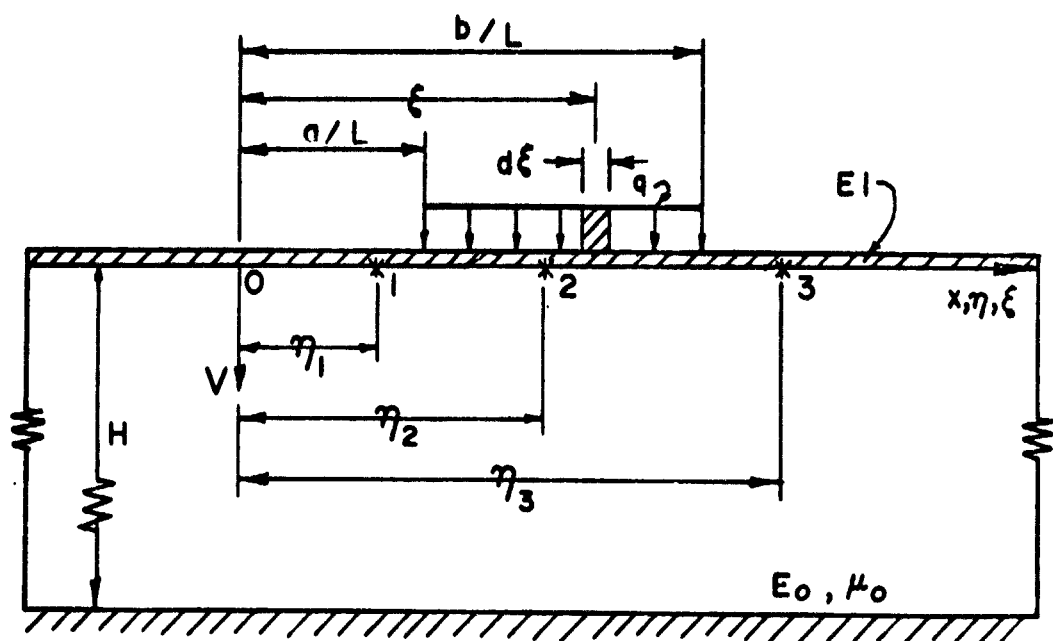


FIGURE B2. UNIFORM LOAD ON MODEL.

zero, the model becomes one for a beam supported by a membrane. All further formulation is restricted to the condition when $s > r$. For this condition the roots of the characteristic equation are

$$m = \pm \bar{\alpha} \pm i\bar{\beta} \qquad (B9)$$

where $\bar{\alpha}$ and $\bar{\beta}$ are real and positive

$$\bar{\alpha} = \frac{s^2+r^2}{2} \quad ; \quad \bar{\beta} = \frac{s^2-r^2}{2} \qquad (B10)$$

The solution of Eqn. (B7) then has the general form

$$V(\eta) = C_1 e^{-\bar{\alpha}\eta}\sin\bar{\beta}\eta + C_2 e^{-\bar{\alpha}\eta}\cos\bar{\beta}\eta + C_3 e^{\bar{\alpha}\eta}\sin\bar{\beta}\eta + C_4 e^{\bar{\alpha}\eta}\cos\bar{\beta}\eta \qquad (B11)$$

Due to symmetry only that portion of the beam for $\eta > 0$ need be considered. Since the deflection of the beam must approach zero as the nondimensional coordinate becomes large ($\eta \to \infty$), the following must occur

$$C_3 = C_4 = 0 \qquad (B12)$$

The deflection equation, Eqn. (B11), then becomes

$$V(\eta) = C_1 F_1 + C_2 F_2 \qquad (B13)$$

where

$$F_1 = e^{-\bar{\alpha}\eta}\sin\bar{\beta}\eta \qquad (B14a)$$

$$F_2 = e^{-\bar{\alpha}\eta}\cos\bar{\beta}\eta \qquad (B14b)$$

The remaining constants $C_1$ and $C_2$ can be determined from the conditions at the origin related to the slope and the shear. Thus for $\eta = 0$

$$\theta(0) = \frac{1}{L}\frac{dV(\eta)}{d\eta} = 0 \qquad (B15)$$

119

$$F(0) = -\frac{EI}{L^3}\left[\frac{d^3 V(\eta)}{d\eta^3} - 2r^2\frac{dV(\eta)}{d\eta}\right] = -\frac{p}{2} \qquad (B16)$$

It should be noted that the shear at any section is composed of two distinct components. The first term Eqn. (B16), results from the shear force developed in the beam whereas the second term arises from the shear force developed in the soil. The latter term is expressed in integral form in Eqn. (A17b).

Substituting the appropriate derivatives of Eqn. (B13) into Eqns. (B15) and (B16) and solving for the constants produces

$$C_1 = \frac{PL^3}{4\bar{\beta}s^2 EI} \qquad (B17a)$$

$$C_2 = \frac{PL^3}{4\bar{\alpha}s^2 EI} \qquad (B17b)$$

Thus the general equation for the deflection of the beam subject to a concentrated load becomes

$$V(\eta) = \frac{PL^3}{4\bar{\alpha}\bar{\beta}s^2 EI}[\bar{\alpha}\, F_1(\eta) + \bar{\beta}\, F_2(\eta)] \qquad (B18)$$

Modification of Eqn. (B18) is necessary when uniformly distributed loads are encountered. Referring to Figure B2, three expressions are developed for the beam deflection which depend upon the location of the uniform load relative to the point at which the deflection is sought. In the development of each expression a differential element is used in conjunction with Eqn. (B18) which is then integrated over the length of the load. Thus for $0 \leq \eta_1 \leq \frac{a}{L}$

$$V(\eta) = \frac{L^3 q(x)}{4\bar{\alpha}\bar{\beta}s^4 EI}\left\{r^2\left[F_1\left(\frac{a}{L}-\eta_1\right)-F_1\left(\frac{b}{L}-\eta_1\right)\right] + 2\bar{\alpha}\bar{\beta}\left[F_2\left(\frac{a}{L}-\eta_1\right)-F_2\left(\frac{b}{L}-\eta_1\right)\right]\right\}$$

$$(B19a)$$

for $\frac{a}{L} < \eta_2 < \frac{b}{L}$

$$V(\eta) = \frac{L^3 \sigma(x)}{4\,\overline{\alpha}\overline{\beta}\,s^4 EI} \left\{ 4\overline{\alpha}\overline{\beta} - r^2 \left[ F_1\left(\eta_2 - \frac{a}{L}\right) + F_1\left(\frac{b}{L} - \eta_2\right) \right] - 2\overline{\alpha}\overline{\beta}\left[ F_2\left(\eta_2 - \frac{a}{L}\right) + F_2\left(\frac{b}{L} - \eta_2\right) \right] \right\} \tag{B19b}$$

an. for $\dfrac{b}{L} \le \eta_3$

$$V(\eta) = \frac{L^3 \sigma(x)}{4\,\overline{\alpha}\overline{\beta}\,s^2 EI} \left\{ r^2 \left[ F_1\left(\eta_3 - \frac{b}{L}\right) - F_1\left(\eta_3 - \frac{a}{L}\right) \right] + 2\overline{\alpha}\overline{\beta}\left[ F_2\left(\eta_3 - \frac{\eta}{L}\right) - F_2\left(\eta_3 - \frac{a}{L}\right) \right] \right\} \tag{B19c}$$

With the use of Eqns. (B19), the deflection of the beam at any point can be determined for a given uniform load. After employing superposition, any number of uniform loads may be handled. The parameters $\overline{\alpha}$, $\overline{\beta}$, $s^4$, and $r^2$ are all functions of the displacement distribution function $\psi_1(y)$.

# APPENDIX C

## STATE VARIABLE FILTER FORMULATION

The procedure for identification of the model parameters presented below follows Kohr [30].

From the data available from prototype tests [ 12 ], a system (relationship) can be established between the known input and the resulting output. The form of this system has been postulated as Eqn. (B3). For this system to reflect adequately the behavior of landing mats, the model parameters must be representative of the test conditions.

By writing Eqn. (B3) as

$$\frac{d^4 V}{dx^4} - a* \; \frac{d^2 V}{dx^2} + b*V = \frac{p(x)}{EI} \qquad (C1)$$

where

$$a* = \frac{2t}{EI} \; ; \; b* = \frac{k}{EI}$$

separation of the unknown quantities can be achieved. The term on the right is exclusively input data; that is, load configuration, expressed by step functions, and mat rigidity.

Let the "model residue", $\varepsilon$, at a point be defined as

$$\varepsilon = \frac{d^4 V}{dx^4} - a* \; \frac{d^2 V}{dx^2} + b*V - \frac{p(x)}{EI} \qquad (C2)$$

and the error functional, $f(\varepsilon)$, for all points be defined as

$$f(\varepsilon) = \int_L \varepsilon^2 dx \qquad (C3)$$

If $V$, $\dfrac{d^2V}{dx^2}$, and $\dfrac{d^4V}{dx^4}$ can be obtained, then the "model residue" and the error functional can be made a minimum through the proper selection of $a^*$ and $b^*$. When this occurs, $a^*$ and $b^*$ are called the "best" estimates of the model parameters.

The derivatives, $\dfrac{d^2V}{dx^2}$ and $\dfrac{d^4V}{dx^4}$ required in Eqn. (C2) may be obtained from the actual deflections by use of a state variable filter [20]. For this operation, it was convenient to represent the "average deflection" patterns by a continuous function rather than by a series of discrete points. To obtain deflection as a function of position, the selected points from the "average deflection" patterns were approximated by a polynomial using a least squares technique. The criterion established for the polynomial was that it approximate the discrete points within a selected standard deviation of 0.05. For the three deflection patterns investigated by this procedure, a sixth degree polynomial was found to satisfy the standard deviation criterion. The polynomial thus obtained, denoted by $\bar{V}$, was established as the expression for the test output and served as the forcing function for the state variable filter. Following Kohr, the state variable filter employed was a differential equation of one order higher than the highest derivative of the model. Thus the filter selected was taken as

$$\frac{d^5V_c}{dx^5} + q_4 \frac{d^4V_c}{dx^4} + q_3 \frac{d^3V_c}{dx^3} + q_2 \frac{d^2V_c}{dx^2} + q_1 \frac{dV_c}{dx} + V_c = \bar{V} \quad (C4)$$

where the coefficients, $q_1$, $q_2$, $q_3$, and $q_4$, for this filter were

$$q_1 = 3.29710$$
$$q_2 = 4.89532$$
$$q_3 = 4.53948 \qquad (C5)$$
$$q_4 = 2.15678$$

These coefficients, called the Paynter filter coefficients, were also given by Kohr [30]. Solution of Eqn. (C4) yielded the values of $\dfrac{d^4V_c}{dx^4}$, $\dfrac{d^2V_c}{dx^2}$, and $V_c$.

123

Once these values were known, they were substituted into Eqn. (C2) and the error functional, Eqn. (C3), was minimized by using the "descent equations" [30, 66]. These equations for a two parameter system are

$$\frac{da*}{dx} = - K_a \ \frac{\partial f(\epsilon)}{\partial a*} = - 2K_a \epsilon \ \frac{\partial \epsilon}{\partial a*}$$

$$\frac{db*}{dx} = - K_b \ \frac{\partial f(\epsilon)}{\partial b*} = - 2K_b \epsilon \ \frac{\partial \epsilon}{\partial b*}$$

(C6)

where $K_a$ and $K_b$ are arbitrary positive constants. These constants, called the "identification gains", stipulate the speed at which the minimum is approached.

Noting from Eqn. (C2) that

$$\frac{\partial \epsilon}{\partial a*} = - \ \frac{d^2 V_c}{dx^2}$$

$$\frac{\partial \epsilon}{\partial b*} = V_c$$

(C7)

and making the appropriate substitutions, the values of a* and b* are obtained by

$$a* = 2K_a \ \int_L \epsilon \ \frac{d^2 V_c}{dx^2} \ dx$$

$$b* = - 2K_b \int_L \epsilon V_c dx$$

(C8)

Solution of Eqns. (C8) was obtained by evaluating the integral between the points of zero deflection and by conveniently setting $K_a$ and $K_b$ equal to 0.5.

124

# APPENDIX D

## STEEP DESCENT METHOD

As demonstrated in Appendix B, the behavior of the mat-soil model is governed by an expression of the form

$$V_{theoretical} = G(E_0, \gamma) \qquad (D1)$$

where $E_0$ and $\gamma$ are unknown parameters and G is the differential equation, Eqn. (B5). The behavior of the prototype tests can be simulated by the model only if the parameters $E_0$ and $\gamma$ are representative of the test subgrade conditions. To determine $E_0$ and $\gamma$, a criterion is established as to minimize the sum of the squares of the deviations of the theoretical deflections from the experimental deflections. As the "average deflection" patterns [12] have been defined by discrete points, let the error functional to be minimized be defined as

$$f(\epsilon) = \sum_{i=1}^{n} \epsilon_1^2 \qquad (i = 1, 2, 3, \ldots n) \qquad (D2)$$

where $\epsilon_i$ represents the deflection deviation at a discrete point and n is the number of discrete points. Equation (D2) can be minimized by a "trial and error" procedure; however, a more direct procedure, "steep descent method"[ 40, 66 ], which is based upon the behavior of the error functional can be employed.

Five combinations of $E_0$ and $\gamma$ are selected in a manner as to form a five point grid, Figure D1, and the error functional is computed for each combination. From this grid a spatial surface is developed which reflects the local behavior of the error functional. Assuming that the error functional possesses a bowl-like surface in the vicinity of the minimum a second order surface of the form

125

M = 33.4    M = 29.7
                    $E_o = 250^{\#}/SQ.IN.$

M = 72.8
                    $E_o = 200^{\#}/SQ.IN.$

M = 195.1    M = 178.8
                    $E_o = 150^{\#}/SQ.IN.$

$\gamma = 2.55$    $\gamma = 2.60$    $\gamma = 2.65$
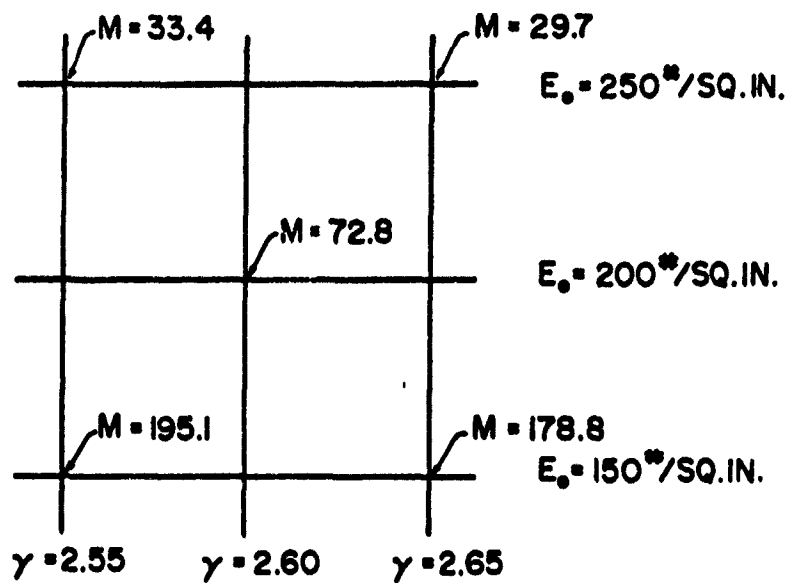
FIGURE D1. TYPICAL FIVE POINT GRID FOR
STEEP DESCENT PROCEDURE.

$$Z = a\gamma^2 + 2h\gamma E_0 + bE_0^2 + 2g\gamma + 2fE_0 + c \qquad (D3)$$

is fitted to the grid. The influence of the quadratic terms, in Eqn. (D3), will become negligible in a region removed from the minimum and a plane containing the central grid can adequately describe the local behavior of the error functional. The equation of this plane is taken as

$$Z = 2g\gamma + 2fE_0 + c \qquad (D4)$$

where $g$ and $f$ are obtained from Eqn. (D3) and $c$ is the value of the error functional at the central grid point. The coefficients, $g$ and $f$ are determined in this manner so as to obtain the most representative plane. The direction of the line of maximum slope, steepest descent, in this plane is given by

$$\tan\delta = \frac{2f}{2g} \qquad (D5)$$

A minimum of the error functional will be rapidly attained by proceeding in the $\delta$ direction from the central grid point.

Reasonably small increments should be used when proceeding along the steep descent line to avoid bypassing the minimum. Also, it is advisable to initiate the procedure from various locations on the error functional surface to determine whether the minimum obtained is global rather than local.

# APPENDIX E

## FORMULATION FOR MOMENT TRANSFER INVESTIGATION

To facilitate the computation of the deflections of a hinged beam, two semi-infinite beams, one on each side of the hinge, are loaded with a concentrated moment as shown in Figure E1. Two distinct expressions are developed, one for the deflection of the semi-infinite beam and the other for the exposed ground surface. The latter is necessitated to insure the continuity of the soil media.

With reference to Figure E1, it is apparent that Eqn. (B7) is applicable for $\eta > 0$ and that the deflection for this region can be expressed by Eqn. (B13). The governing differential equation for the exposed foundation surface from Eqn. (A14) for $x < 0$ is

$$2t \frac{d^2 V(x)}{dx^2} - kV(x) = 0 \qquad (E1)$$

of which the general integral is

$$V(x) = D_1 e^{-\alpha x} + D_2 e^{\alpha x} \qquad (E2)$$

where

$$\alpha = \sqrt{\frac{k}{2t}} \qquad (E3)$$

Applying the boundary condition that the deflection $V(x)$ approaches zero as $x$ approaches minus infinity yields

$$D_1 = 0$$

128
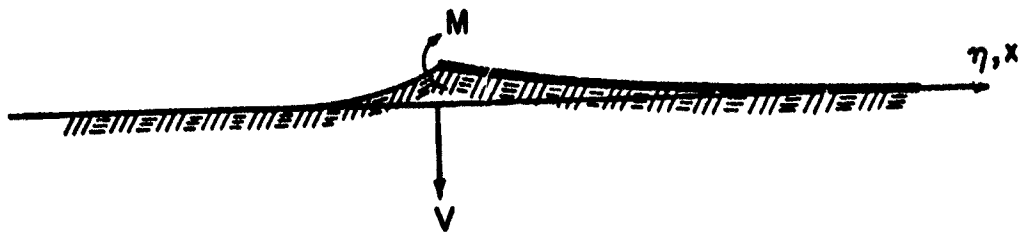
FIGURE E1. MOMENT LOADING ON END OF
SEMI - INFINITE BEAM.

The deflection of the foundation surface for $x < 0$ is

$$V(x) = D_2 e^{\alpha x} \qquad (E4)$$

To determine the constants $C_1$, $C_2$, of Eqns. (B13), and $D_2$, the following boundary conditions are used at the origin

$$V(-0) = V(0)$$

$$M = - \frac{EI}{L^2} V(0) \qquad (E5)$$

$$N(-0) = N(0)$$

where $N(-0) = 2tV' = 2_\alpha tD_2$ is the generalized shear at minus zero. Applying the first of Eqns. (E5) produces

$$D_2 = C_2 \qquad (E6)$$

From the second of Eqns. (E5) after substituting the second deviatives of the F functions, Eqns. (B14), at the origin there results

$$- \frac{ML^2}{EI} = - 2\bar{\alpha}\bar{\beta} C_1 + r^2 C_2 \qquad (E7)$$

where $\bar{\alpha}$, $\bar{\beta}$, and $r^2$ are as defined in Eqns. (B6a) and (B10). The third boundary condition gives

$$2_\alpha tD_2 = - \frac{EI}{L^3} \left[ \frac{d^3 V(0)}{d \eta^3} - 2r^2 \frac{dV(0)}{d\eta} \right]$$

Multiplying by $-L^3/EI$ and making the appropriate substitutions for the derivatives of the F functions, Eqns. (B14), one obtains

$$\frac{-2 \alpha L^3 D_2}{EI} = [\bar{\beta}(3\bar{\alpha}^2 - \bar{\beta}^2) - 2r^2 \bar{\beta}] C_1 + [\bar{\alpha}(3\bar{\beta}^2 - \bar{\alpha}^2) + 2r^2 \bar{\alpha}] C_2 \quad (E8)$$

130

From the simultaneous solution of Eqns. (E6), (E7), and (E8), the integration constants are found to be

$$D_2 = C_2 = \frac{ML^2}{EID} \, [\bar{\beta} s^2]$$

$$C_1 = - \frac{ML^2}{EID} \left[ \bar{\alpha} s^2 + \frac{2\alpha_t L^3}{EI} \right] \tag{E9}$$

where

$$D = - \left[ \bar{\beta} s^2 (3\bar{\alpha}^2 - \beta^2) + \frac{4\bar{\alpha}\alpha_t L^3}{EI} \right]$$

and $s^2$ is as defined by Eqns. (B6b). Thus the deflection for the semi-infinite beam is given by

$$V(\eta) = C_1 F_1 + C_2 F_2 \tag{E10}$$

and the deflection of the ground surface by

$$V(x) = \frac{ML^2}{EID} \, \bar{\beta} s^2 e^{\alpha x} \tag{E11}$$

If the semi-infinite beam extends to the left of the origin, the coordinate system is reversed and Eqns. (E10) and (E11) are then applicable.

COMPUTER PROGRAM FOR PARAMETER IDENTIFICATION

```
C     *********************************************************************   A    1
C              PARAMETER IDENTIFICATION PROGRAM                              A    2
C     *********************************************************************   A    3
C        INFINITE BEAM ON A VLASOV AND LEONTEV MODEL                         A    4
C        DOWNWARD DEFLECTION IS TAKEN AS POSITIVE                            A    5
C     *********************************************************************   A    6
C        DEFINITION OF VARIABLES USED                                        A    7
C        KNK = NUMBER OF TEST SECTIONS TO BE INVESTIGATED                    A    8
C        KNN = INTEGER COUNTER                                               A    9
C        E = YOUNGS MODULUS OF THE MAT MATERIAL   (KIPS/SQ.IN.)              A   10
C        I = MOMENT OF INERTIA OF THE MAT PER FOOT OF WIDTH   (IN.**4)       A   11
C        DELTA = WIDTH OF THE MAT - TAKEN AS THE LENGTH OF A RECTANGLE       A   12
C        WHOSE AREA IS EQUAL TO THAT OF THE TIRE PRINT AND WHOSE WIDTH       A   13
C        IS THE MAXIMUM WIDTH OF THE TIRE PRINT   (IN.)                      A   14
C        KKK = NUMBER OF SETS OF DATA PER SECTION - A SET IS A               A   15
C        DEFLECTION PATTERN FOR A PARTICULAR COVERAGE WITHIN THE TEST        A   16
C        NN5 = NUMBER OF STATIC UNIFORM LOADS - WHEEL LOADS                  A   17
C        POIS = POISSONS RATIO OF THE SOIL                                   A   18
C        H = THICKNESS OF SOIL LAYER - 1000 USED FOR  H= INFINITY            A   19
C        SAI = DISTANCE TO THE BEGINNING OF STATIC UNIFORM LOAD FROM         A   20
C        THE ORIGIN  (IN.)                                                   A   21
C        SQ0 = MAGNITUDE OF STATIC UNIFORM LOAD (KIPS/INCH)                  A   22
C        SBI = DISTANCE TO THE END OF STATIC UNIFORM LOAD FROM THE           A   23
C        ORIGIN  (IN.)                                                       A   24
C        NN = INTEGER COUNTER                                                A   25
C        IH = INTEGER VARIABLE ASSOCIATED WITH THE TYPE OF STRESS            A   26
C        DISTRIBUTION                                                        A   27
C                        1 = LINEAR                                          A   28
C                        2 = HYPERBOLIC - FINITE DEPTH                       A   29
C                        3 = HYPERBOLIC - INFINITE DEPTH                     A   30
C        NDP = NUMBER OF DEFLECTION POINTS PER SET                           A   31
C        I1 = SECTION NUMBER                                                 A   32
C        I2 = LANE NUMBER                                                    A   33
C        I3 = ITEM NUMBER                                                    A   34
C        I4 = LOCATION NUMBER                                                A   35
C                        1 = CENTER OF PANEL                                 A   36
C                        2 = QUARTER POINT OF PANEL                          A   37
C                        3 = JOINT                                           A   38
C        ICOVER = NUMBER OF COVERAGES FOR THE SET                            A   39
C        XS = DISTANCE FROM ORIGIN TO POINT AT WHICH DEFLECTION IS GIVEN     A   40
C        (IN.)                                                               A   41
```

```
C          DS = MEASURED DEFLECTION AT THE POINT XS                    A  42
C          GAMMA = RATE OF DECREASE OF STRESS WITH DEPTH               A  43
C          EO = YOUNGS MODULUS OF THE SOIL                             A  44
C          *************************************************           A  45
C                                                                      A  46
       REAL I,L,KS,MOME,MSMAL,MOMES                                    A  47
       DIMENSION SAI(5), SQO(5), SBI(5), XS(20), DS(20), XDEFL(20)     A  48
       COMMON L,A,B,A3,S2,S4,R2,E,I,V5,X(60),AI(5),QO(5),BI(5),DEFL(60),S A 49
      1LOPE(60),MOME(60),SHEAR(60)                                     A  50
       READ (5,15) KNK                                                 A  51
       KNN=0                                                           A  52
       KNN=KNN+1                                                       A  53
1      IF (KNN.EQ.(KNK+1)) STOP                                        A  54
C                                                                      A  55
C      READ INFORMATION ABOUT BEAM PROPERTIES                          A  56
C                                                                      A  57
       READ (5,16) E,I,DELTA                                           A  58
       I=I*DELTA/12.                                                   A  59
C                                                                      A  60
C      READ INFORMATION ABOUT FOUNDATION PROPERTIES                    A  61
C                                                                      A  62
       READ (5,20) KKK,NN5,POIS,H                                      A  63
C                                                                      A  64
C      READ LOADING INFORMATION                                        A  65
C                                                                      A  66
       READ (5,16) (SAI(K),SQO(K),SBI(K),K=1,NN5)                      A  67
       NN=0                                                            A  68
2      NN=NN+1                                                         A  69
       IF (NN.EQ.(KKK+1)) GO TO 1                                      A  70
C                                                                      A  71
C      READ INFORMATION ABOUT DISTRIBUTION OF STRESS                   A  72
C                                                                      A  73
       READ (5,17) IH,NOP                                              A  74
C                                                                      A  75
C      READ TEST SECTION IDENTIFICATION                               A  76
C                                                                      A  77
       READ (5,18) I1,I2,I3,I4,ICOVER                                  A  78
C                                                                      A  79
C      READ DATA POINTS                                                A  80
C                                                                      A  81
       READ (5,19) (XS(J),DS(J),J=1,NOP)                               A  82
       WRITE (6,21)                                                    A  83
       WRITE (6,22) I1,I2,I3,I4,ICOVER                                 A  84
       WRITE (6,23)                                                    A  85
       WRITE (6,24)                                                    A  86
       WRITE (6,25)                                                    A  87
       GAMMA=1.                                                        A  88
C                                                                      A  89
C      ERRS = STORED VALUE OF ERROR - SET INITIALLY TO 10000.          A  90
C                                                                      A  91
3      ERRS=10000.                                                     A  92
       EO=.1                                                           A  93
4      L=((2.*E*I*(1.-POIS**2.))/(EO*DELTA))**0.33333333               A  94
C                                                                      A  95
```

```
C        SELECT EQUATION FOR PROPER STRESS DISTRIBUTION          A  96
C                                                                A  97
         IF (IH.EQ.1) GO TO 5                                    A  98
         IF (IH.EQ.2) GO TO 6                                    A  99
         IF (IH.EQ.3) GO TO 7                                    A 100
5        R11=DELTA*H/3.                                          A 101
         S11=DELTA/H                                             A 102
         T=(EO*R11)/(4.*(1.+POIS))                               A 103
         KS=(EO*S11)/(1.-POIS**2.)                               A 104
         R2=(T*L**2.)/(E*I)                                      A 105
         S4=(KS*L**4.)/(E*I)                                     A 106
         GO TO 8                                                 A 107
C                                                                A 108
6        GHL=(GAMMA*H)/L                                         A 109
         PSIK=0.5*GHL*((SINH(GHL)*COSH(GHL)+GHL)/(SINH(GHL)**2.)) A 110
         PSIT=1.5/GHL*((SINH(GHL)*COSH(GHL)-GHL)/(SINH(GHL)**2.)) A 111
         T=(EO*DELTA*H*PSIT)/(12.*(1.+POIS))                     A 112
         KS=(EO*DELTA*PSIK)/(H*(1.-POIS**2.))                    A 113
         R2=(H*(1.-POIS)*PSIT)/(6.*L)                            A 114
         S4=(2.*L*PSIK)/H                                        A 115
         GO TO 8                                                 A 116
C                                                                A 117
7        KS=(EO*DELTA*GAMMA)/(2.*L*(1.-POIS**2.))                A 118
         T=(EO*DELTA*L)/(8.*GAMMA*(1.+POIS))                     A 119
         R2=(1.-POIS)/(4.*GAMMA)                                 A 120
         S4=GAMMA                                                A 121
8        S2=S4**0.5                                              A 122
C                                                                A 123
C        TEST TO DETERMINE IF FOLLOWING EQUATIONS ARE APPLICABLE A 124
C                                                                A 125
         IF (R2.GT.S2) GO TO 14                                  A 126
         A=((S2+R2)/2.)**0.5                                     A 127
         B=((S2-R2)/2.)**0.5                                     A 128
         AB=2.*A*B                                               A 129
         N5=NN5                                                  A 130
         DO 9 K=1,N5                                             A 131
            AI(K)=SAI(K)                                         A 132
            QO(K)=SQO(K)                                         A 133
9        BI(K)=SBI(K)                                            A 134
         DO 10 J=1,NDP                                           A 135
            X(J)=XS(J)                                           A 136
            CALL ULOAD (J)                                       A 137
            XDEFL(J)=DEFL(J)                                     A 138
10       CONTINUE                                                A 139
         ERROR=0.0                                               A 140
         DO 11 J=1,NDP                                           A 141
11       ERROR=ERROR+ABS(XDEFL(J)-DS(J))**2.                     A 142
         IF (ERROR.GT.ERRS) GO TO 13                             A 143
         ERRS=ERROR                                              A 144
         IF (ERRS.LT.1.1) GO TO 12                               A 145
         EOS=EO                                                  A 146
         SKS=KS                                                  A 147
         TS=T                                                    A 148
         EO=EO+0.05                                              A 149
```

```
          GO TO 4                                                 A 150
C                                                                 A 151
12        EOS=EO                                                  A 152
          SKS=KS                                                  A 153
          TS=T                                                    A 154
          EO=EO+0.01                                              A 155
          GC TO 4                                                 A 156
C                                                                 A 157
13        SUBR=SKS/DELTA                                          A 158
          TT=TS/DELTA                                             A 159
          WRITE (6,26) EOS,GAMMA,SUBR,TT,L,ERRS                   A 160
          IF (GAMMA.GE.8.) GO TO 2                                A 161
          GAMMA=GAMMA+1.                                          A 162
          GO TO 3                                                 A 163
C                                                                 A 164
14        WRITE (6,27)                                            A 165
C                                                                 A 166
15        FORMAT (I10)                                            A 167
16        FORMAT (3F20.5)                                         A 168
17        FORMAT (2I15)                                           A 169
18        FORMAT (5I10)                                           A 170
19        FORMAT (2F20.5)                                         A 171
20        FORMAT (2I15,2F15.5)                                    A 172
21        FORMAT (//10X,7HSECTION,10X,4HLANE,10X,4HITEM,10X,8HLOCATION,10X,9  A 173
         1HCOVERAGES)                                             A 174
22        FORMAT (I14,I16,I14,I16,I19)                            A 175
23        FORMAT (/5X,9HE OF SOIL,9X,5HGAMMA,5X,8HSUBGRADE,12X,1HT,13X,1HL,1  A 176
         12X,5HERROR)                                             A 177
24        FORMAT (37X,7HMODULUS)                                  A 178
25        FORMAT (3X,11HK IPS/SQ.IN.,20X,15HKIPS/SQ.IN./IN.,5X,8HKIPS/IN./)   A 179
26        FORMAT (6F15.5)                                         A 180
27        FORMAT (/10X,34HR2 IS GREATER THAN S2  NO SOLUTION)     A 181
          END                                                     A 182-
```

## COMPUTER PROGRAM FOR PERFORMANCE PREDICTION

```
C      **********************************************************
C                 PERFORMANCE PREDICTION PROGRAM
C      **********************************************************
C          INFINITE BEAM ON A VLASOV AND LEONTEV MODEL
C          HYPERBOLIC STRESS DISTRIBUTION
C          DOWNWARD DEFLECTION IS TAKEN AS POSITIVE
C      **********************************************************
C          DEFINITION OF VARIABLES USED
C          KNK = NUMBER OF TEST SECTIONS TO BE INVESTIGATED
C          KNN = INTEGER COUNTER
C          I1 = SECTION NUMBER
C          I2 = LANE NUMBER
C          I3 = ITEM NUMBER
C          INCA = ACTUAL NUMBER OF COVERAGES AT WHICH THE SECTION FAILED.
C          E = YOUNGS MODULUS OF THE MAT MATERIAL  (KIPS/SQ.IN.)
C          I = MOMENT OF INERTIA OF THE MAT PER FOOT OF WIDTH  (IN.**4)
C          DELTA = WIDTH OF THE MAT - TAKEN AS THE LENGTH OF A RECTANGLE
C          WHOSE AREA IS EQUAL TO THAT OF THE TIRE PRINT AND WHOSE WIDTH
C          IS THE MAXIMUM WIDTH OF THE TIRE PRINT  (IN.)
C          NN5 = NUMBER OF STATIC UNIFORM LOADS - WHEEL LOADS
C          WGAMMA = THE PRODUCT OF THE AVERAGE WATER CONTENT (PERCENT)
C          AND THE AVERAGE DRY UNIT WEIGHT OF THE TOP 18 INCHES OF SOIL.
C          CBR = AVERAGE C.B.R. VALUE FOR THE TOP 18 INCHES OF SOIL
C          WL = MAGNITUDE OF THE LOAD - FOR DUAL WHEELS USE TOTAL LOAD ON
C          THE ASSEMBLY - FOR SINGLE WHEEL USE WHEEL LOAD.  (IN KIPS)
C          CA = CONTACT AREA (IN SQ.IN.) - FOR BOTH SINGLE AND DUAL
C          ASSEMBLY USE CONTACT AREA OF ONE WHEEL.
C          TP = TIRE INFLATION PRESSURE. (IN LBS./SQ.IN.)
C          SAI = DISTANCE TO THE BEGINNING OF STATIC UNIFORM LOAD FROM
C          THE ORIGIN  (IN.)
C          SQO = MAGNITUDE OF STATIC UNIFORM LOAD (KIPS/INCH)
C          SBI = DISTANCE TO THE END OF STATIC UNIFORM LOAD FROM THE
C          ORIGIN  (IN.)
C          POIS = POISSONS RATIO OF THE SOIL
C          GAMMA = RATE OF DECREASE OF STRESS WITH DEPTH
C          EO = YOUNGS MODULUS OF THE SOIL
C      **********************************************************
       REAL I,KS,L,INTKS,II,MOME
       DIMENSION SAI(5),SQO(5),SBI(5)
       COMMON X(60),AI(5),QO(5),BI(5),L,A,B,AB,S2,S4,R2,E,I,N5,DEFL(60),
      1    SLOPE(60),MOME(60),SHEAR(60)
```

```
      READ (5,420) KNK
  420 FORMAT (I10)
C     KNK=NUMBER OF SECTIONS INVESTIGATED
      KNN=0
  410 KNN=KNN+1
      IF (KNN.EQ.(KNK+1)) STOP
C     READ SECTION IDENTIFICATION
      READ (5,101) I1,I2,I3,INCA
C     READ PROPERTIES OF MAT
      READ (5,100) E,I,DELTA
C     READ NUMBER OF WHEELS AND SOIL PROPERTIES.
      READ (5,102) NN5,WGAMMA,CBR
C     READ WHEEL LOAD, CONTACT AREA,TIRE PRESSURE.
      READ (5,100) WL,CA,TP
C     READ LOAD PLACEMENT AND MAGNITUDE.
      READ (5,100) (SAI(K),SQO(K),SBI(K),K=1,NN5)
      JIK=1
      II=1
      I=I*DELTA/12.
      POIS=0.4
      INTKS=164.+3.*CBR-5.45*WGAMMA
      ICOVER=1
      IF (JIK.EQ.1) GO TO 69
   73 ICOVER=1
      IF (JIK.EQ.2) GO TO 70
   69 ICOVER= INCA
   70 EIM=E*II
      NNNK=1
  501 SUBR=INTKS/(FLOAT( ICOVER)**0.048455)
      GAMMA=FLOAT(ICOVER)**0.25
      GAMMA=GAMMA+(13680.-EIM)/EIM
      KS = SUBR*DELTA/1000.
      EO=((2.*(1.-POIS**2.))/DELTA)*((E*I*KS**3.)/(GAMMA**3.))**0.25
      L=((2.*E*I*(1.-POIS**2.))/(EO*DELTA))**0.33333333
      T=(EO*DELTA*L)/(8.*GAMMA*(1.+POIS))
      TT=T/DELTA
      R2=(1.-POIS)/(4.*GAMMA)
      S4= GAMMA
      S2=S4**0.5
      A=((S2+R2)/2.)**0.5
      B=((S2-R2)/2.)**0.5
      AB=2.*A*B
      N5=NN5
      DO 111 K=1,N5
      AI(K)=SAI(K)
      QO(K)=SQO(K)
  111 BI(K)=SBI(K)
      J=1
      IF (NN5.EQ.2) X(J)=AI(1)+(BI(2)-AI(1))/2.
      IF (NN5.EQ.1) X(J)=AI(1)+(BI(1)-AI(1))/2.
      CALL ULOAD(J)
      IF (JIK.EQ.1) GO TO 71
      IF (NN5.EQ.1) GO TO 78
      EIC=(E*II/13680.)**2.5
```

```
      CAC=CA**0.5
      WLC=(WL//0.)**1.75
      TPC=100./TP
      FAILN=FLOAT(ICOVER)**.325
      CRITER=(EIC*CBR*CAC*TPC)/(WLC*FAILN)
      CRITER=(CRITER**0.945924)/(10.0**0.50524)
      IF (NNNK.EQ.1) ICOVER=ICOVER-1
      IF (CRITER.LE.DEFL(1)) GO TO 80
      GO TO 79
   73 EIC=(E*II/13680.)**0.5
      WLC=(WL/35.)**1.3
      CAC=CA**0.72
      CBRC=CBR**0.9
      FAILN=FLOAT(ICOVER)**0.3
      CRITER=(WLC*FAILN)/(EIC*CAC*CBRC)
      CRITER=(10.**1.156626)*(CRITER**0.599264)
      IF (NNNK.EQ.1) ICOVER=ICOVER-1
      IF (CRITER.GE.DEFL(1)) GO TO 80
   79 IF (ICOVER.CT.5000) GO TO 81
      IF (ICOVER.GE.200) ICOVER =ICOVER+20
      IF (ICOVER.LT.200) ICOVER=ICOVER+5
      NNNK = 2
      GO TO 501
   80 WRITE (6,10)
   10 FORMAT (//10X,7HSECTION,10X,4HLANE,10X,4HITEM,10X,8HCOVERAGE   )
      WRITE (6,129) I1,I2,I3,INCA
  129 FORMAT (I14,I16,I14,I19)
      WRITE (6,82) ICOVER
   82 FORMAT (/10X,25HTHIS SECTION WILL FAIL AT ,I4,11H COVERAGES.   )
      GO TO 410
   81 WRITE (6,10)
      WRITE (6,129) I1,I2,I3,INCA
      WRITE (6,83)
   83 FORMAT (/10X,48HPREDICTED FAILURE IS GREATER THAN 5000 COVERAGES )
      GO TO 410
  100 FORMAT (3F20.5)
  102 FORMAT (I20,2F20.5)
  110 FORMAT (2F20.5)
  101 FORMAT (4I10)
  120 FORMAT (4F20.5)
   71 WRITE (6,72) ICOVER,DEFL(1)
   72 FORMAT (I10,5X,21HFAILURE DEFLECTION IS    ,F10.5)
      JIK=2
      GO TO 73
      END
```

E-O-J

COMPUTER PROGRAM FOR ASYMMETRIC LOAD MODEL

```
C     *********************************************************************
C                          ASYMMETRIC LOAD MODEL
C     *********************************************************************
      REAL I
      DIMENSION AX1(20),AX2(20),BX1(20),BX2(20),XDEFL(25),ADDEFL(25)
      COMMON X(60),DEFL(60),AI(5),BI(5),QO(5),N5
C         READ SECTION IDENTIFICATION
C         I1=SECTION NUMBER
C         I2= LANE NUMBER
C         I3= ITEM NUMBER
      READ (5,101) I1,I2,I3
C         READ INFORMATION ABOUT BEAM PROPERTIES
C         E=MODULUS OF ELASTICITY OF BEAM - KIPS/SQ.IN.
C         I= MOMENT OF INERTIA OF BEAM PER FOOT OF WIDTH - IN.**4
      READ (5,100) E,I
C         NLOAD=NUMBER OF WHEELS.
C         WHEELS=WHEEL SPACING IN INCHES.
C         WIDLAN=WIDTH OF THE TRAFFIC LANE IN INCHES.
      READ (5,2) NLOAD,WHEELS,WIDLAN
C         NSHIFT=NUMBER OF POSITIONS OF THE ASSEMBLY BEFORE IT IS
C         MOVED LATERALLY THE WIDTH OF THE ASSEMBLY. THIS VALUE IS USED
C         ONLY FOR MULTIPLE-WHEEL TESTS. FOR THE LOADING SEQUENCE SHOWN
C         IN FIGURE 24 OF THIS REPORT - NSHIFT=3.0. THIS VALUE FOR
C         SINGLE-WHEEL TESTS IS SET EQUAL TO UNITY.
C         CONTA=CONTACT AREA OF TIRE IN SQ.IN.
C         Q=TOTAL LOAD ON ONE WHEEL IN KIPS.
      READ (5,2) NSHIFT,CONTA,Q
C         NPOSIT=NUMBER OF POSITIONS OF WHEEL ASSEMBLAGES TO COVER THE
C         TRAFFIC LANE WIDTH.
      READ (5,421) NPOSIT
C         TIREW=WIDTH OF THE TIRE PRINT IN INCHES.
C         TIREL=LENGTH OF THE TIRE PRINT IN INCHES.
C         ABOVE TWO VALUES BASED UPON A RECTANGULAR TIRE PRINT.
      IF (NLOAD.EQ.1) TIREW=WIDLAN/(FLOAT(NPOSIT))
      IF (NLOAD.EQ.2) TIREW=WIDLAN/(2.*FLOAT(NPOSIT))
      TIREL=CONTA/TIREW
      I=I*TIREL/12.
      WLK=Q
      Q=Q/TIREW
C         AT=LENGTH OF TIME THAT THE LOAD IS APPLIED.
C         BT=LENGTH OF TIME THAT THE LOAD IS OFF BEFORE THE LOAD IS
```

```
C          APPLIED AGAIN.
           READ (5,100) AT,BT
C              * NETHOW
C              AT AND BT MUST BE SO SELECTEC THAT
C                  (AT+BT)*NPOSIT =1
C              THE ABOVE PEQUIREMENT IS NECESSARY FOR 1 COVERAGE TO BE THE
C              BASIC TIME UNIT.
C              READ INFCRMATICN CF VARIATION OF MODULUS OF SOIL
C              IN THIS PROGRAM ONLY THE RESIDUAL DEFORMATIONS ARE OF
C              INTEREST, THUS THE VALUE OF C CAN BE ARBITRARY.
C              IN THIS PROGRAM AD=1.0 ( SEE REPORT-SECTION ON A SYMMETRIC
C              LOAD MODEL).
           READ (5,1) C,CI,EN,AD
C              XC=DISTANCE FROM CRIGIN TO ECGE OF TRAFFIC LANE,IN THIS
C              PROGRAM THE ORIGIN HAS BEEN SELECTED AS A POINT 10 FEET LEFT
C              OF THE EDGE CF THE TRAFFIC LANE.
           X0=120.
           IF (NLCAD.EC.1) GO TO 650
           DO 651  J=1,NPOSIT
           IF (J.GT.NSHIFT) GO TO 720
           AX1(J)=X0+FLCAT(J-1)*TIREW
           AX2(J)=AX1(J)+FLCAT(NSHIFT)*TIREW
           PX1(J)=AX1(J)+TIREW
           BX2(J)=AX2(J)+TIREW
           GO TO 651
       720 AX1(J)=X0+2.*FLOAT(NSHIFT)*TIREW+FLOAT(J-1-NSHIFT)*TIREW
           AX2(J)=AX1(J)+FLOAT(NSHIFT)*TIREW
           PX1(J)=AX1(J)+TIREW
           BX2(J)=AX2(J)+TIREW
       651 CONTINUE
           GC TO 652
       650 DO 653  J=1,NPOSIT
           AX1(J)=X0+FLOAT(J-1)*TIREW
       653 PX1(J)=AX1(J)+TIREW
       652 NS=NLCAD
           DO 654 KK=1,NS
       654 CC(KK)=C
C              ESTABLISH DISTANCES TO WHERE DEFLECTIONS ARE TO BE COMPUTED.
C              LET THIS ARRAY BE X(J).
C              COMPUTED DEFLECTION AT ONE-TENTH POINTS ACROSS TRAFFIC LANE.
           DO 303 JJ=1,11
       303 X(JJ)=X0+FLCAT(JJ-1)*WICLAN/10.
           WRITE (6,10)
           WRITE (6,129) I1,I2,I3
C              NUMCOV= NUMBER OF COVERAGES.
C              NPASS= NUMBER CF SPECIFIC PASS WITHIN A COVERAGE AT THE END OF
C              WHICH THE DEFLECTION IS DESIRED.
C              NPASS MUST BE LESS THAN OR EQUAL TO NPOSIT.
C              NCPASS= TOTAL NUMBER OF PASSES NECESSARY TO COMPLETE THE GIVEN
C              NUMBER CF COVERAGES.
       810 READ (5,420) NUMCOV , NPASS
           NCPASS=NUMCOV*NPOSIT
C              LUP=COMPLETE NUMBER OF PASSES FOR ALL FULL AND PARTIAL COVER.
           LUP=NOPASS+NPASS
```

```
C         FTIME = FINAL TIME TO WHERE CEFLECTION IS DESIRED
      FTIME=FLOAT(LUP)*AT+FLOAT(LUP)*BT
C         LET THE TCTAL CEFLECTICN AT EACH POINT BE REPRESENTED BY
C         XCEFL(J). ZERC ALL OF  THESE LOCATIONS INITIALLY
      DO 444 J=1,11
  444 XDEFL(J)=0.
C         COMPUTE THE CEFLECTIONS FOR EACH LOAC APPLICATION AND RELEASE.
      II=1
      M3=NFOSIT
      NUMCC2=NUMCOV+2
      DO 301 NN=2,NUMCO2,2
      IF (NN.EC.NUMCC2) M3=NPASS
      IF (M3.EQ.0) GC TO 301
      DC 302 MM=1,M3
      IF (NLCAD.EC.1) GO TC 660
      AI(1)=AX1(MM)
      AI(2)=AX2(MM)
      BI(1)=BX1(MM)
      BI(2)=BX2(MM)
      KMM=0
      GC TO 661
  660 AI(1)=AX1(MM)
      BI(1)=BX1(MM)
      KMM=0
  661 NM1=NN*NFOSIT-(2*NPOSIT-2*MM+2-KMM)
      TSTART=FLOAT(NM1)*AT+FLOAT(NM1)*BT
      TIME=FTIME-TSTART
      T1=AT
      COMF=D+D1*(T1*(1./AC-1.)+TIME)**EN-(C+D1*(TIME-T1)**EN)
      BKS=TIREL/COMP
      WLAMCA=(BKS/(4.*E*I))**0.25
      DO 309 J=1,11
      CALL WULOAD (J,WLAMCA,BKS)
  309 ADDEFL(J)=DEFL(J)
      DO 663 J=1,11
  663 XDEFL(J)=XDEFL(J)+ACCEFL(J)
      II=II+1
      KMM=KMM+1
      IF (KMM.EQ.1) GO TO 661
  302 CONTINUE
  301 CONTINUE
      KII=II-1
      JNN=NN-2
      WRITE (6,130) JNN
      WRITE (6,131) MM,KII
      WRITE (6,132) C1,EN
      WRITE (6,133)
      WRITE (6,134)
      WRITE (6,135) ( XDEFL(J),X(J),J=1,11)
      GO TO 810
    1 FORMAT (4F10.5)
    2 FORMAT (I5,2F10.5)
   10 FORMAT (//10X,7HSECTION,10X,4HLANE,10X,4HITEM )
  100 FORMAT (2F10.5)
```

```
101 FORMAT (3I10)
129 FORMAT (I14,I16,I14)
130  .ORMAT (6X,41HTHE FOLLOWING RESULTS OCCUR AT THE END OF /
    *   17X,I4,1X,9HCCVERAGES)
131 FORMAT (6X,33HTHE LAST POSITION OF THE LOAD WAS  ,I5,1X,3HAND/
    *2X,11HA TOTAL CF ,I5,1X,38HLOADS HAVE BEEN APPLIED TO THE SYSTEM.)
132 FORMAT(15X,19HTHE VALUE OF C1 IS ,F6.3/15X,19HTHE VALLE CF EN IS ,
    *   F6.3)
133 FORMAT (8X,37HTHL CEFORMATION PATTERN IS AS FOLLOWS)
134 FORMAT (4X,20HRESIDUAL CEFORMATION ,4X,2CHDISTANCE FROM ORIGIN/
    *   10X,6HINCHES ,19X,6HINCHES  )
135 FCRMAT  (10X,F8.5,15X,F10.5)
420 FORMAT (2I10)
421 FCRMAT (I10 )
    END
```

# APPENDIX I

## CCMPUTER FROGRAM FOR MOMENT TRANSFER INVESTIGATICN

```
C     ***************************************************************
C                      MOMENT TRANSFER ANALYSIS
C     ***************************************************************
C        VLASOV ANC LEONTEV MOCEL
C        HYFERBOLIC STRESS DISTRIBUTION
      REAL I,KS,INTKS,MOEFL,MOEFLL,MOMES,MOME,L,II
      DIMENSICN SAI(5),SGC(5),SEI(5),XS(2C),DS(2C),XDEFL(2C),MDEFL(20),
     1      FDEFL(20),MCEFLL(20),CCEFL(2C)
      COMMON X(60),AI(5),CC(5),EI(5),L,A,E,AB,S2,S4,R2,F,I,N5,DEFL(60),
     1      SLCFE(60),MOME(60),SHEAR(60),CM(51),DIST(5),N2,AA,T
C        KNK= NUMBER CF SECTIONS INVESTIGATED
      REAC (5,420) KNK
      KNN=0
  410 KNN=KNN+1
      IF (KNN.EQ.(KNK+1)) STOP
C        READ INFCRMATION ABOUT BEAM PROPERTIES
      REAC (5,100) E,I,CELTA
C        DELTA=WIDTH OF BEAM IN INCHES.
C        READ INFORMATICN ABOUT FOUNCATION PROPERTIES.
      REAC (5,102) KKK,NN5,POIS
C        KKK= NUMBER CF SETS OF CATA PER SECTION.
C        NN5= NUMBER CF STATIC UNIFORM LOACS.
      READ (5,100) (SAI(K),SCO(K),SEI(K),K=1,NN5)
      II=I
      I=I+UELTA/12.
      EIM=E+II
      NN=0
  402 NN=NN+1
      IF (NN.EQ.(KKK+1)) GO TO 410
      READ (5,4) N2,NDP
C        N2= NUMBEF CF MCMENT RELEASES.
      READ (5,101) II,I2,I3,I4,ICOVER
C        INTKS= SUEGRACE MOCULUS IN LBS./CU.IN.
      READ (5,999) INTKS
      READ (5,110) (XS(J),CS(J),J=1,NCP)
C        SAI= CISTANCE TO BEGINNING OF STATIC UNIFORM LOAD IN INCHFS.
C        SBI= CISTANCE TO ENC OF STATIC UNIFORM LOAD IN INCHES.
C        I1= SECTICN NUMBER
C        I2= LANE NUMBER
C        I3= ITEM NUMBER
C        I4= LOCATICN NUMBER
```

```
C         ICOVER=NUMBER OF COVERAGES
C         LET 1=CENTER OF PANEL 2=QUARTER POINT OF PANEL 3=JOINT
      WRITE (6,3)
      WRITE (6,129)I1,I2,I3,I4,ICOVER
      SUBR=INTKS
      IF (ICOVER.GT.0) GO TO 501
      GAMMA=1.0
      GAMMA=GAMMA+(13680.-EIM)/EIM
      GO TO 502
  501 GAMMA=FLOAT(ICOVER)**0.25
      GAMMA=GAMMA+(13680.-EIM)/EIM
  502 KS=SUBR*CELTA/1000.
  403 EO=((2.*(1.-PCIS**2.))/CELTA)*((E*I*KS**3.)/(GAMMA**3.))**0.25
      L=((2.*E*I*(1.-FCIS**2.))/(EO*CELTA))**0.33333333
      T=(EO*DELTA*L)/(8.*GAMMA*(1.+POIS))
      TT=T/DELTA
      R2=(1.-FOIS)/(4.*GAMMA)
      S4=GAMMA
      S2=S4**0.5
      AA=SQRT(KS/(2.*T))
C         A=ALFHA
C         B=BETA
      A=((S2+R2)/2.)**0.5
      B=((S2-R2)/2.)**0.5
      AB=2.*A*B
      N5=NN5
      DO 111 K=1,N5
      AI(K)=SAI(K)
      COI(K)=SCO(K)
  111 BI(K)=SBI(K)
      DO 114 J=1,NCP
      X(J)=XS(J)
      CALL ULOAD (J)
      XDEFL(J)=CEFL(J)
  114 CCNTINUE
C         CALCULATE THE MOMENT AT THE JOINT LOCATION ASSUMING THE
C         BEAM TC BE CONTINUOUS.
      J=1
      X(J)=AI(1)+(BI(2)-AI(1))/2.
      CALL ULOAD(J)
      ACTMON=MOME(J)
      ERRS=10000.
      JIJ=1
      N2=1
      DIST(1)=X(J)
      CM(1)=-    (ACTMON*0.01)
  117 DO 115 J=1,NCP
      X(J)=XS(J)
      CALL SEMIM(J)
      MDEFL(J)=CEFL(J)
  115 CONTINUE
      DO 116 J=1,NDP
      X(J)=DIST(1)+(DIST(1)-XS(J))
      CALL SEMIM(J)
```

```
      MDEFLL(J)=DEFL(J)
      CDEFL(J)=MDEFL(J)+MCEFLL(J)
116   FDEFL(J)=XCEFL(J)+CCEFL(J)
      PERC= CM(1)/ACTMON*100.
      ERROR=0.0
      DO 200 J=1,NDP
200   ERROR=ERROR+ABS(FDEFL(J)-CS(J))**2.
      IF (JIJ.EQ.2) GC TO 401
      IF (ERROR.GT.ERRS) GO TO 400
      ERRS=ERROR
      CM(1)=CM(1)-     (ACTMON*0.01)
      GC TC 117
400   CM(1)=CM(1)+     (ACTMON*0.01)
      JIJ=2
      GO TO 117
401   WRITE (6,130) ACTMON
      WRITE (6,131) CM(1)
      WRITE (6,132) PERC
      WRITE (6,133) ERROR
      WRITE (6,134)
      WRITE (6,135)
      WRITE (6,136)
      WRITE (6,137)
      WRITE (6,138)
      WRITE (6,113) (XS(J),CS(J),XCEFL(J),MCEFL(J),MDEFLL(J),CDEFL(J),
     1      FDEFL(J),J=1,NDP)
      GO TO 402
3     FORMAT(//10X,7HSECTION,10X,4HLANE,10X,4HITEM,10X,8HLOCATION,
     1      10X,9HCOVERAGES   )
4     FORMAT (2I15)
100   FORMAT (3F20.5)
101   FORMAT (5I10)
102   FORMAT (2I15, F15.5)
110   FORMAT (2F20.5)
113   FORMAT (7F15.5)
129   FORMAT (I14,I16,I14,I16,I19)
130   FORMAT(//5X,65HTHE MOMENT AT THE LOCATION OF THE HINGE IN THE CONT
     *INUOUS BEAM IS ,F9.2,1X,8HKIP-INS. )
131   FORMAT(/5X,88HTHE MAGNITUDE OF THE CONCENTRATED MOMENT APPLIED TO
     *THE END OF THE SEMI-INFINITE BEAM IS ,F9.2,1X,8HKIP-INS. )
132   FORMAT(/5X,78HTHE RATIO OF THE APPLIED CONCENTRATED MOMENT TO THE
     *MOMENT AT THE HINGE IN THE /5X,18HCONTINUOUS BEAM IS ,F9.2,1X,
     *8HPERCENT. )
133   FORMAT(5X,23HTHE SIMULATION ERROR IS ,F9.5)
134   FORMAT(/3X,13HDISTANCE FROM ,6X,6HACTUAL ,7X,10HDEFLECTION ,5X,
     *10HDEFLECTION ,5X,10HDEFLECTION ,5X,10HDEFLECTION ,7X,5HTOTAL )
135   FORMAT(7X,6HORIGIN ,7X,10HDEFLECTION ,5X,11HOF INFINITE ,5X,
     *8HOF SEMI- ,7X,8HOF SEMI- ,6X,9HOF HINGED ,8X,5HMODEL )
136   FORMAT(38X,4HBEAM ,6X,13HINFINITE BEAM ,2X,13HINFINITE BEAM ,6X,
     *4HBEAM ,9X,10HDEFLECTION )
137   FORMAT(51X,7H(RIGHT) ,9X,6H(LEFT) )
138   FORMAT(7X,6HINCHES ,6(9X,6HINCHES)//)
420   FORMAT (I10)
999   FORMAT (F10.0)
      END
```

## SUBROUTINES FOR COMPUTER PROGRAMS

```
      SUBROUTINE ULOAD(J)
      REAL I,MOMES,MSMAL,MOME,L
      COMMON X(60),AI(5),QO(5),BI(5),L,A,B,AB,S2,S4,R2,E,I,N5,DEFL(60),
     1     SLOPE(60),MOME(60),SHEAR(60),CM(5),DIST(5),N2,AA,T
      DEFL(J)=0.0
      SLOPE(J)=0.0
      MOME(J)=0.0
      SHEAR(J)=0.0
      DO 600 K=1,N5
      IF (X(J).GT.AI(K)) GO TO 601
      ALETA=(AI(K)-X(J))/L
      BLETA=(BI(K)-X(J))/L
      C1= (L**4.)/(4.*A*B*S4*E*I)*R2
      C2= (L**4.)/(4.*A*B*S4*E*I)*AB
      GO TO 603
601   IF (X(J).GT.BI(K)) GO TO 602
      ALETA=(X(J)-AI(K))/L
      BLETA=(BI(K)-X(J))/L
      C1=-(L**4.)/(4.*A*B*S4*E*I)*R2
      C2=-(L**4.)/(4.*A*B*S4*E*I)*AB
      GO TO 603
602   ALETA=(X(J)-AI(K))/L
      BLETA=(X(J)-BI(K))/L
      C1= (L**4.)/(4.*A*B*S4*E*I)*R2
      C2= (L**4.)/(4.*A*B*S4*E*I)*AB
603   AAX=A*ALETA
      BAX=B*ALETA
      ABX=A*BLETA
      BBX=B*BLETA
      FA1=SIN(BAX)/(EXP(AAX))
      FA2=COS(BAX)/(EXP(AAX))
      FA11=B*FA2-A*FA1
      FA21=-(A*FA2+B*FA1)
      FA12=R2*FA1-AB*FA2
      FA22=R2*FA2+AB*FA1
      FA13=B*(3.*A**2.-B**2.)*FA2+A*(3.*B**2.-A**2.)*FA1
      FA23=B*(B**2.-3.*A**2.)*FA1+A*(3.*B**2.-A**2.)*FA2
      FB1=SIN(BBX)/(EXP(ABX))
      FB2=COS(BBX)/(EXP(ABX))
      FB11=B*FB2-A*FB1
      FB21=-(A*FB2+B*FB1)
```

```
      FB12=R2*FB1-AB*FB2
      FB22=R2*FB2+AB*FB1
      FB13=3*(3.*A**2.-B**2.)*FB2+A*(3.*B**2.-A**2.)*FB1
      FB23=B*(B**2.-3.*A**2.)*FB1+A*(3.*B**2.-A**2.)*FB2
      IF (X(J).GT.AI(K)) GO TO 604
      VSMAL=C1*(FA1-FB1)+C2*(FA2-FB2)
      OSMAL=C1*(FB11-FA11)+C2*(FB21-FA21)
      MSMAL =C1*(FA12-FB12)+C2*(FA22-FB22)
      CSMAL=C1*(FB13-FA13)+C2*(FB23-FA23)
      OSMAL=-OSMAL
      CSMAL=-CSMAL
      GO TO 606
  604 IF(X(J).GT.BI(K)) GO TO 605
      CC=(L**4.)/(S4*E*I)
      VSMAL=C1*(FA1+FB1)+C2*(FA2+FB2)+CC
      CSMAL=C1*(FA11-FB11)+C2*(FA21-FB21)
      MSMAL=C1*(FA12+FB12)+C2*(FA22+FB22)
      QSMAL=C1*(FA13-FB13)+C2*(FA23-FB23)
      OSMAL=-OSMAL
      CSMAL=-QSMAL
      GO TO 606
  605 VSMAL=C1*(FB1-FA1)+C2*(FB2-FA2)
      OSMAL=-(C1*(FB11-FA11)+C2*(FB21-FA21))
      MSMAL=C1*(FB12-FA12)+C2*(FB22-FA22)
      QSMAL=-(C1*(FB13-FA13)+C2*(FB23-FA23))
  606 DEFLS=QO(K)*VSMAL
      SLOPES=QO(K)/L*OSMAL
      MOMES=-(QO(K)*E*I)/(L*L)*MSMAL
      SHEARS=-(QO(K)*E*I)/(L**3.)*QSMAL
      DEFL(J)=DEFL(J)+DEFLS
      SLOPE(J)=SLOPE(J)+SLOPES
      MOME(J)=MOME(J)+MOMES
  600 SHEAR(J)=SHEAR(J)+SHEARS
      RETURN
      END


      SUBROUTINE WULOAD (J,WLAMDA,BKS)
C     INFINITE BEAM ON WINKLER MODEL
C     UNIFORM LOADS
      COMMON X(60),DEFL(60),AI(5),BI(5),QO(5),N5
      DEFL(J)=0.0
      DO 800 K=1,N5
      IF (X(J).GT.AI(K)) GO TO 801
      AW= AI(K)-X(J)
      BW= BI(K)-X(J)
      GO TO 803
  801 IF (X(J).GT.BI(K)) GO TO 802
      AW= X(J)-AI(K)
      BW= BI(K)-X(J)
      GO TO 803
  802 AW=X(J)-AI(K)
      BW=X(J)-BI(K)
  803 ALAMDA= AW*WLAMDA
```

```
      BLAMDA= BW*WLAMDA
      CLA= COS(ALAMDA)/(EXP(ALAMDA))
      CLB= COS(BLAMDA)/(EXP(BLAMDA))
      IF (X(J).GT.AI(K)) GO TO 804
      DEFLS=(QO(K)*(DLA-DLB))/(2.*BKS)
      GO TO 800
  804 IF (X(J).GT.BI(K)) GO TO 805
      DEFLS=(QO(K)*(2.-DLA-DLB))/(2.*BKS)
      GO TO 800
  805 DEFLS=-(QO(K)*(DLA-DLB))/(2.*BKS)
  800 DEFL(J)=DEFL(J)+DEFLS
      RETURN
      END


      SUBROUTINE SEMIM(J)
      REAL I,MOMES,MOME,L
      CCMMON X(60),AI(5),QO(5),BI(5),L,A,B,AB,S2,S4,R2,E,I,N5,DEFL(50),
     1      SLOPE(60),MOME(60),SHEAR(60),CM(5),DIST(5),N2,AA,T
      DEFL(J)=0.0
      SLOPE(J)=0.0
      MOME(J)=0.0
      SHEAR(J)=0.0
      DO 300 K=1,N2
      D=-B*(S2*(3.*A**2.-B**2.)+(4.*A*AA*T*L**3.)/(E*I))
      C1=-((CM(K)*L**2.)/(E*I*D))*(A*S2+(2.*4*T*L**3.)/(E*I))
      C2=(CM(K)*S2*B*L**2.)/(E*I*D)
      IF (X(J).GE.DIST(K)) GO TO 301
      XDIST=DIST(K)-X(J)
      AANEG=AA*XDIST
      DEFLS=C2/(EXP(AANEG))
      DEFL(J)=DEFL(J)+DEFLS
      GO TO 300
  301 XDIST=X(J)-DIST(K)
      AX=A*XDIST/L
      BX=B*XDIST/L
      F1=SIN(BX)/(EXP(AX))
      F2=COS(BX)/(EXP(AX))
      F11=B*F2-A*F1
      F21=-(A*F2+B*F1)
      F12=R2*F1-AB*F2
      F22=R2*F2+AB*F1
      F13=B*(3.*A**2.-B**2.)*F2+A*(3.*B**2.-A**2.)*F1
      F23=B*(B**2.-3.*A**2.)*F1+A*(3.*B**2.-A**2.)*F2
      DEFLS=C1*F1+C2*F2
      SLOPES=C1*F11+C2*F21
      MOMES=C1*F12+C2*F22
      SHEARS=C1*F13+C2*F23
      DEFL(J)=DEFL(J)+DEFLS
      SLOPE(J)=SLOPE(J)+SLOPES
      MOME(J)=MOME(J)+MOMES
      SHEAR(J)=SHEAR(J)+SHEARS
  300 CONTINUE
      RETURN
      END
```